University of Nairobi

Faculty of Engineering

ASSESSING THE IMPACT OF CLIMATE CHANGE ON AGRO-ECOLOGICAL ZONES AND AGRICULTURE IN KENYA'S LOWER EASTERN REGION

Lilian Wangui Ndungu

(F80/54871/2019)

B.Sc. (Business Information Systems) (Kenya Methodist University), M.Sc. (GIS) (University of Nairobi)

A thesis submitted in fulfillment of the requirements for the degree of Doctor of Philosophy in the Department of Geospatial and Space Technology of the University of Nairobi

May 2024

Declaration of Originality

I declare that this research proposal is my original work and has not been submitted elsewhere for examination, award of a degree or publication. Where other works or my own work has been used, this has properly been acknowledged and referenced in accordance with the University of Nairobi's requirements.

Signed: Lilian Ndungu

11-05-2024

Approval

This thesis has been submitted for examination with our approval as university supervisor(s).

Prof. Dr.-Ing John B. Kyalo Kiema   SIGNATURE   DATE…11-05-2024

Dr.-Ing David N. Siriba   SIGNATURE   DATE…11-05-2024

Dedication

To my father, Moses Ndungu Wamathai, words fail me. And to my children Grace and Asher who have made the commitments and sacrifices with me to complete this research. And to my family, Mum Grace, Irene, Sam, Eric, Joan and Tony for your love and unwavering support in every chapter of my life. And to the ecosystem of scientists and friends whose faith in my capacity has never wavered. Thank you for giving me the courage to do this.

Acknowledgement

I would like to acknowledge my supervisors Prof. Dr.-Ing John B. Kyalo Kiema and Dr.-Ing David N. Siriba for agreeing to be part of this journey, for their understanding and encouragement in scoping and finishing the research. And to the Kenya Climate Smart Agriculture Program (KCSAP) and by extension the World Bank for facilitating my research. To the KCSAP program team and especially Dr. Kevin Obiero and Ms. Priscilla Muiruri for believing in me.

ABSTRACT

Kenya's vulnerability to climate variability and change has been compounded by dependence on rain-fed agriculture with constrained capacity to adapt and a rapidly growing population. Changes in Agro-Ecological Zones (AEZ) is a notable response to climate change, and it alters and influences cropping patterns. This research implements a replicable and scalable workflow for mapping past, present and future agro-ecologies to demonstrate a forward future-based thinking for climate adaptation and investments. Google Earth Engine and R Statistics were used for satellite and station data analysis. Fuzzy logic was used in normalizing the layers and in computing the AEZ. Change was evaluated at two checkpoints (1990-2005, 2006-2020). 2020 was used as the baseline year to evaluate change in the "near future" 2040 through two Representative Concentration Pathways 4.5 and 8.5. Interesting results emerge from the study, validating the hypothesis that the seasons and production potential is shifting. Lowland drylands (Kitui, Machakos, Makueni) experienced an increase in the Length of the Growing Period (LGP) ranging from 1 to 20 days in the short rains, but no change in the long rains. However, in future, the lowlands drylands experience an increasing LGP, surface runoff, creating potential for diversifying production systems with the capacity to grow more drought resistant crops and harvest water. Midland highland areas (Embu, Tharaka-Nithi, Meru) experienced a loss in LGP ranging from 1 to 10 days in most areas in both seasons and a reduction in agro-ecological potential. This change is already evident with the negative trend continuing. In these areas, resilience mechanisms will need to consider the expected future reduction in rain-fed agricultural potential and drought resilience focused diversification. The research proposes policy focusing on use of digital technologies, cloud computing and future projections.

Keywords: Climate change, AEZ, Kenya, hotspots, geospatial, IPCC, agriculture, predictions.

TABLE OF CONTENTS

4

List of figures

List of tables

List of equations

List of abbreviations

Abbreviation	Meaning
ACZ	Agro Climatic Zones
AEZ	Agro- Ecological Zones
AI	Aridity Index
ASAL's	Arid and Semi-Arid Areas
CABI	Centre for Agriculture and Bioscience International
NCCAP	National Climate Change Action Plan
CHIRPS	Climate Hazards Infra-Red Precipitation with Stations data
CHIRTS	Climate Hazards Infra-Red Temperature with Stations data
CIMP5	Coupled Model Intercomparison Project
CV	Coefficient of Variation
DM	Dry Matter
DMP	Dry Matter Productivity
ECMWF ERA	European Centre for Medium Range Weather Forecasts Reanalysis
EO	Earth Observation
EOS	End of the Season
FAO	Food and Agriculture Organization
GCM	Global Climate Models
GDP	Gross Domestic Product
GEE	Google Earth Engine
GHG	Green House Gas
GIS	Geographic Information Systems
GIZ	German Gesellschaft für Internationale Zusammenarbeit GmbH
GoK	Government of Kenya
HadGEM-ESM	Hadley Centre Earth System Models
ICIPE	International Centre of Insect Physiology and Ecology
ICPAC	IGAD Climate Prediction and Application Centre
IPCC	Inter-governmental Panel on Climate Change
IPCC AR5	Fifth Assessment Report of the Intergovernmental Panel on Climate Change
ISRIC	International Soil Reference and Information Centre
KCSAP	Kenya Climate Smart Agriculture Programme

KENSOTER	Kenya Soil and Terrain database
KMC	Kenya Meat Commission
KMD	Kenya Meteorological Department
KSS	Kenya Soil Survey
LGP	Length of the Growing Period
LR	Long Rains
MAM	March April May
MCDM	Multi Criteria Decision Making
MI	Moisture Index
MOALFC	Ministry of Agriculture Livestock Fisheries and Cooperatives
MR	Moisture regimes
NAP	Kenya National Adaptation Plan
NCCAP	National Climate Change Adaptation Plan
NDVI	Normalized Difference Vegetation Index
NPP	Net Primary Productivity
OND	October November December
PCA	Principal Component Analysis
PET	Potential Evapotranspiration
QGIS	Quantum GIS
RCP	Representative Concentration Pathways
RS	Remote Sensing
SDG	Sustainable Development Goals
SOS	Start of Season
SPEI	Standardized Precipitation Evapotranspiration Index
SR	Short Rains
SRTM	Shuttle Radar Topography Mission
SSA	Sub-Saharan Africa

1 INTRODUCTION

1.1 The intensifying effect of a changing climate on rain-fed systems

A changing and varying climate is one of the extremely notable causes influencing agricultural production and food security because it negatively impacts on crop suitability due to shifting weather patterns (Gleixner et al., 2020; Lin et al., 2013). Smallholder rainfall dependent farming systems, which are highly gendered, are likely to be highly impacted, as their capacities to cope with the shifting climate is already constrained by low incomes, small parcels of land and soil fertility challenges(Lane & Jarvis, 2007). A change in the viability or feasibility of production systems due to climate change affects agricultural productivity. (Mulinge et al., 2015). For instance, a rise in temperature shortens the growing season, requiring agricultural systems to be adjusted to maintain productivity (Lane et al., 2007; Lin et al., 2013).

Climate projections show that the suitable area for growing major food crops will reduce as the climate changes. In some African countries, including Kenya, the change in climate was projected to halve yields from rain-fed production systems by 2020, with net revenues projected to drop by 90% by 2100 (FAO, 2010; IPCC, 2007). Kenya is already experienced the predicted chaotic variations in its crop growth season, low productivity, as well as sudden occurrences of diseases and vectors (IPCC, 2007). Kenya's agricultural sector faces heightened vulnerability to climate change due to its reliance on rain-fed crops, a growing population requiring more food, limited use of machinery, and resource-constrained small farms with deteriorating soil quality (Boitt et al., 2016; EroHerr et al., 2010; Obwocha et al., 2022; Ojwang et al., 2010).

The increasing frequency of extreme events, like droughts and floods, with shorter recovery periods, weakens the resilience of ecosystems. This can lead to a cascade of problems, including crop failures, the spread of invasive species, and the emergence of new diseases in agricultural systems (Manzi et al., 2020). Intensifying production in already-degraded ecosystems has been one of the response

mechanisms (FAO, 2010; Liu, 2015) which calls for striking a careful balance between managing degradation and optimizing food supply and returns on agricultural investments.

This is crucial in nations like Kenya where agriculture significantly contributes to the GDP of the nation. Agriculture contributes 33% of the GDP and employs more than 40% of the workforce that represents 70% of the rural population. Evidence is overwhelming that the shorter recovery period between extreme events will worsen poverty, trapping smallholder farmers, in a cycle of vulnerability (Eichsteller et al., 2022). The ability to produce enough food has already been impacted by frequent droughts, increasing floods, and unexpected deviations to regular weather patterns, which result in high rates of human and cattle mortality and decreased productivity (FAO, 2010; C. Nakalembe et al., 2021).

After a third straight below-average rainy season that was brought on by the effects of poor crop and livestock output, resource-based violence, livestock sickness and mortality, and the COVID-19 pandemic; over 3.1 million Kenyans experienced severe food shortages in 2022(FEWSNET, 2022). Further, the capacity to optimize production is affected by land fragmentation and land ownership issues. In the high production areas, land fragmentation hampers the capacity to leverage economies of scale and mechanization. In the rangelands, land ownership and shift from purely pastoral to agro-pastoral systems has also led to an increase in conflicts as livestock and wildlife migration routes become closed.

The global financial and economic crisis' disruption of agricultural supply networks and marketplaces has made it more difficult for the nation to sustainably manage the issue of food security (Breisinger et al., 2022; Manzi et.al., 2020). The Russia-Ukraine war occurred when the country was already grappling with the effects of the COVID-19 pandemic and the desert locust invasion, resulting in record high food prices due to shortages, pushing millions more people into severe poverty and hunger. Food prices reached record highs due to the crisis in Ukraine, supply chain interruptions, and the

persisting negative economic consequences of the COVID-19 pandemic, undoing years of development progress (Breisinger et al., 2022).

Adaptation strategies, decisions and priorities are based on historical baselines, to define Agro-ecological potential, and sometimes combined with short term forecasts. But the past, and especially the last fifteen years when the clarion call on approaches to responding to a changing climate was amplified, means that the current adaptation decisions have not achieved the desired effect of stabilizing the increasing constraints posed by climate change.

Climate projections are pointing to major region-specific shifts in rainfall and temperature and specifically, probabilities of long-term wetting, which will manifest through an increase in annual mean precipitation (RCMRD, 2018). At the same time, higher risks of drought are also anticipated, along with decreases in rainfall especially in the long rains, since much of the stability is expected in the short rains (Schlenker et al., 2010).

1.2   Problem statement

To optimize the efficacy of resilience investments, there is a pressing need to reevaluate our strategies for mitigating and adapting to the declining agricultural productivity in Kenya (Antony, 2017; Ochieng et al., 2016). The classification of geographical regions into Agro-Ecological Zones (AEZs) based on their meteorological, edaphic, and biophysical similarities is fundamental in determining their capacity for rain-fed agriculture. However, the shifting seasonality and climate patterns lead to changes in AEZs, significantly impacting agricultural practices (Lin et al., 2013).

The accuracy of AEZ mapping relies heavily on data availability, affecting the precision of adaptation recommendations, particularly in regions with similar temperature and precipitation patterns but varying soil properties within microclimates (Herrick et al., 2016). It is imperative to conduct thorough assessments to account for these microclimate differences, especially for smallholder farmers dependent on agriculture for sustenance, employment, and income. The existing AEZ dataset and maps, primarily developed by the Food and Agricultural Organization (FAO) in 1983 with partial

updates in 1993 and 1996, lack recent and comprehensive profiling that incorporates microclimate variations (Jaetzold et al. 1983, Boitt et al., 2016). The resource-intensive nature of earlier mapping approaches hinders regular updates, compromising the quality of decisions regarding agricultural interventions and adaptation to shifting climate.

1.3   Objectives

1.3.1   Overall objective

The study assessed how climate variability and change will affect AEZ and impact agriculture Lower Eastern Region.

1.3.2   Specific objectives

1.   The study assessed past and present AEZ based on biophysical and climatic factors and evaluated hotspots of significant change.

2.   The study interpreted the observed changes in predicted future climate and AEZ and their anticipated influence on agriculture in the lower eastern region and recommended opportunities for adaptation.

1.4   Research questions.

How did climate variability and change affect AEZ in the lower Eastern Region?

2.   What was the interpretation of these changes on agriculture?

3.   What opportunities did these changes present in improving adaptation in the region's agricultural production systems?

1.5   Justification of the study

The continued reliance on the rain-fed production systems emphasizes the need for a closer examination of adaptation and mitigation strategies and their effectiveness in boosting agricultural production and food security (Manzi et al., 2020). This is possible if decisions are made using timely, accurate and appropriate data, because climate adaptation recommendations are often expensive and have long-term consequences. In this situation, precise climate data is essential for building a system

that is climate-resilient and for developing responses and methods that lessen the country's vulnerability to the various climatic risks (Boitt et al., 2016). Yet, relying solely on climate-driven assessments proves insufficient in capturing the complexities of both climate and human-induced vulnerabilities. This study recognizes the need to bridge this gap by incorporating a comprehensive understanding of the potential of the land in the Lower Eastern Region and its susceptibility to climatic and anthropogenic factors.

Despite extensive research on variations in inter-annual and inter-seasonal changes in climatic conditions, and their effect on agricultural production cycles in Kenya, significant gaps remain.

The central focus of this research is to address these gaps, particularly the challenges in consistently providing current and accurate information essential for supporting agricultural decisions and maximizing adaptation objectives. The Ministry of Agriculture, vital in this regard, relies on Agro-Ecological Zone (AEZ) definitions from the farm management handbook for crucial decisions on crop insurance, adaptation recommendations, and resilience strengthening.

 Aligned with the Kenya Climate Smart Agriculture Program, which aims to enhance climate adaptation mechanisms, this research employs technological innovations to deliver practical applications. Through the integration of satellite data and earth observation (EO) datasets, this study brings forth timely and actionable insights, transforming adaptation priorities. For instance, the prediction of increased rainfall and surface runoff in certain Arid and Semi-Arid Areas (ASALS) during short rains presents opportunities for mixed agro-pastoral systems and water harvesting (Muthoni et al., 2019; RCMRD, 2018). Furthermore, the research challenges the status quo by highlighting that farming systems in transition zones no longer align with recommendations in the farm management handbook. The proposed technologies offer a proactive and pre-emptive understanding of past, current, and anticipated future changes, charting a new data-driven trajectory for enhancing adaptation recommendations.

The increasing availability of high-quality, high-resolution remote sensing and model-based datasets, combined with ground data, provides a cost-effective means to evaluate past, present, and future trends at micro-scales. As decision-making trends towards forecast-based assessments, the research advocates for leveraging these resources to de-risk agriculture. The study builds upon the findings of RCMRD (2018), which projected a reduction in rainfall and runoff in Western Kenya and other high production areas. Simultaneously, it anticipates increased rainfall in Eastern Kenya, emphasizing the need to evaluate the agricultural potential and identify opportunities for improving adaptation and resilience mechanisms considering these anticipated shifts.

This research offers a pioneering approach to transforming adaptation strategies in Kenya's Lower Eastern Region, integrating technological advancements and innovative methodologies to address the challenges posed by climate change. The proposed methodologies, grounded in robust data and forecasts, aim to guide proactive decision-making for sustainable agricultural development and resilience in the face of evolving climatic patterns.

1.6 Scope and limitations of the work

The research was conducted in the Lower Eastern Region in Kenya, covering Meru, Embu, Tharaka Nithi, Makueni, Machakos and Kitui Counties. The region was selected since the counties represent diverse AEZ from arid to high potential zones. Leveraging satellite datasets, the study aimed to provide scalable methods for mapping agro potential across Kenya.

Following FAO guidelines for AEZ, the research utilized both climatic and biophysical parameters to define AEZs. Rainfall, temperature, potential evapotranspiration (PET), length of growing period (LGP), and aridity index were some key climatic variables analysed. Freely available datasets meeting spatial and temporal requirements were selected, including daily data from 1990 to 2020 with a resolution of 5km or less for the baseline assessments. Weather station data from the Kenya Meteorological Department and satellite precipitation and temperature were utilized and improvements made.

Downscaling techniques were applied to Climate Model Intercomparison Project Phase 5 (CMIP5) data, with a focus on Representative Concentration Pathways (RCP) 4.5 and 8.5 for future projections from 2020 to 2040 representing the near future. The study evaluated and adopted the General Circulation Models (GCMs) due to research showing they performed better over Eastern Kenya, which was crucial for accurate climate projections.

Biophysical characteristics like soil profiles, soil constraints, slope and land productivity (biomass) were included in the research. The study focused on shifts in agricultural potential which are known to affect productivity, food security, and livelihoods in the region.

The study acknowledges a limitation in capturing land management practices and in this case an assumption that proper land management practices increase productivity and biomass are used to identify the proxy dataset for land management. At the same time, lack of localized solar radiation data also influenced the calculation methods for the potential evapotranspiration instead resulting in the use of the Thornthwaite's calculations instead of penman monteith equations as adopted by FAO. Trade-offs were made on data selection in order to meet the requirements for workflow scalability and replicability.

1.7 Organization of the report

Chapter 1 is the background section that provides an overview of the impact of climate change on rain-fed agricultural systems in Kenya, particularly in the Lower Eastern Region. It highlights the vulnerability of smallholder farmers, who face challenges such as low incomes, limited land, and soil fertility issues. The section also discusses the recent disruptions, including resource-based violence, the COVID-19 epidemic, and the Russia-Ukraine war, which have amplified food security issues. The subsequent problem statement emphasizes the need to reassess mitigation and adaptation strategies given the decline in agricultural production.

Chapter two focuses on a literature review introducing and further elaborating on concepts and tools that have been applied in this study. It demonstrates the urgency to think outside the box to respond to

the climate change crisis. Further, showing the opportunities that emerging technologies provide in transforming business-as-usual ways of deriving information for decision making.

Chapter three explains in detail the methodology adopted for the study, the study area, the data type used and data sourcing techniques, the analysis performed on the data and the integrated visualization. This chapter forms the core of the project and as such a lot of emphasis has been put on the systematic approach taken. It proposes a new and sustainable methodology approach for mapping agro-ecological zones to maintain recency in data available for decision making. It utilizes freely available satellite imagery with the best spatial coverage, and cloud computing to map past, present, and future agro-ecological zones.

Chapter Four presents the deliverables from chapter three such as maps showing the shifts past, present and future climatic conditions and agro-ecological zones. Followed by textual descriptions and discussions providing more information about the data displayed on the maps and the interpretations and implications of the same.

Chapter Five concludes the project report by providing policy and decision support conclusions and recommendations.

2   LITERATURE REVIEW

2.1   Background

Globally, the increased frequency and intensity of precipitation changes, heat waves, droughts, and floods have all contributed to an increased focus on adapting to and minimizing responses to climate change (Kotir, 2011; Ochieng et al., 2016). Globally, the growing focus on optimizing responses to climate change and adaptation has been catalysed by the increasing climate extreme events that have been manifest through frequent and more intense variations in precipitation, heat waves, drought, and floods (Kotir, 2011; Ochieng *et al*., 2016).

By the end of the 21st century, climate change is predicted to raise the average temperature by 1.4 to 5.5°C and the average amount of precipitation by 2% to 20%. (Adhikari et al., 2015). Despite varying forecasts for rainfall, the general view is that whether a rise or reduction in temperature is evident, it will primarily hurt agricultural production because of increased evapotranspiration (Adhikari et al., 2015; Kotir, 2011; Ochieng et al., 2016).

The largest contribution to Green House Gas emissions, according to a report from the Intergovernmental Panel on Climate Change (IPCC, 2014), came from agricultural production and its effects on land use. Future predictions offer a bleak picture, with the demand to create more; fuelling the anticipated rise in population and resource consumption, creating a vicious cycle wherein growing competition for finite resources will result in further degradation. Global and national goals have been established to encourage change with the purpose of mitigating these changes through Sustainable Development Goals (SDG) targets due to the growing need to combat climate change and global warming while lowering carbon dioxide emissions (Holzkämper, 2017).

2.2   Drivers of climate change in Kenya

In Kenya, the drivers of climate change encompass a multifaceted array of natural and anthropogenic factors that interact to shape the country's climate system. One of the primary drivers is anthropogenic

greenhouse gas emissions, primarily stemming from the burning of fossil fuels for energy production, industrial activities, transportation, and deforestation(Vermeulen et al., 2014).

Rapid population growth and urbanization aggravate these emissions, increasing the carbon footprint of human activities. Changes in the use of land, such as deforestation for agriculture, infrastructure development, and urban expansion, further contribute to carbon dioxide levels while disrupting local weather patterns and ecosystems. Additionally, agricultural practices, including livestock rearing and land degradation, emit methane and nitrous oxide, potent greenhouse gases that amplify climate change (Ngigi & Muange, 2022).

Moreover, Kenya's vulnerability to climate change is compounded by natural factors such as its geographical location near the equator, which exposes it to intense solar radiation and influences seasonal rainfall patterns. Variability in sea surface temperatures, particularly in the Indian Ocean, also influences rainfall distribution through phenomena like the El Niño-Southern Oscillation (ENSO) and the Indian Ocean Dipole (IOD), exacerbating droughts or floods (Indeje et al., 2005).

The geographic suitability of crops in Kenya is expected to undergo significant modifications due to climate change, with these changes becoming more pronounced in the near future, particularly by 2040(RCMRD, 2018). Climate projections indicate alterations in temperature and precipitation patterns, which will directly impact the agro-ecological zones and suitability of different crops across the country(Lane, Annie; Jarvis, 2007).

Rising temperatures are projected to shift the boundaries of suitable growing areas, with higher elevations becoming more conducive to certain crops while lowland areas may experience decreased suitability. Additionally, changes in precipitation patterns, including shifts in the timing and intensity of rainfall, will affect water availability and soil moisture, further influencing crop suitability (EroHerr et al., 2010; IPCC, 2007).

For instance, areas currently suitable for rainfed agriculture may face increased water stress, necessitating shifts to drought-resistant crops or alternative irrigation methods. Conversely, regions

experiencing increased rainfall may see expanded opportunities for crop cultivation, albeit with potential challenges related to soil erosion and waterlogging. These modifications in crop suitability pose significant challenges to Kenya's agricultural sector, requiring proactive adaptation strategies such as crop diversification, improved water management practices, and the development of climate-resilient varieties (Cairns et al., 2013; Silvestri et al., 2012). Understanding these projected changes is crucial for policymakers, farmers, and other stakeholders to effectively plan and implement measures to sustain food production and enhance agricultural resilience in the face of a changing climate (Musafiri et al., 2022; Rios, 2015).

2.3 The effect of a changing and varying climate on agriculture

Because so many people depend on agriculture and are at threat of food insecurity in low-income countries, effects of climatic fluctuations are anticipated to be the most severe there (Liu, 2015). In Africa, where agriculture is highly reliant on weather and climate factors including temperature, precipitation, and light and extreme events, these effects are anticipated to be more pronounced and to have higher ramifications (Cairns et al., 2013; Knox et al., 2012; Liu, 2015).

In all the agro-systems which are predominantly rain-fed, climate variability and change has resulted in losses in livestock and livelihoods and human lives (Ojwang et al., 2010). Further, these impacts are expected to worsen with projections anticipating an increase in temperatures and unpredictability of rainfall (Kotir, 2011; Ochieng et al., 2016).

The adaptive capacity is also negatively affected by the growing population and agricultural production systems that are characterized by smallholder subsistence, labour intensive low input and poorly mechanized farming(FAO, 2010; Liu, 2015).Adaptation strategies demonstrated in the changing cropping patterns such as increase in area under agricultural production and deserting unproductive land is only exacerbating the situation.

To meet the needs of the population, which is projected to continue expanding, this trend is predicted to continue, requiring not less than one hundred million hectares of new land globally for agricultural use in 2050 (FAO, 2010; Liu, 2015).

With a changing climate, new patterns in crop and livestock diseases are emerging. Changes in biodiversity due to shifts in the use of land and cover, coupled with new moisture and temperature patterns has resulted in new hotspots due to modified pest and disease propagation dynamics. Global warming has also resulted in emergence of new strains of pest and diseases in new environments with the frequency of these outbreaks expected to increase (Kabubo-Mariara et al. 2015; Liu, 2015).

While quantifying climate change requires large time and scale specific datasets, the gradual shifts in seasonality and especially through a fluctuation in the frequency and intensity of both rainfall and temperature; has had the considerable impact on agricultural production. Delays in onset and cessation of rainfall means farmers cannot rely on the crop calendars to plant. Sustaining required production then becomes a game of chance. Where every option undertaken by the farmer represents a set of risks. For example, early planting means delays in onset of rainfall will result in losses of seed. Intermittent rainfall also results in wilting and crop failure.

The delays in onset of the rainfall, result in a reduction in planted area, and in effect seasonal production. Early cessation of rainfall during the flowering stages will lower yields, while an increase of rainfall during the end of season results on post-harvest losses. As the seasonality changes, so does the viability for production of domain crops (Kazembe & Kenya, 2014). With farmers growing the domain crops due to distinct reasons, switching to more viable crops takes time. For example, with ugali as a staple food, farmers continue to grow maize even in areas where it has ceased to be viable. Advisories to adjust the crops planted then requires a cultural shift over time, within which farmers might continue to experience considerable losses in their production systems (Gebre et al., 2023; Musafiri et al., 2022).

2.4 Efforts in addressing climate change in Kenya

Food security in Kenya remains a key challenge despite increased investments in agricultural production assistance (FAO, 2010; Kotir, 2011), with Kenya importing over 50% of its food supply (EroHerr et al., 2010). To effectively manage the effects being felt, it is important to reassess our mitigation and adaptation measures considering the country's clearly dropping agricultural productivity (FAO, 2010; Muok et al., 2012). Particularly given that forecasted the variations in climatic conditions are expected to result in decreased food production in "food basket areas," while population growth will increase competition for already depleting natural resources.

Many programs have been initiated focused on adaptation with the goal of decreasing the effects of a changing and erratic climate on the country's agricultural production systems. The government has led the research and development of adaptive plants and animals that thrive even in drought prone areas. Other measures include diversification of the sources of livelihoods and water management (Ochieng et al., 2016; Ojwang et al., 2010).

National initiatives including Vision 2030, the NCCAP-2013-2017(National Climate Change Action Plan), and NAP-2015-2030 (Kenya National Adaptation Plan) were created to set goals for managing the implications of a fluctuating climate (Ochieng et al., 2016). These plans emphasized putting important initiatives into action, including stepping up irrigation to increase food security, putting safety nets in place to lessen livestock losses during drought in ASALs, reviving the Kenya Meat Commission (KMC), and putting government crop and livestock insurance programs into action.

2.5 Gendered and indigenous adaptation efforts

Local communities in Kenya possess valuable traditional knowledge and practices that have enabled them to adapt to environmental changes for generations. However, these communities are often overly affected by the ravages of a frequently changing climate due to their reliance on natural resources and their marginalization from mainstream society.

Indigenous climate adaptation efforts involve community-based approaches that draw on local knowledge and cultural practices. For instance, traditional ecological knowledge is used to monitor the weather patterns, enhance agricultural practices, water management systems, and natural resource conservation (Gebre et al., 2023; Musafiri et al., 2022).

Due to cultural divisions of labour, women often till the land and look for water, making them particularly susceptible to changes in rainfall patterns and agricultural productivity. Recognizing the distinct experiences and knowledge of different genders and Indigenous communities is essential for developing effective and inclusive strategies to cope with climate-related challenges(Ngigi & Muange, 2022).

2.6 Assessing climate change projections for Kenya

Research shows various projections for various regions of the nation. Nevertheless, despite divergent climatic predictions in the East Africa Region, there is consensus on the anticipated increase in rainfall in some parts of Kenya (Adhikari et al., 2015; EroHerr et al., 2010; Knox et al., 2012; Kotir, 2011; Ochieng et al., 2016) (see Table 2.1). A second indication of this is the stabilizing trend in the brief rains (important in the ASALs), which is in line with projections for an increase in rainfall there (RCMRD, 2018).

Table 2.1 An analysis of climate projections and general impacts on agriculture in different periods leading to 2100.

Author	Temperature	Rainfall	Impacts on agriculture
EroHerr *et al*. 2010	Increase	Increase	Increases might cancel out due to increased potential evapotranspiration, but opportunities for water harvesting and diversification of livelihoods
Adhikari *et al*. 2015	Increase	Increase	Although a rise in temperature may result in an increase in crop productivity, it will also raise the risk of water stress in lowland areas. Climate change-related precipitation variability increases the need for irrigation water.

Knox et al. 2012	Increase	Decrease	Expected to be a significant decrease in the yields of wheat, sorghum, millet, and corn.
Kotir, 2011	Increase	Increase	Despite advances, it is anticipated that the length of growing seasons will decrease by more than 20%.
Kabubo-Mariara et al. 2015	Increase	Increase	Erratic weather is anticipated to have an impact on crop revenue, with higher crop revenue being related with higher winter temperatures (June to August) and lower crop revenue being connected with higher summer temperatures (March to May).

Further, the projected increase in temperature might improve suitability for agricultural production in Kenyan highlands, potentially leading to higher yields (EroHerr et al., 2010). In the Kenya ASAL's, projected increase in frequency of droughts, is expected to negatively impact livestock production compromising food security (Silvestri et al., 2012). However, projected increase in precipitation in the ASAL's, coupled by an understanding of soils and crop suitability would provide invaluable insights on where diversification of incomes through crop production would be viable.

Increasing capacity to downscale predictions is yielding more interesting results that align with trends observed in baselines. These downscaled predictions, provide a localized understanding and improve the quality of information available to inform the proposed forward-thinking approach to climate adaptation, where decisions are based on past and present trends, as well as in future trends.

The recent downscaling of Coupled Model Intercomparison Project (CIMP5) projections by RCMRD is an example, which provides country wide insights on the changes expected in climate and the near future in Kenya. The research by RCMRD predicts a reduction in rainfall and runoff in Western Kenya and other high production areas (RCMRD, 2018). At the same time, stability in the short rains which is already evident, and projected increase in rainfall is expected in Eastern Kenya (RCMRD, 2018).

2.7 AEZ and their role in adapting agriculture to climate change

Considerable research has been done on how climate change is affecting Kenyan agriculture. Still, there are gaps. For example, the FAO recommended using agro ecological zones to do more thorough

evaluations of the influences of climate variations on agriculture, including changes in temperature, rainfall, humidity, as well as other variables under various climate scenarios (Liu, 2015).

This is crucial since maintaining and sustaining food security presents unique problems for each AEZ (Ojwang et al., 2010). Furthermore, altering AEZ, which affects and influences cropping patterns, has been identified as one of the main responses of production systems to climatic changes and variations (Lin et al., 2013). Therefore, looking at the variations in AEZ through time is necessary to assess the effects that a changing climate has on agriculture.

2.8 The case for a technology-driven approach for replicable, scalable, and sustainable mapping

Over the last 20 years, there has been an increasing availability of free medium resolution datasets at different spatial and temporal scales from satellites and other earth observation instruments. EO creates limitless opportunities to provide precise, dependable, and timely information to decision-makers across various agricultural systems and for resource-constrained organizations due to the emerging improvements in technologies and methodologies for archiving and processing EO data using cloud services (C. Nakalembe et al., 2021; Shukla et al., 2021) .

Cloud computing provides opportunities to create scalable and replicable processes that utilize the available data and computing systems. Locally, many studies have demonstrated the value of EO-derived information in improving the understanding of the agricultural productivity and variability within micro-climates, improving the quality of agricultural decisions (Kenduiywo et al., 2020; Miller et al., 2019; Ndungu et al., 2019). EO data and methods are increasing being used in agriculture systems, especially by governments, with their demand being driven by the growing availability of decision-support information and tools (Nakalembe et al., 2019).

2.9 Technology as a key enabler to food security policies and investments

The government has set up several policy-driven investments to inform adaptation and mitigate the consequences of climatic changes on the nation's agricultural production systems. These include

initiatives supported by the government and donors that encourage livelihood diversification, the approval and implementation of national irrigation plans, the promotion of drought-tolerant plants and animal breeds, among others (Ochieng et al., 2016; Ojwang et al., 2010).

Governments are already investing in technology-driven tools because they have realized that to maximize agriculture's potential for mitigating climate change, investments will be needed in both technological advancements and agricultural intensification linked to increased input efficiency, as well as the development of inducements and observatory systems that focus on smallholder farmers (Vermeulen et al., 2014). This research therefore seeks to assess past and present agro-ecological zones, providing insights into the drivers of observable changes. Furthermore, the study seeks to develop an automated, scalable workflow using cloud computing to demonstrate the value of technology driven AEZ mapping. The mapping process endeavors to identify and evaluate hotspots of change in AEZ in the lower eastern region.

2.10 Rethinking adaptation based on future climate projections.

While numerous efforts have been made to increase Kenyan communities' ability to adapt to climate change, commensurate success on investments to climate adaptation and resilience have not been realized. The growing climate change-related issues continue to have a greater impact on smallholder farmers. Even if long-term climate predictions have some uncertainty, it is crucial to look at how vulnerable to climate change social and environmental systems and economically significant assets are affected (Macharia et al., 2020; Silvestri et al., 2012).

Adaptation strategies, decisions and priorities are either based on historical baselines, which are sometimes combined with short-term forecasts. But the past, and especially the last fifteen years when the clarion call on addressing a changing climate was amplified, means that the current adaptation decisions have not achieved the desired effect of stabilizing the increasing constraints posed by climate change.

The increasing availability of satellite and earth observation (EO) datasets and systems for future predictions; provides opportunities for evaluating past, present and future trends at micro-scales. Superior and also high-resolution remote sensing and predictive-derived datasets that are blended and unbiased using station and ground data, are now easily available and provide an opportunity to improve the quality of information available for decision making (RCMRD, 2018; Shukla et al., 2021).

The future of decision making, and indeed the current direction is a move from past baselines-based decision systems to future based anticipatory and early action driven decision making and investments. Already, de-risking of agriculture is being driven by forecast-based assessments. In Kenya, study by RCMRD (2018) developed downscaled EO based climate projections that found a reduction in rainfall and runoff in western Kenya and other high production areas. These climate projections are pointing to major region-specific shifts in rainfall and temperature (RCMRD, 2018) .

2.11 Defining future emission-based trajectories

The primary tools for predicting climate change are global climate models (GCMs), which are compiled with scenarios of the evolution of greenhouse gas (GHG) and aerosol concentrations. They work well at replicating both global and continental climate characteristics, such as global and continental temperature and precipitation patterns, and are intended to assess the behavior of the global climate system (Indeje et al., 2005). The most recent GCMs from the Coupled Model Intercomparing Project's (5th Phase) employed the Hadley Center Earth System Models from the UK Met Office (HadGEM-ESM), and they contributed to the IPCC's fifth Assessment Report (IPCC AR5) (Jones et al., 2011).

Since implementation can involve subjective decisions and may differ between modeling groups conducting the same experiment, it is crucial to have a clear understanding of how the GCM/ESM has been derived to diagnose the simulated climate response and compare responses across different models (Jones et al., 2011).

The outputs from CIMP5 correspond to the three distinct scenarios that constitute the RCPs, which are designated as 2.6, 4.5, and 8.5, respectively. In the moderate emission scenario represented by RCP4.5, greenhouse gas concentrations progressively increase until around 2040 before dropping subsequently. This scenario assumes that linked reference situations will be changed by the employment of climate policy. The most pessimistic scenario, known as RCP8.5, envisions a future in which greenhouse gas concentrations rise continuously (Jones et al., 2011).

2.12 Future proofing adaptation through leveraging emerging technologies

The complexity of updating AEZs demands substantial resources, time, and data, necessitating a robust methodology (Jatzold & Kutsch, 1982). Climate variability and change implicitly affect agriculture potential and productivity (Adhikari et al., 2015; Antony, 2017; EroHerr et al., 2010; Holzkämper, 2017; Knox et al., 2012; Kotir, 2011; Kurukulasuriya & Mendelsohn, 2008; Stige et al., 2006).The proposed solution, leveraging on cloud computing and satellite imagery, transcends these challenges by harnessing 50 years of data to construct workflows spanning past, present, and future scenarios. This approach ensures real-time access to spatial data, facilitating seamless integration with additional data sources for deeper insights and automated processes tailored to users with limited modelling skills as has already been demonstrated in several research in different parts of Kenya (Boitt et al., 2016; Manzi & Gweyi-onyango, 2020; Sagero et al., 2021). This approach, and especially downscaling models to predict the near future has been successfully done in several studies in east Africa and in Kenya ((Endris et al., 2013; RCMRD, 2018) .

Embracing gender-sensitive adaptation and capitalizing on emerging opportunities in a changing climate, this approach optimizes investments and production (Ngigi & Muange, 2022; Ratcheva et al., 2022). While not entirely novel, the transition towards forecast-based decision-making, as opposed to past baseline-driven methods, is gaining traction. Recent studies, such as the one conducted by the Regional Centre for Mapping of Resources for Development (RCMRD) in 2018, underscore the necessity of adapting to projected climate shifts. Leveraging open-source satellite data and cloud

computing, the scalable and replicable workflow presented here offers an efficient means to map AEZs, paving the way for enhanced adaptation strategies and resilient agricultural practices in Kenya.

2.13 Summary

Climate is changing and will continue to change into the future. The government and local communities are responding to these changes using different measures to adapt. AEZ are a good indicator of the effect of the changing climate on the production potential. This means that as climate changes, viability to grow domain crops change, but the new agro-potential represent opportunities to grow new crops.

Information driving adaptation, like the farm management handbook, is often outdated, and based on historical information. This is due to the resource's intensity required to update the maps over large areas. Emerging technologies provide opportunities to improve AEZ mapping, and with increasing accuracy such as the capacity to downscale climate projections, the capacity to map future AEZ changes. These innovations represent an opportunity to provide more accurate and updated information to support structuring of climate adaptation mechanisms. Further, these technologies can support frequent updating of the maps to ensure information remains relevant, even as climate continues to change. It also provides the opportunity to base current adaptation mechanisms with an understanding of future changes in climate and agro-potential, allowing for a more informed transition to more suitable adaptation options.

By understanding how climate change will impact different Agro-Ecosystems in Kenya and specifically in the Lower Eastern region, this study seeks to leverage technologies to identify measures that can be implemented to modify agricultural methods to lessen the negative implications of climatic variations; and leverage new developing prospects.

3 DATA AND METHODS

3.1 Conceptual framework

This part highlights relationships between climate change, adaptation mechanisms, agro potential, methodology development, and the implications for agricultural prioritization and adaptation approaches in Kenya. The goal is to validate the hypothesis that climate is changing and will continue changing into the future in Kenya. These changes and variability will continue to have varying impacts on production systems even in the future. In a highly varying environment consisting of smallholder farming systems, the difference in success of adaptation recommendations will rely on accurately capturing the micro-variations in agro potential.

While there has been increasing investments in adapting our production systems to the changing climate, these changes are not bearing commensurate gains since production keeps dropping. Further, future predictions continue to paint a grim picture of the future where the currently observed trends and changes continue. Adaptation mechanisms have at most used historical baselines as the point of learning to inform design and recommendation of adaptation mechanisms. Effecting any change in a system takes time. There is time lost between recommendations on adaptation to effecting the cultural change that is required to drive adoption of these new recommendations. Farmers who plant maize and depend on maize for food and trade will not be quick to switch to other more viable drought resistance crops immediately.

The study proposes a new line of thought, where current adaptation recommendations learn not only from the past and present changes, but account for anticipated future changes. This would create a convergence in adaptation mechanisms that account and respond to these future changes, potentially creating the tipping point in successful adaptation and contribute to strengthening agriculture production.

Further, while climate may be homogenous over relatively large areas, biophysical characteristics vary over small areas such as soil. Soil characteristics can vary even within the same unit area of land. Therefore, climate predictions alone might not fully represent the changing agro potential.

This research proposes the use of agro-ecological zonation changes as a better predictor to the impact of the evolving and varying climate on agricultural potential and a change in production potential. Existing methods for mapping agro-ecological zones are often time consuming and requiring considerable resources and investments. But the same time, technology, methods, computing resources, algorithms are emerging and opening a new world of opportunities that overcome the existing limitations of updating information required for adaptation. These resources remove the barrier of accessibility of data, reducing the need for personal computing resources to manipulate enormous amounts of data. Development of libraries reduce the amount of coding required to develop outputs, reducing computation time for large volumes of spatial temporal data. This research leverages on this advance in technology and in remote sensing to develop a scalable and replicable methodology for assessing agro potential.

With the government of Kenya relying on Agro-Ecological Zonation as defined in the farm management handbook to inform agricultural prioritization, advisory and investments, the FAO methodology used in developing the AEZ for Kenya is adopted. However, it is refined to allow incorporation of the datasets that allow for improvement of spatial and temporal qualities of data to improve and localize the mapping outputs. Improved mapping outputs can inform agricultural advisory and investments. Finally, while climate change has been seen as all doom and groom, this research evaluates emerging opportunities and consolidates the case for rethinking adaptation approaches.

3.2   Area of study

The area of research comprises of six counties that were selected since they represent diversity in Agro-Ecological and agroclimatic zones. Agroclimatic zones (ACZ) are characterized by moisture

regimes defined by precipitation, potential evapotranspiration, and temperature. The agroclimatic zones in the region range from humid to arid areas. The Agro-Ecological zones (AEZ), as seen in Figure 3.1, include medium potential to low potential zones. AEZ combine Agroclimatic zones with other factors such as soils, landforms, land use to evaluate potential for agricultural production.
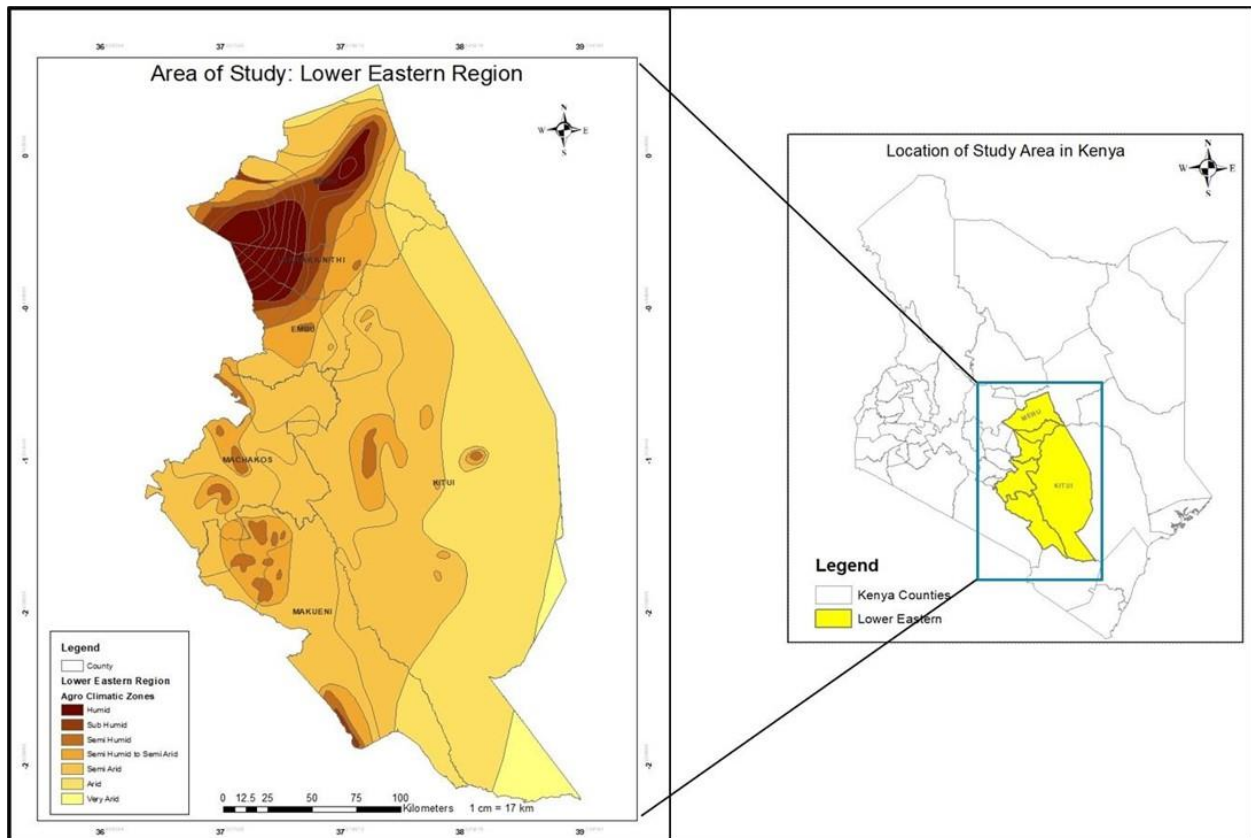
Figure 3.1 The study area and the agro-ecological zones as previously mapped by FAO.

The area of study is represented by humid to arid agroclimatic zones which translate to zone I to zone VI. Possible crop and cropping systems viable in the area include agriculture and livestock production as described in Figure 3.1.

The counties in study area, are represented by humid to arid agroclimatic zones which translate to zone I to zone VI (Table 3.1); where the category of farmers is dependent on rainfed agriculture for livelihood, with diversity in cropping and livestock production. The crops grown in these areas are food crops such as maize, beans, green grams, pigeon peas, sorghum, millet; cash crops such miraa cotton, and tobacco; and fruit trees such as bananas, avocadoes, oranges, mangoes, macadamia,

34

papaws. The farm management handbook describes the cropping patterns as ranging from uncertain, noticeably short and short cropping seasons (Jaetzold et al. 1983)

Table 3.1 The FAO definition of Kenya's agro-ecological zones (Source: Jaetzold, et al. 1983)

AEZ no.	Ratio of Rainfall to PET	Agro-Ecological Zone	Crops and cropping systems
0	> 1.20	Per humid	Forest zone
i	0.80-1.20	Humid	Tea-dairy
ii	0.65-0.79	Sub humid	Wheat, maize, beans, Irish potatoes
iii	0.50-0.64	Semi humid	Beans and other pulses, maize, wheat, cotton, cassava
Iv	0.40-0.49	Transitional	Barley, cotton, maize, groundnut, sorghum
V	0.24-0.39	Semi-arid	Livestock, beans, pigeon peas, sweet potatoes, sorghum, millet
Vi	0.10-0.24	Arid	Ranching and cropping only under irrigation
vii	< 0.10	Per arid	rangeland

The typical precipitation as well as temperature in Tharaka Nithi, Meru, Makueni, Kitui, and Machakos lowland midland areas spans between 0 to 1400mm with definite variations in the length of the rainfall during the short and long rains as shown in Figure 3.2.
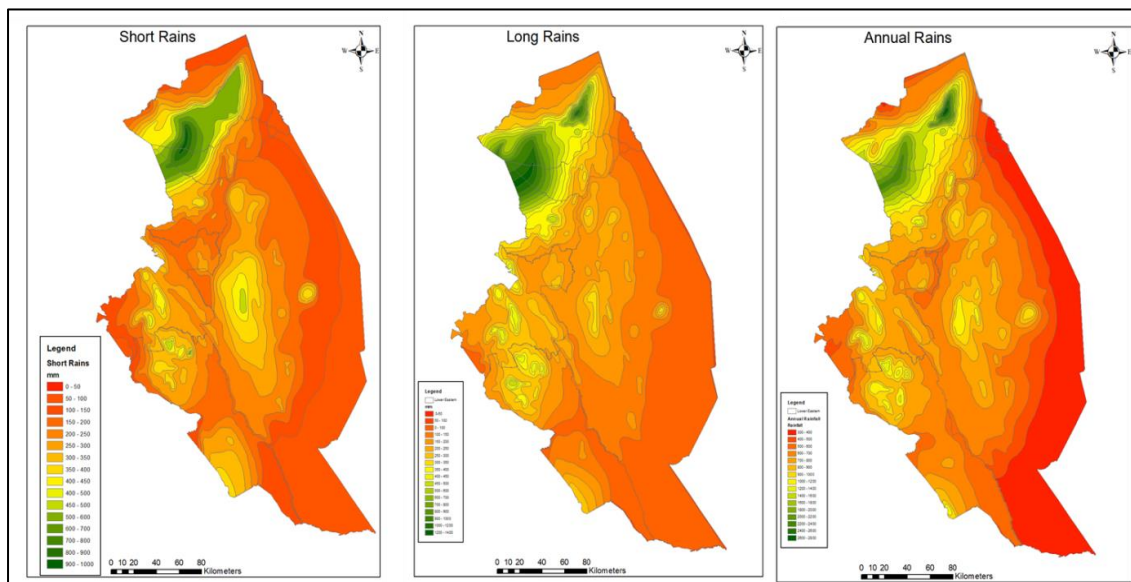
Figure 3.2 Seasonal and annual rainfall variation in the study area

3.3 Selection of methodology

The selection of methodology in this research was carefully considered, with a focus on enhancing the existing FAO framework for defining Agro-Ecological Zones (AEZs) in Kenya. Given the critical role

of AEZ definitions in informing governmental decisions related to agriculture, such as crop insurance and adaptation recommendations, adherence to established guidelines was paramount. The reliance of the Government of Kenya, particularly the Ministry of Agriculture, Livestock, Fisheries, and Cooperatives (MOALFC), on AEZ definitions from the farm management handbook underscores the significance of this research's methodology.

By adhering to the FAO methodology, this research ensures comparability with past data, maintaining consistency in AEZ definitions over time. However, recognizing the need for improvement in the quality and scale of mapped outputs, adjustments were made to incorporate more spatially and temporally detailed datasets. This refinement allows for the integration of satellite-derived data and cloud computing techniques, enabling the utilization of more continuous and comprehensive spatial information.

The value addition from using satellites and cloud computing is substantial. Satellite imagery provides a wealth of information on land cover, vegetation health, and climatic variables, allowing for a more nuanced understanding of agricultural landscapes. Cloud computing facilitates the processing and analysis of large volumes of satellite data, enabling the generation of high-resolution maps and models. By leveraging these technologies, this research produced more localized and accurate AEZ maps. These refined maps hold immense potential in informing agricultural advisories and investments, thereby benefiting Kenyan farmers and decision-makers. The incorporation of spatially continuous datasets enhanced the precision of AEZ delineations, enabling more targeted interventions and resilience-building measures. Moreover, the research aligns with broader initiatives such as the Kenya Climate Smart Agriculture Program, which seeks to strengthen capacities for adopting effective climate adaptation mechanisms

3.4 Data selection

3.5 Baseline assessment data

The research leveraged on existing earth observation data which allowed for assessment of spatial variation in the parameters. While station data is usually ideal, especially for climate parameters, the distance between stations introduces challenges especially when interpolating. For replicability and scalability, freely available datasets matching the required spatial temporal scales for localizing the assessments were selected. The selection criteria required daily data, covering the evaluation period of 1990-2020, and with a resolution of 5km or less. Weather station data for precipitation and temperature was acquired from the Kenya Meteorological Department (KMD). The datasets used in the baseline assessment are listed in Table 3.2.

Table 3.2 Baseline data sources and their properties (1990-2020)

Category	Dataset	Frequency	Source	Scale	Time
Climatology	Rainfall (Precipitation) - PPT	Daily	Climate Hazards Infrared Precipitation with stations (CHIRPS)	5km	1990 - 2020
	Temperature - TMP	Daily	European Center for Medium-Range Weather Forecasts (ECMWF) Re-Analysis (ERA)	2km	1990 - 2020
	Potential Evapotranspiration (PET)	Daily	Computed	5km	1990 - 2020
	Moisture Index	Daily	Computed	5km	1990 - 2020
	Aridity Index	Daily	Computed	5km	1990 - 2020
Station Data	Rainfall, Temp, PET	Daily	KMD	Stations	1990 - 2020
Biophysical	Soil		KENSOTER database ver. 2.0		Static layer
	Slope		SRTM (Shuttle Radar Topography Mission)	90 m	2020
	Land Productivity	8-day	MOD13A2 NDVI (Normalized Difference Vegetation Index)		1990 - 2020

3.6 Future projections assessments data

The Climatic Research Unit (CRU) station derived gridded data (CRU time series 3.24.01), is available at 0.5 degrees from 1901-2015, was used to downscale the CIMP5 data that was gotten from RCMRD. For this study, RCP 4.5 and RCP 8.5 were used. From the downscaling, it was noted that the GCM performs better over Eastern Kenya as compared to Western Kenya hence making it a suitable choice for this research. Kenya's rainfall is bimodal, with two distinct wet seasons that support most of the rainfed agriculture production (Antony, 2017; RCMRD, 2018; Vrieling et al., 2013). Table 3.3 provides a list of all datasets used or derived for the future projections .

Table 3.3 Projected data sources and their properties (2020-2040)

Category	Dataset	Frequency	Source	Scale	Temporal resolution used
Downscaled Climate Projections	Precipitation	Daily	RCMRD improved CIMP5	5km	2040- RCP 4.5 & 8.5
	Temperature-TMP	Daily	RCMRD improved CIMP5	5km	2040- RCP 4.5 & 8.5
Climate Parameters	Potential Evapotranspiration (PET)	Daily	Computed	5Km	2040- RCP 4.5 & 8.5
	Moisture Index	Daily	Computed	1km	2040- RCP 4.5 & 8.5
	Aridity Index	Daily	Computed	1km	2040- RCP 4.5 & 8.5
Biophysical Parameters	Soil		KENSOTER database ver. 2.0		Static layer
	Slope		SRTM (Shuttle Radar Topography Mission)	90m	2020

4 METHODOLOGY

This study employed a stock taking approach that seeks to develop an agro-specific climatic baseline, investigated the implications of continuing trends and linked this to future projected climate trends under different mitigation strategies (Table 4.1). This was in in response to identified climate and agriculture adaptation gaps.

Table 4.1 Outline of Methodology

Objectives	Research question	Methods	Output
Assessed past and present AEZ based on biophysical and climatic factors and evaluate hotspots (of significant change)	How climate variability and change affected AEZ in the lower Eastern Region?	Adjusted FAO methodology for mapping baseline time Agro-Ecological zones, but utilizing scalable satellite datasets	Maps and graphs that show the variations in climate, length of growing period and agro-ecological zones and the hotspots is the study area
	What was the interpretation of these changes on agriculture?	An analysis of the results and interpretation of impact of observed changes on agriculture	A description of the visible impacts in the identified hotspots
Evaluated implications of observed changes in predicted future climate and AEZ on agriculture in the lower eastern region and identified opportunities for adaptation.	What opportunities did these changes present in improving adaptation in the region's agricultural production systems?	Adjusted FAO methodology utilizing climate predictions in 2040 and other scalable satellite datasets, to map the change in agro-ecological zones and length of growing period.	Maps and graphs showing change from baseline to the future climate and agro-ecological zones in the study area.

4.1 Mapping the past and present Agro-Ecological Zones

An adjusted methodology for Agro-Ecological Zones mapping was adopted from the FAO (Food and Agriculture Organization) farm management handbook development guidelines (Jaetzold *et.al.* 1983). The FAO methodology was used to define the inputs to the AEZ mapping, with adjustments focusing on including satellite indices as proxies for parameters that were unavailable. For example, Dry Matter Productivity (DMP) was used to define land productivity.

Climate parameters were all derived by blending daily satellite estimates with station data to improve spatial quality in the region. Further, indicators such as Aridity index were used to define climatic constraints. With research demonstrating that AI is a better indicator for monitoring increasing aridity than direct climate assessments such as those relying on rainfall, in at least half of the total land area with considerable change, aridity index (AI) provides a good depiction of the multifaceted nature of estimated aridity changes (Greve et al., 2019) .

Potential Evapotranspiration was also derived using *Thornthwaite's* equation due to unavailability of a continuous PET dataset for the assessment period. FAO uses the *Penman Monteith* equation which required inputs such as solar radiation which even when available, are too coarse to provide daily input for estimating PET for the assessment area.

Statistical assessment was conducted on inputs such as rainfall and temperature. Evaluation of change was done using statistical tests such as regression, correlation tests, coefficient of variation and pair plots. Coefficient of variation (CV) was used to explain the change between the two evaluation periods. CV provides an understanding of the intensity of the change in variables. The greater the coefficient of variation, the greater the degree of dispersion around the mean. It is generally expressed as a percentage. The full implementation of the adjusted methodology is shown in Figure 4.1.
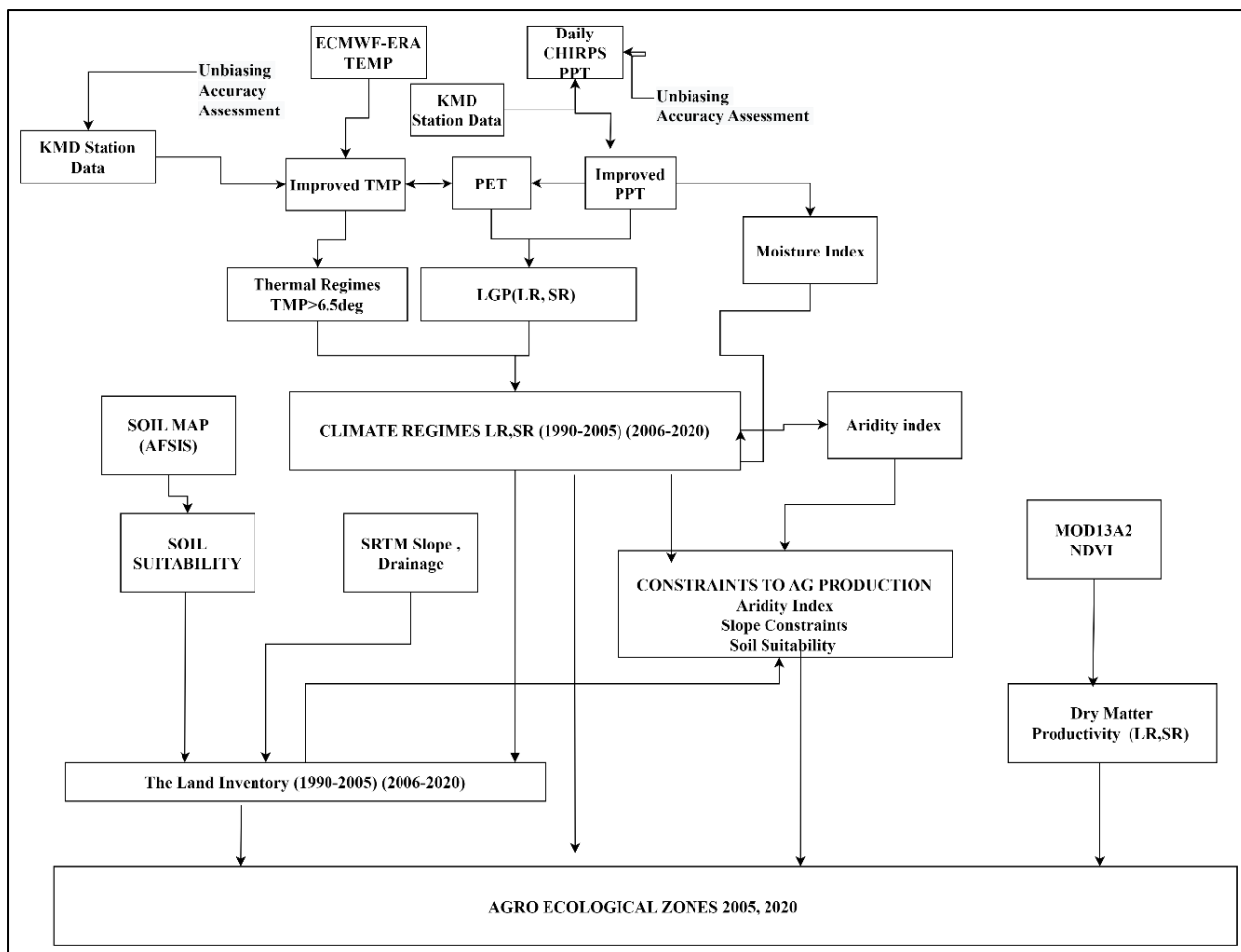
Figure 4.1 Implementation workflow for mapping Agro-Ecological Zones

4.2   Mapping future Agro-Ecologies

A similar adaptation of the FAO methodology was used to map future Agro-Ecologies (see Figure 4.2). However, Climate projections were adopted, and baseline biophysical characteristics layers adopted, under the assumption that change in landforms happens slowly over time.
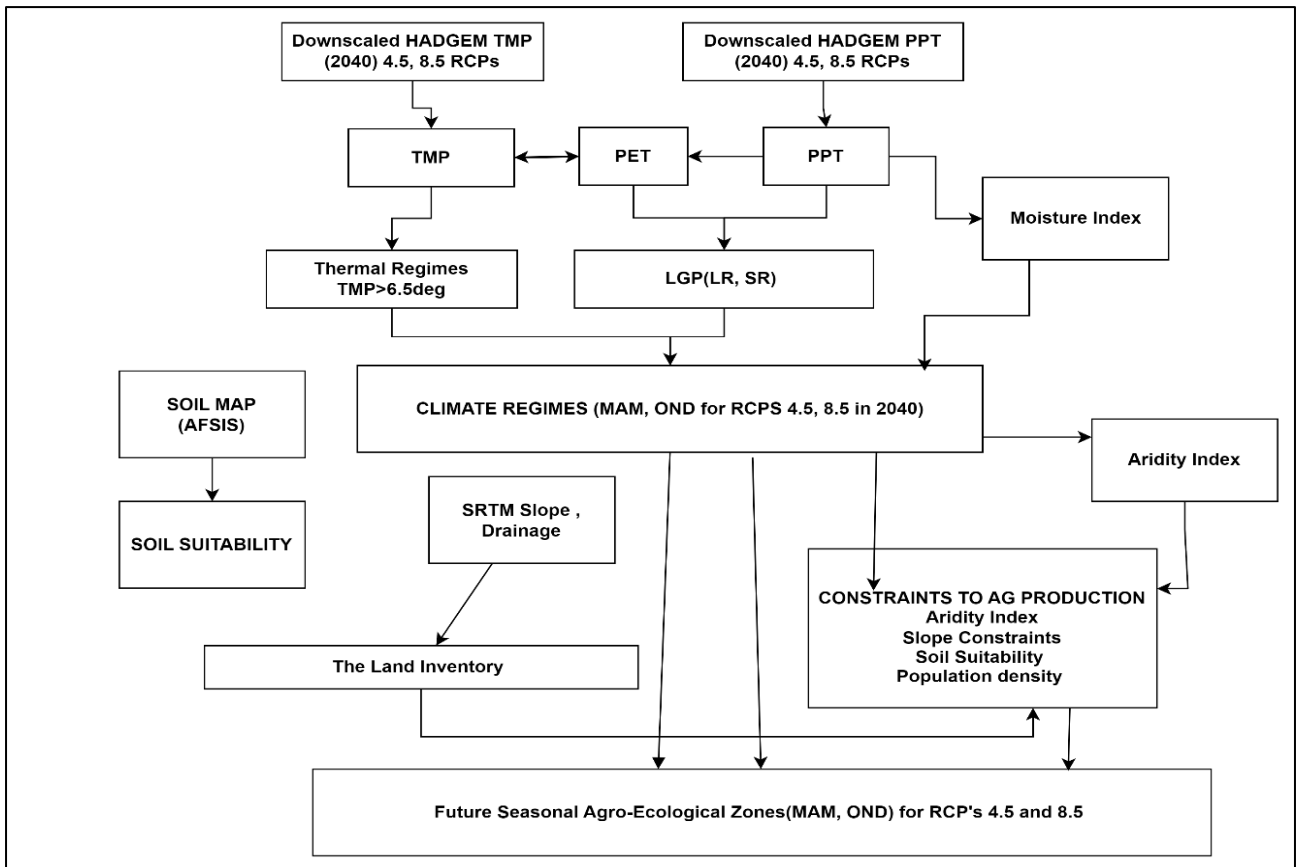
Figure 4.2 Methodology for mapping future Agro-Ecological Zones

4.2.1   Determining seasonality

Kenya's rainfall is bimodal, with two distinct wet seasons that support most of the rainfed agriculture production (Antony, 2017; RCMRD, 2018). The Long Rains (LR), which occur in March, April, and May (MAM), and the Short Rains (SR), which occur in October, November, and December (OND), are used to define the seasons. The seasons are defined as the Long Rains(LR) that are experienced from March, April and May (MAM) and the Short Rains (SR) that come from October November and December (OND)(Kazembe & Kenya, 2014). The defined seasonality has been adopted for this research. To capture the microvariations, all layers were acquired at a scale of 1km or less where possible and resampled to the same scale, but the use of satellite derived information provides more variation in information per pixel. Further the use of the most recent data provided value addition in recency of the outputs. Resampling data to a uniform resolution is a common practice in research, particularly when working with mixed datasets containing continuous and non-continuous data . While

it doesn't inherently improve data quality, it facilitates smoother computations and enables direct comparisons across different data layers. This is because analyses often rely on spatial alignment and overlapping regions, and a consistent resolution ensures all data points contribute equally, simplifying calculations and interpretation of results (Manzi & Gweyi-onyango, 2020).

4.2.2 Identifying distinct zones

The greatest challenge in identifying distinct AEZs, is the uncertainty in delineating the boundaries between two consecutive zones, especially when continuous and categorical variables are used. Researchers have employed different approaches when using satellite data such as wavelet analysis, geographic clustering, fuzzy theory, and multivariate clustering, although there is no single method that has been deemed best (Boitt et al., 2016; Ojwang et al., 2010; Praseyto et al., 2013; Quiroz et al., 2000; Sharma et al., 2007). Fuzzy logic is a process of grouping the analysed indicator established in form of membership function. The membership function is a curve demonstrating the mapping of data input points into the membership value.

Fuzzy logic was used in normalizing both continuous and categorical variables with direct and inverse relationships applied to inform the derivation of the AEZs. Linear normal relationship fuzzification process transforms the data normally with a normal scale, where the large values have high prominence, and they are transformed to approximate value of 1. Small membership function gives the small value prominence so that their contribution is accounted for in the AEZ generation. Fuzzy logic was chosen due to its ability to handle data uncertainties and remove excessive "noise" in the final maps as seen in Figure 4.3.
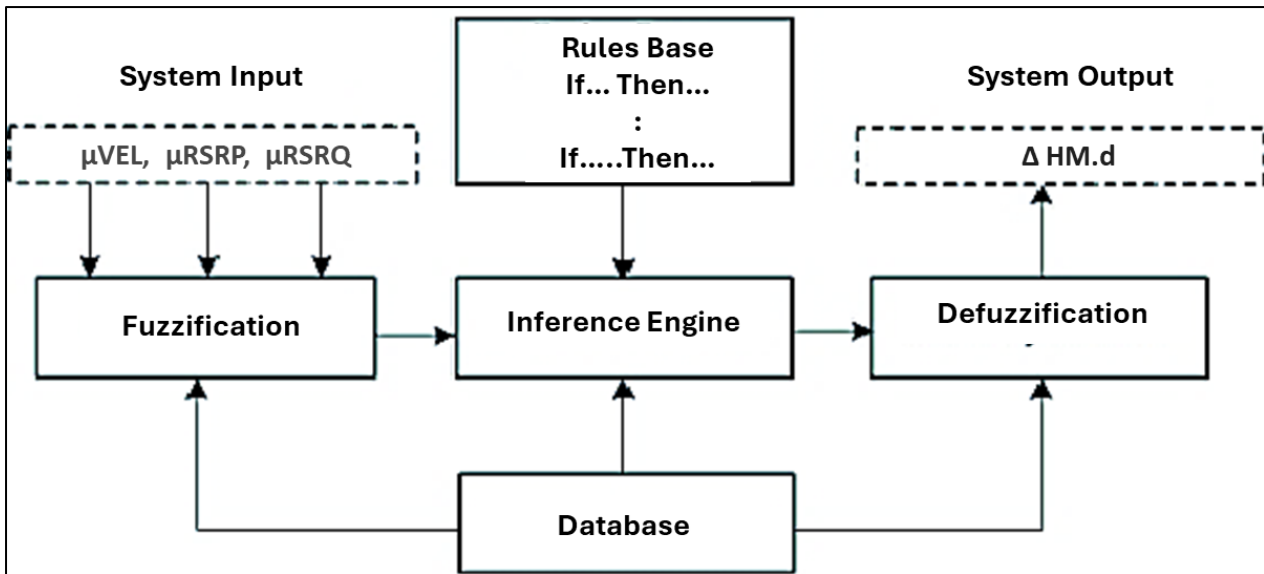
Figure 4.3 Implementation of Fuzzy logic

4.3 Data collection

4.3.1 Strategy for sampling and definition of sample size

A multistage sampling process that blended stratified random sampling with purposeful sampling was used. In the preliminary stage, consideration of research gaps informed the choice of the subject area. There was emphasis on extending agricultural production and research beyond the main food basket areas, as well as the need to select a representative area with the diversity in agro ecologies led to the selection of the six eastern counties (Embu, Meru, Tharaka Nithi, Machakos, Kitui and Makueni). The counties represent the seven agro-ecological zones in Kenya.

The next step in sampling involved an assessment of the micro-climatic variations and homogeneity. Using Multi-Criteria Dimension Analysis (MCDA) function in R, the rainfall and temperature data and derivatives were used to generate a climate homogeneity map as shown in Figure 4.4. MCDA was selected due to its capacity to map relationships through proximity analysis and derive homogenous zones. From the map, areas representing unique and mixed micro-climates were identified and used to select 17 wards (Meru county - Antubetwe-Kiongo, Akachiu and Nyaki east; Embu county - Nthawa and Muminji wards; Tharaka Nithi county - Mwimbi and Igambangombe; Makueni - Kiimakiu-

Kalanzoni, Kiteta-Kisau and Muvau-Kikumini; Machakos - Matungulu North and Upper Kaewa-Iveti;

Kitui - Tseikuru, Mumoni, Mutongoni, Mulango and Mutha). Within these selected wards, further

stratification was done by overlaying agricultural areas. From the agricultural areas, sampling points

were derived.
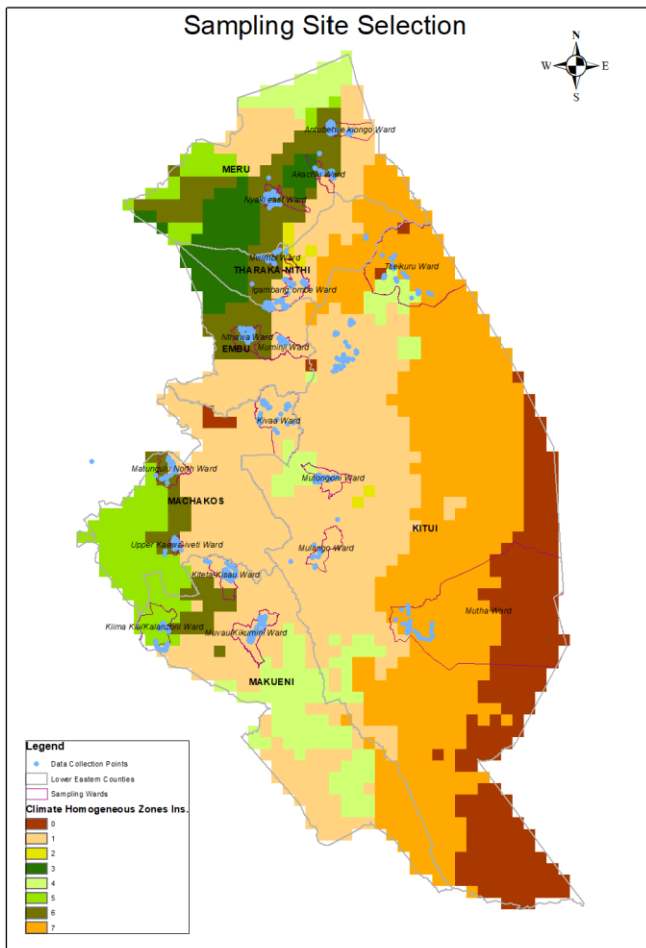
Figure 4.4 Sampling site selection based on climate homogeneity and variability.

A limited population (p) was used to generate the representative sample, which was then calculated

using a 99% confidence level and a 5% degree of variability in Equation 4.1 below.

$$n' = \frac{n}{1 + \dfrac{z^2 \times p(1-p)}{\varepsilon^2 N}}$$

Equation 4.1 Calculating the representative sample.

Calculations based on a finite population sample n, where z defines the z score, ε defines the error

margin, N represents the size of the population and p the proportion of the population. The population

proportion was represented by the total farming households in the lower eastern region identified from the Kenya National Bureau of Statistics 2019 Census ((KNBS, 2019)). Using N = 1,042,046, ε = 5%, confidence level = 99% and p = 50% and the standard z-score for the selected confidence level = 2.58 the study arrived at a 666 representative farming households sample size.

To assist data collectors in navigating to the nearest farming household based on the sampling location, maps were generated using google maps overlays with landmarks added and each sub-location split into detailed maps associated with the landmarks as shown in Figure 4.5.
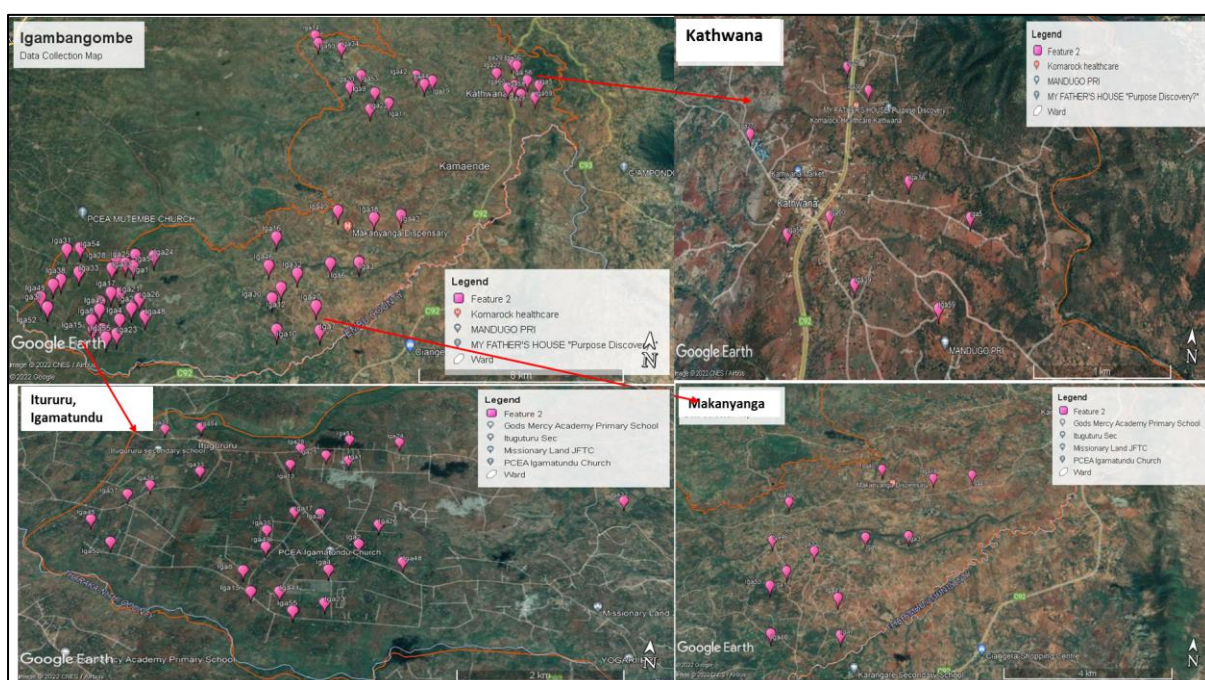
Figure 4.5 Google maps for navigation for Igamba-Ngombe ward in Tharaka Nithi county

4.3.2   Data collection tools

The questionnaire for data collection (see Appendix A1) was designed to collect data on the population, their demographics, as well as perceptions and understanding of climate change, access to information and resources, their coping and adaptation mechanisms, sensitivities that negatively impact their capacity to produce, gendered capacities to decision making, and their priorities. The questionnaire was created and coded into Kobo toolbox with functionality for data collection on web and mobile developed. All automation and hard coding in the fields was done to optimize the quality of data

collected. Once the tool was evaluated, accounts for data collectors were created ahead of the field training. The kobo toolbox mobile application called Kobo Collect was used during the training of 17 data collectors, identified through the county extension officers and KCSAP county offices. After the training and testing of the tool, the questionnaire and form were improved, and the final version was used to collect the data. Slight variations in locations of data collection were made due to accessibility issues and all collected data points are indicated in Figure 4.6.
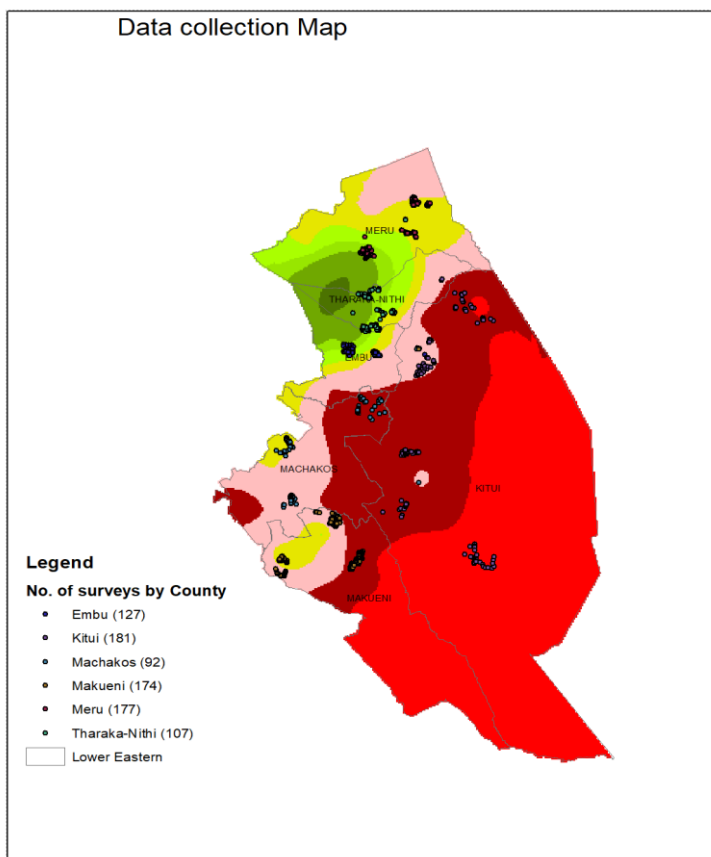
Figure 4.6 Valid questionnaires by county

After data cleaning, a total of 860 samples were used in the analysis spread across the area of study as shown in Figure 4.5. The full questionnaire as used on Kobo Toolbox is available as Appendix A1.

4.4 Data processing

4.4.1 Tools

With its free cloud-based computing capabilities for geospatial data analysis and access to most of the publicly accessible, multi-temporal Remote Sensing (RS) data, Google Earth Engine (GEE) offers a

scalable, cloud-based geospatial retrieval and processing platform. Artificial intelligence is a significant enabler for automating RS imagery interpretation, especially with object-based domains, hence integrating AI techniques into GEE is one way to operationalize automated RS-based monitoring systems (Yang et al., 2022).Other tools such as R-Statistics provide open-source, freely available libraries that ease spatial and statistical data exploration and visualization, with a recent increase in geospatial data manipulation tools (Minegishi et al., 2020). The codes are available under Appendix 2A.

4.5   Developing historical baselines
4.5.1   Rainfall

The CHIRPS dataset has been widely calibrated in Africa with demonstrated skill for estimating rainfall with higher temporal and spatial accuracies especially over East Africa(Gleixner et al., 2020; Muthoni et al., 2019; Shukla et al., 2021). To assess the quality of the sensor (satellite) data, pair plots in R statistics using a combined sensor-station stack, were derived across the epochs and seasons (MAM and OND). Pair plots helps to visualize the distribution of single variables and relationships between two variables.

Pearson's correlation was used to give an indication of the measure of the relationship between sensor and station data, with values closer to one representing strong positive correlation. CHIRPS and station rainfall data showed good correlation across MAM and OND in the two epochs (1990-2005, and 2006-2020) at **0.87, except during the 2006-2020 OND where the correlation was **0.55. However, across the two epochs, station data was used to unbias the sensor (satellite) estimates to improve the quality of input as shown in Figure 4.7.
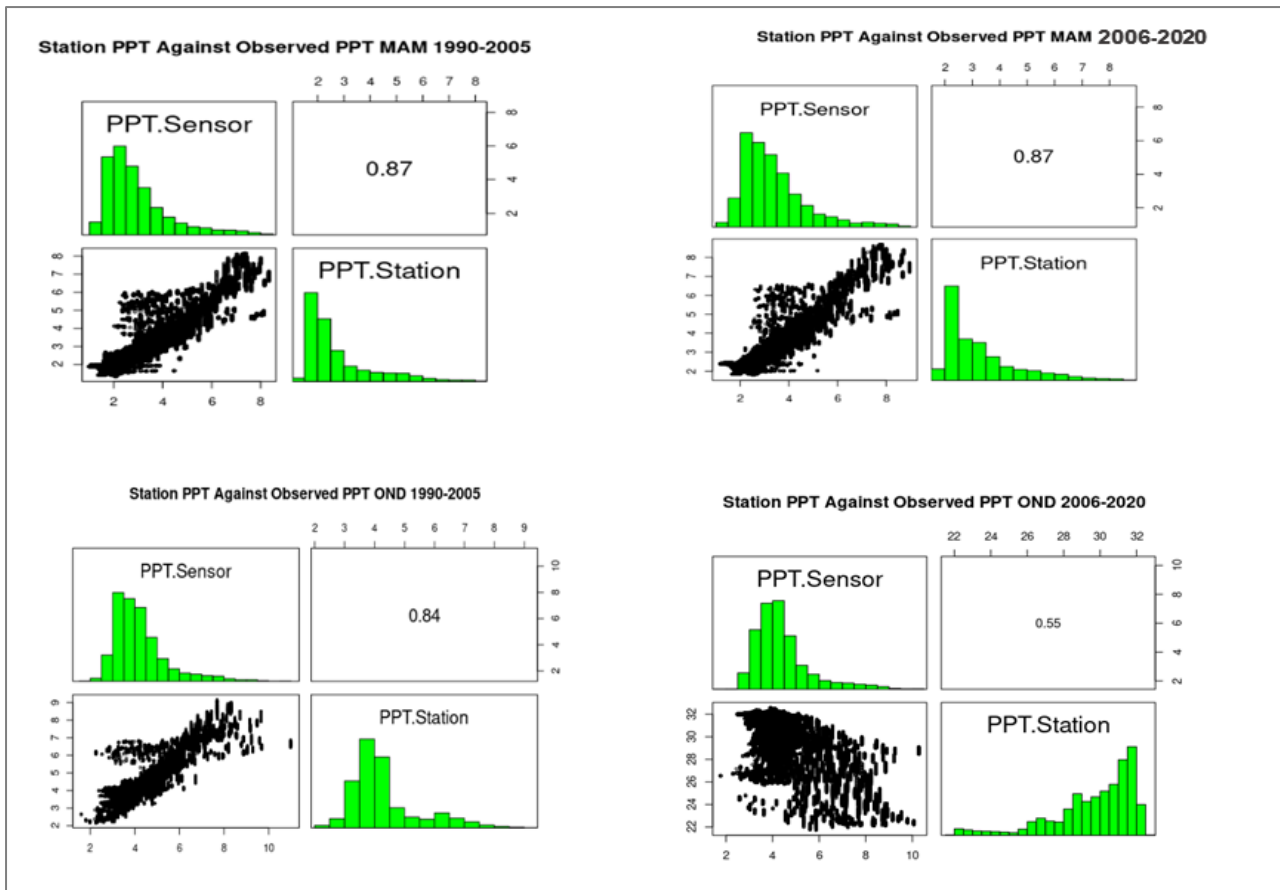
Figure 4.7 Assessing Precipitation correlation between Station and Sensor (CHIRPS) blended data across MAM and OND

4.5.2 Temperature

Despite the increasing availability of stations improved satellites dataset, there is a gap in daily temperature datasets that overlooks their role in land surface interactions. Reanalysis products provide complete and coherent climate datasets to get over these data limits, generating the best estimates of climate data without geographical or temporal gaps. This is done by combining forecast model estimates with observations through data assimilation. However, there are significant regional, variable, and terrain-specific variations in the reanalysis data's accuracy (Gleixner et al., 2020). The European Centre for Medium-Range Weather Forecasts (ECMWF) Re-Analysis (ERA) component provides continuous daily 2m land surface temperature. The land surface temperature from ECMWF-ERA, was regressed against weather station temperature data. In preparing the data for regression, the two datasets were merged into an equal length data frame, and ERA data transformed from Kelvin to

Celsius. Station and sensor data compared well with a positive correlation of approx. **0.87 across

the epochs and seasons. Station data was used to unbias the sensor data (see Figure 4.8).
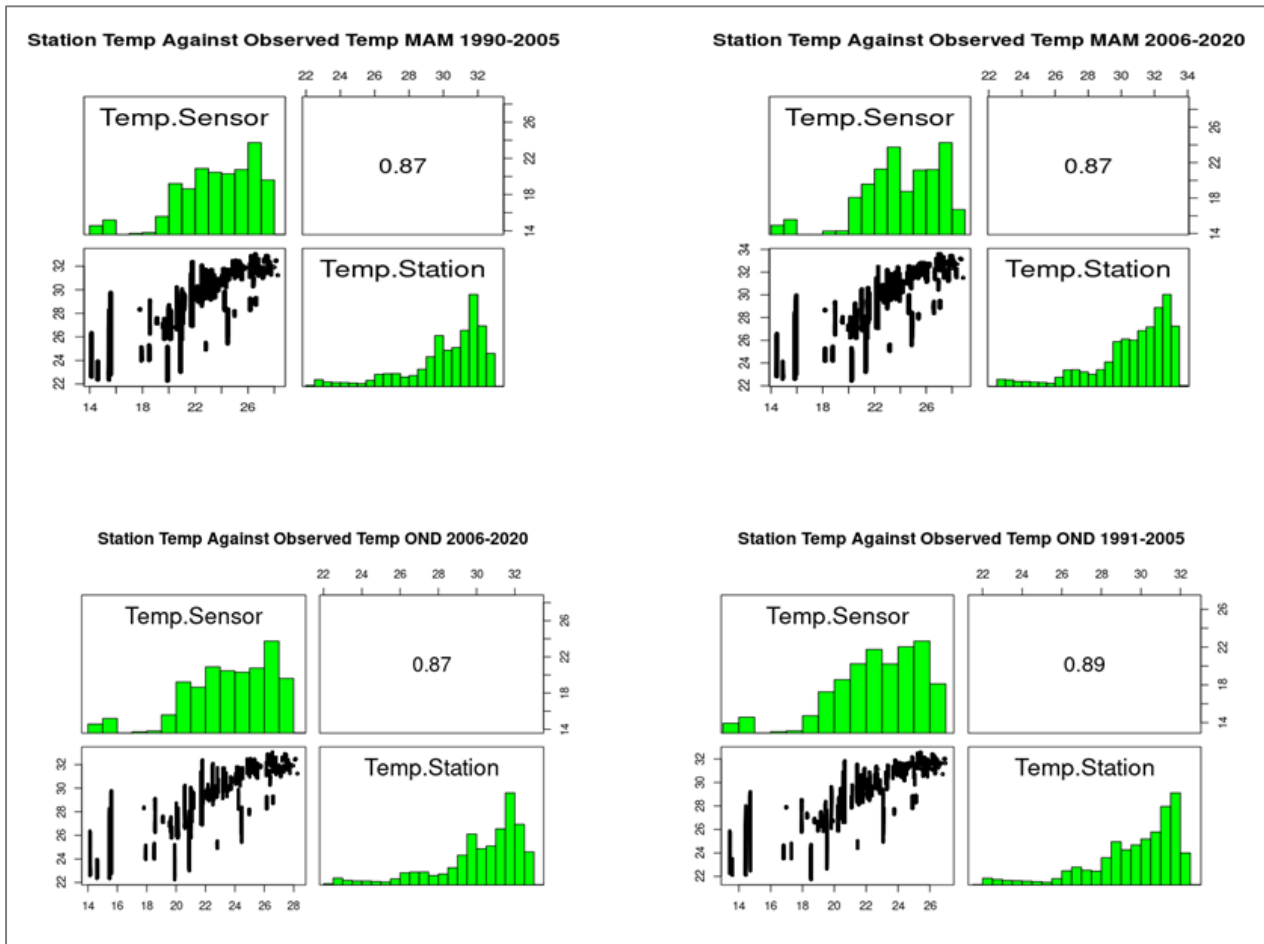
Figure 4.8 Assessing Temperature correlation between Station and Sensor (ERA) blended data across MAM and OND

Given the quality of temperature data and the localized study area size, a further test was done using

Pearson's coefficient to derive line of best fit and a heatmap was produced across temporal scales. The

NumPy python library's statistics package np.corrcoef, that return a matrix of Pearson correlation

coefficients was used. The satellite and sensor data had an r value of **0.78 in sampled stations

demonstrating a strong relationship in the estimates and providing value in the use of the ERA

temperature data for this research. Sample outputs from Machakos are depicted (Figure 4.9).
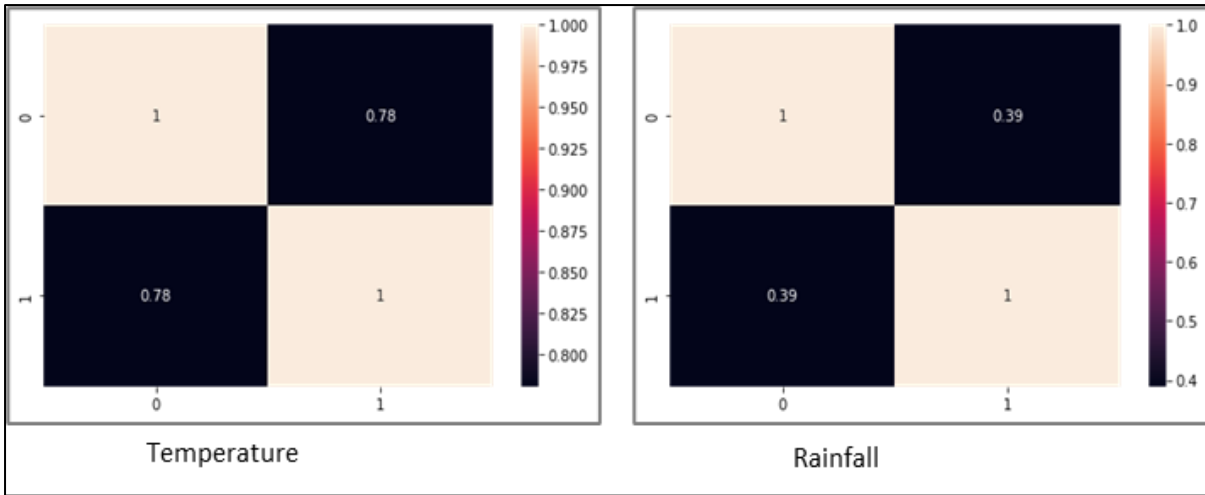
Figure 4.9 Demonstrating Pearson's correlation between ERA satellite and station temperature data and rainfall for Machakos County using box plots.

4.5.3 Uncertainty management in precipitation and temperature data

To unbias station versus sensor (satellite) temperature and precipitation data, we employed several techniques. Firstly, we utilized calibration to address systematic biases originating from consistent errors within instruments or data processing. This involved comparing station data with reliable satellite data or well-maintained reference stations, allowing us to adjust the station data to a known standard and reduce systematic offsets, thus ensuring a more accurate representation of climatic conditions. Additionally, data homogenization was employed to account for non-climatic factors affecting station data, such as instrument changes or land-use modifications. Through statistical analysis, historical data was adjusted to reconcile these changes and maintain consistency with current data, effectively isolating the true climatic signal.

In terms of outlier removal, we implemented thresholding with historical averages and the interquartile range (IQR) method. Thresholding with historical averages involved setting thresholds based on deviations from historical averages to identify potential outliers, while the IQR method identified outliers based on deviations from the median within the interquartile range. This method offers a more robust approach to outlier identification. The IQR represents the spread of data between the 25th and 75th percentiles, capturing the central portion of the data distribution. Points falling outside 1.5 times the IQR from the median are considered potential outliers. This method is less sensitive to the influence

51

of extreme values within the data compared to simple thresholding. The IQR was sufficient since the data was already thresholded with historical averages hence the data wasn't skewed as also demonstrated in (Liu et al., 2018).

Outlier removal was prioritized before unbiasing to ensure that the unbiasing process did not inadvertently introduce further uncertainties by adjusting for biases based on potentially erroneous outliers. By removing outliers first, we created a cleaner dataset for subsequent unbiasing steps, improving the quality of the final temperature and precipitation data. By combining these techniques, we effectively addressed both bias and outliers in station and satellite data, resulting in a more accurate and reliable representation of climatic conditions for our analysis. Plots of station and sensor data after removal of outliers visible in previous assessments and unbiasing, are shown in Figure 4.10.
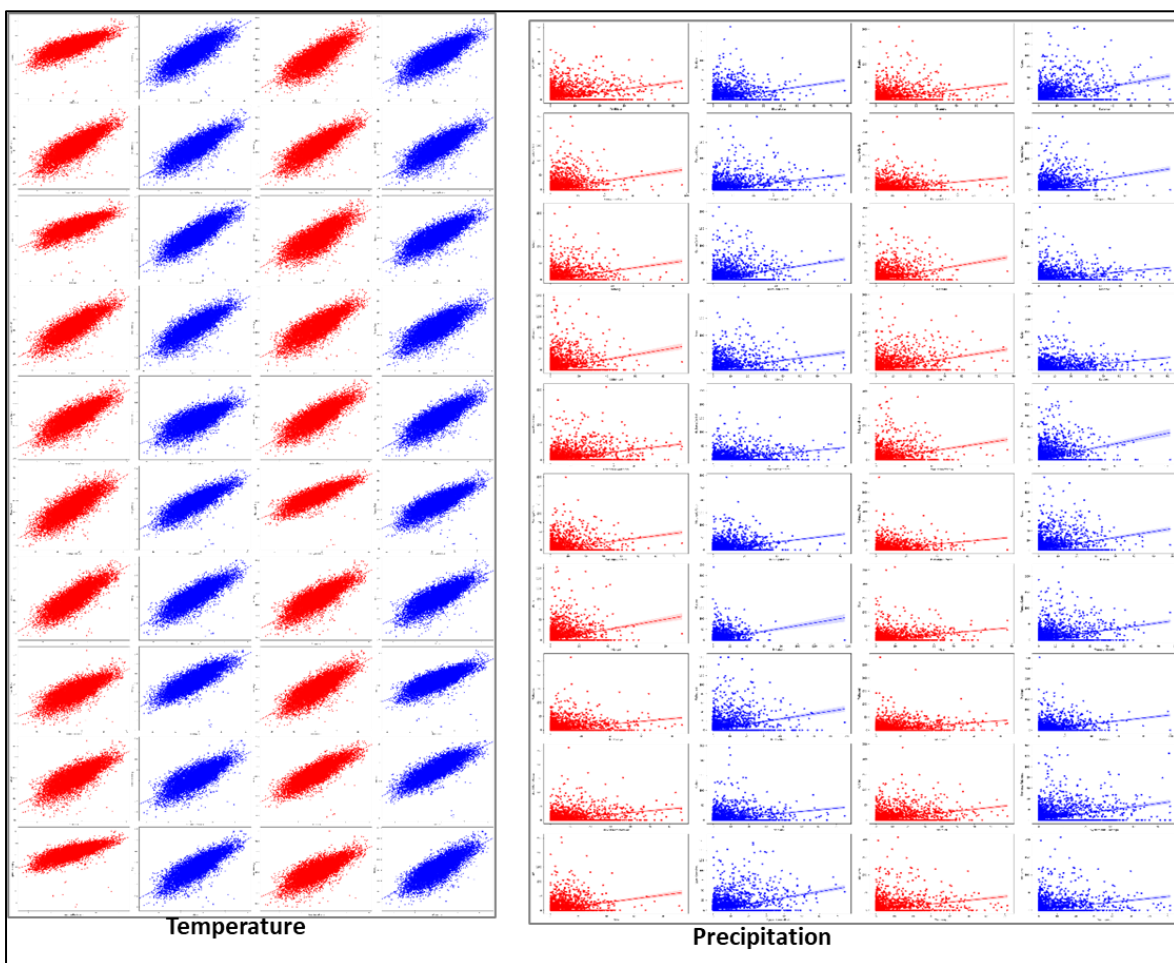
Figure 4.10 Station-Sensor graphs across weather stations in Machakos for Temperature and Precipitation

4.5.4 Potential Evapotranspiration (PET)

PET was computed from the improved rainfall and precipitation. While the Penman-Monteith equation is mostly used to compute PET, it requires many inputs including solar radiation which was not available. A popular empirical technique for calculating potential evapotranspiration is the Thornthwaite (1948) equation (PET). The only quantities required are the average monthly air temperature and the average daily daylight hours for each month, which can both be calculated from latitude (Patel, 2007). PET is normally expressed millimetres (mm) per unit time (see Equation 4.2).

$$PET = 16(\frac{L}{N})(\frac{N}{30})(\frac{10Td}{N})^{\propto}$$

Equation 4.2 Computing Potential Evapotranspiration using Thornthwaite equation.

The potential Evapotranspiration, PET is estimated in mm/month, with the daily average represented by Td, days in the month represented by N, L length of day average and $\propto= (6.75x10^{-7})I^3 - (7.71 - 10^{-5})I^2 + (1.792x10^{-2})I + 0.49239$ is the heat index which depends on T_{mi} which represents the 12 monthly average temperatures.

4.5.5 Length of the Growing Period (LGP)

LGP is a crucial statistic in determining the agricultural potential and subsequent zonation since it shows days with the right precipitation, temperature, and soil moisture for growing crops (Kabubo-Mariara *et al.*, 2015; Seo, 2014; Vrieling *et al.,* 2013). LGP is defined as the time of year when precipitation + soil moisture exceeds 50% of the PET and average temperatures are greater than or equal to 5oC. (Refer to Equation 4.3). A normal growth phase that satisfies the complete evapotranspiration needs of crops and refills the moisture requirements of the soil characteristics is defined by an excess of precipitation over PET. Utilizing historical rainfall data to assess LGP for

specific years allows for estimation of risk and potential output under average climatic circumstances while also accounting for inter-annual changes and the resulting adaptability of land (FAO, 1996) .

$$LGP = (P > 0.5PET)$$

Equation 4.3 Computing the length of growing period.

4.5.6   Moisture Index

The moisture regimes are particularly helpful in recording the cyclical oscillations of effective moisture and are used to denote moist or dry climates (Patel, 2007).The improved moisture index of Thornwaite and Mather's (1955) methodology, was derived using annual rainfall and potential evapotranspiration, using the previously computed PET and unbiased rainfall as inputs. (See Equation 4.4).

$$MI = [(P - PET)/PET] * 100$$

Equation 4.4 Calculating Moisture Regimes

Where MI defines the Moisture Index

P is the Rainfall (mm)

PET represents the Potential Evapotranspiration in mm.

4.5.7   Slope and drainage constraints

The Shuttle Radar Mission Topography elevation (SRTM) corrected to remove voids was used to derive slopes which were used and classified into the following categories. 0–2%, 2–5%, 5–8%, 8–16%, 16–30%, 30–45% and >45%. Constraints for agricultural production due to slope were defined as follows: <8% no constraint, 9-15% slight constraint,16-30% moderately constrained, >30% severely constrained according to the Agro-Ecological zonation guidelines (FAO, 1996).

4.5.8   NDVI Dry Matter (DM) as a proxy for productivity

Standing green biomass can be accurately estimated using the NDVI (Normalized Difference Vegetation Index), which is a good indication of biomass and vegetation production (Miller et al.,

2019; Ndungu et al., 2019). The National Oceanic and Atmospheric Administration's Advanced Very High-Resolution Radiometer (NOAA-AVHRR) MOD13A2 NDVI is the continuity index to the current NDVI data for the full assessment period. The 16-day imagery of the maximum seasonal MOD13A2 NDVI was used to calculate plant dry matter (DM), or biomass (Aravind, 2006; Patel, 2007). Dry Matter Productivity is also known as Net Primary Productivity and it is used as an indicator of both crops and pasture productivity (Rodigheri *et al.,* 2020). DMP was computed from max NDVI (Equation 4.5) by season for the two epochs.

$$DM = (1.615 * NDVI_{max})^{1.318}$$

Equation 4.5 Computing Dry Matter as a proxy for seasonal biomass.

4.5.9   Soil suitability for agricultural production

The soil maps were downloaded using the Soil and Terrain database for Kenya (KENSOTER) (at a scale of 1:1,000,000), version 2.0, from the International Soil Reference and Information Centre (ISRIC) geo-data hub. According to the FAO criteria on soil suitability in creating AEZ, the soil parameters were evaluated and recoded into eight groups, defining soil suitability from extremely appropriate to unsuitable (Batjes & Gicheru, 2004).

4.5.10 Predicting the future

The future predictions applied similar computations as the baseline but utilizing the downscaled climate projections and identified baseline biophysical characteristics.

The acquired daily rainfall (precipitation) and average temperature data was processed for the 2040 climate predictions for the RCP's 4.5 and 8.5 representing the intermediate scenario and the dire scenarios of climate change, respectively. While climate projections are available up to year 2100, the goal of this thesis was to understand the near future changes in climate that are important to inform structuring of climate adaptation and mitigation priorities and investments. RCP 4.5 represents future scenarios where climate policies have reducing effect on the severity of climate change, while 8.5 represents the worst or dire scenarios as seen in Fig. 4.11.
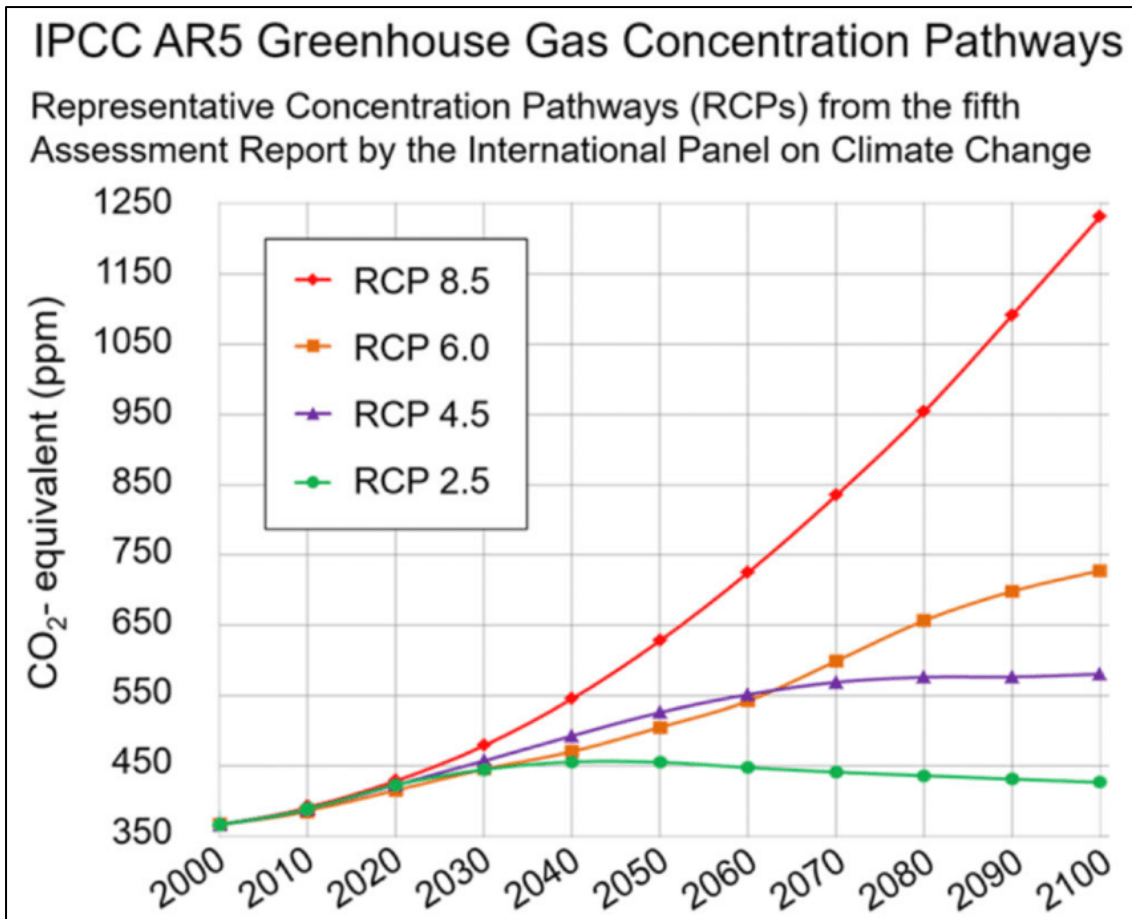
Figure 4.11 The Representative Concentration Pathways

Projected MAM, OND potential evapotranspirations for 2040 RCP 4.5 and 8.5 were derived using the Thornthwaite (1948) equation in R. LGP was derived from the predicted temperature and rainfall for RCPs 4.5 and 8.5 across the two seasons. Moisture Regimes were computed using the predicted rainfall and PET for both RCPS and seasons. Predicted Aridity index was derived from the Terra-Climate database in GEE.

Baseline period biophysical parameters including soil suitability and drainage were used and assumed to remain constant. Soil suitability for agricultural production was categorized from the Kenya Soil Survey (KSS) map and account for soil characteristics including texture and their relationship to supporting agricultural production. The baseline drainage map, which was produced using elevation data from the SRTM (Shuttle Radar Topography Mission), was used to build the soil suitability map (FAO, 1996; Jaetzold *et.al.,*1983).

5   RESULTS AND DISCUSSIONS

5.1   Insights from tracking 30 years of change in AEZ in Kenya's Lower Eastern Region

In this section we focus on responding to the first and second research questions. To provide insights on how climate variability and change affected AEZ in the lower Eastern Region and the interpretation of the changes on agriculture.

5.1.1   Interpreting the maps

The methodology utilized both continuous and categorical variables, requiring fuzzification to create a normalized unit where direction and contribution of values accounts for its influence in the final Agro-Ecological zonation.

5.1.2   Understanding the legends

The fuzzified layers were stretched to a range of 0-1 representing a move from low to higher intensity in the variables.

5.1.3   The Climate inventory

The research evaluated historical change in 30 years at two checkpoints 1990-2005 and 2006-2020 and across the two distinct wet seasons. Kenya's rainfall is bimodal, with rain-fed production supported by the Long Rains (LR) and the Short Rains (SR) (Antony, 2017; RCMRD, 2018). This defined seasonality aligns with the Kenya Meteorology Department (KMD) definitions of growing seasons in Kenya and was adopted for this research since it captures the inter-annual variability in rainfall (Ericksen *et al.,* 2018). To improve the quality of data and capacity to capture micro climatic variations, both station and sensor (satellite) datasets were used to create blended improved seasonal climatologies. The climate inventory was computed by combining normalized rainfall, temperature, PET, LGP and the Moisture index using AND logic and were assigned similar weights. Rainfall was unbiased using stations and the trends across the epochs and by seasons were evaluated using Coefficient of Variation (CV), allowing highlighting of significant change.

While research across East Africa presents diverse climatic projections for various regions (e.g., Adhikari et al., 2015; EroHerr et al., 2010; Knox et al., 2012; Kotir, 2011; Ochieng et al., 2016), a notable consensus emerges for specific areas within Kenya. Several studies consistently predict an increase in rainfall for certain regions. This finding aligns with the observed stabilization of short rains in the ASAL (Arid and Semi-Arid Lands) region (RCMRD, 2018), which often coincides with projections for increased precipitation in these areas. This convergence of evidence from both future projections and observed trends strengthens the likelihood of increased rainfall in specific parts of Kenya.
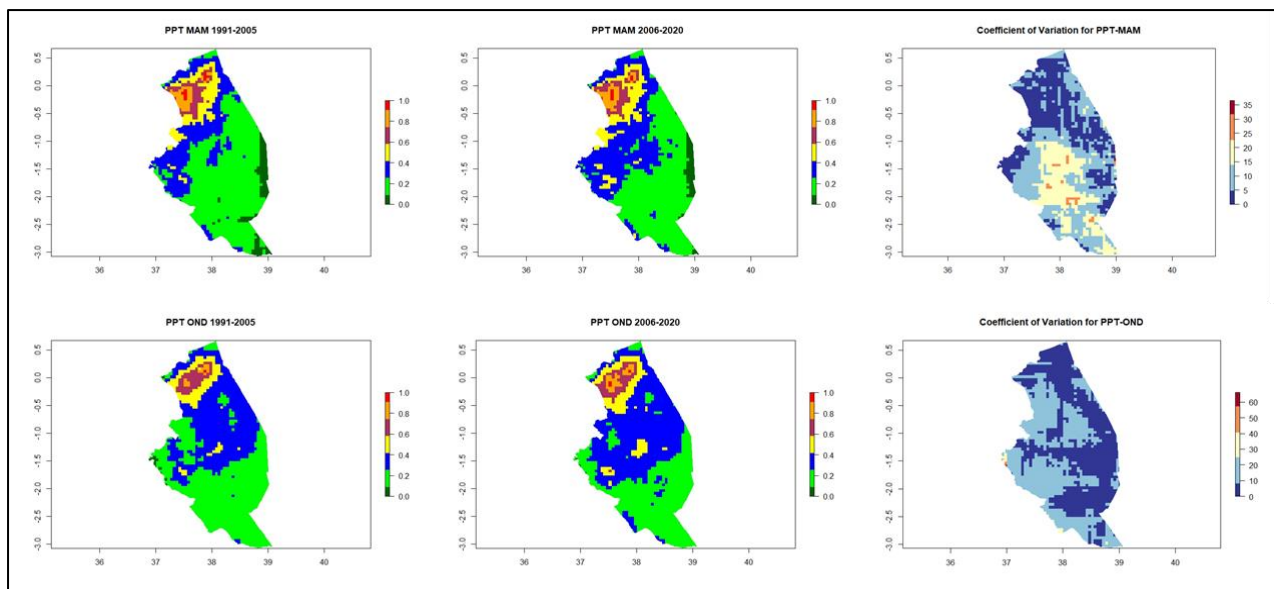
Figure 5.1 Trends in precipitation change for MAM and OND in 1990-2005 and 2006-2020

The maps shown in Figure 5.1 represent the precipitation zones that have been normalized using fuzzy logic with the highest rainfall experienced towards the mountainous regions in Embu, Meru and Tharaka Nithi, and more rainfall received during OND than MAM. The lower eastern regions of Machakos, Kitui and Makueni received the least rainfall during MAM, but with higher amounts during OND which is the main planting season. Some meaningful change was observed during the MAM season, more predominantly across Machakos, Kitui and Makueni . This agrees with most projections that have predicted continued stability in OND and instability in the MAM season with greater gains anticipated in ASALS with the anticipated increase in precipitation (Adhikari et al., 2015; EroHerr et

al., 2010). The Standardized Precipitation-Evapotranspiration Index (SPEI) package, which contains the set of functions necessary for computing potential evapotranspiration and other drought indices, was used to implement the Thornthwaite-based PET computation in R statistics (Equation 2). Considerable change in PET was observed during both seasons with the arid areas in Kitui and north of Meru (Antubetwe Kiongo) and Tharaka Nithi, parts of Machakos and Makueni demonstrating the most change as shown in Figure 5.2.
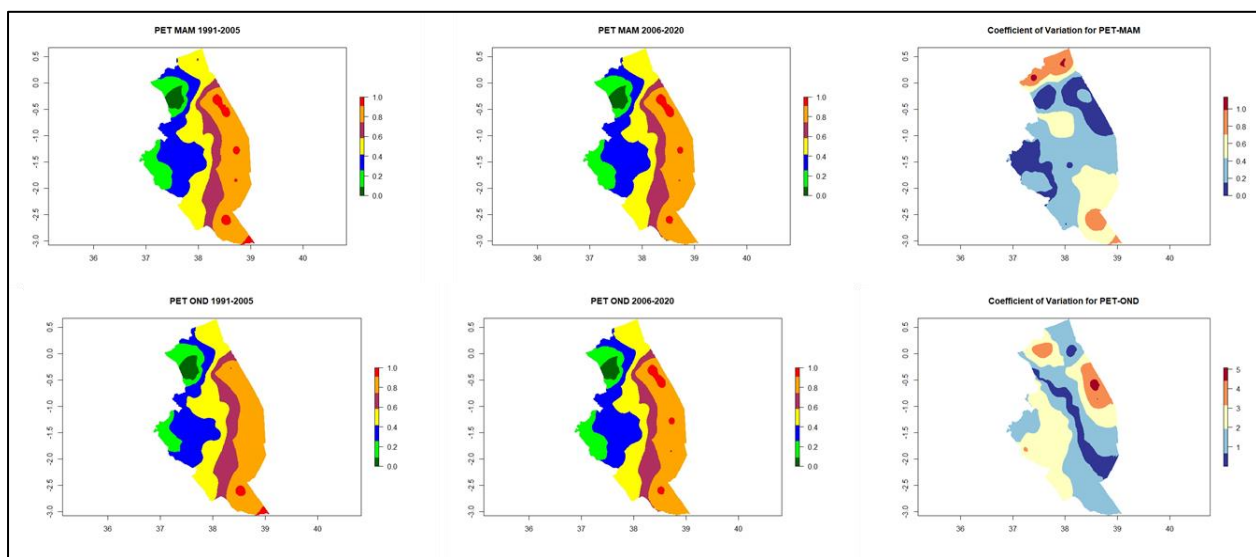
Figure 5.2 Potential Evapotranspiration and change for MAM and OND in 1990-2005 and 2006-2020

However, increases in PET can override potential gains in precipitation as more water is lost through evaporative processes (Adhikari et al., 2015; Antony, 2017; EroHerr et al., 2010; Lane, Annie; Jarvis, 2007) . LGP was computed in R with demonstrable shifts represented as change in number of days and through coefficient of variation. The lowland dryland areas of Kitui, Machakos and Makueni experienced a deterioration in the LGP during the short rains (OND) which represents the primary growing season with a loss ranging from -1 to -20 days. The highland regions of Embu, Tharaka Nithi and northern dryland parts of Meru experienced a slight loss ranging from -1to -10 days in most areas during both seasons. The lowlands drylands did not experience notable change during the long rains (MAM) season (see Figure 5.3).
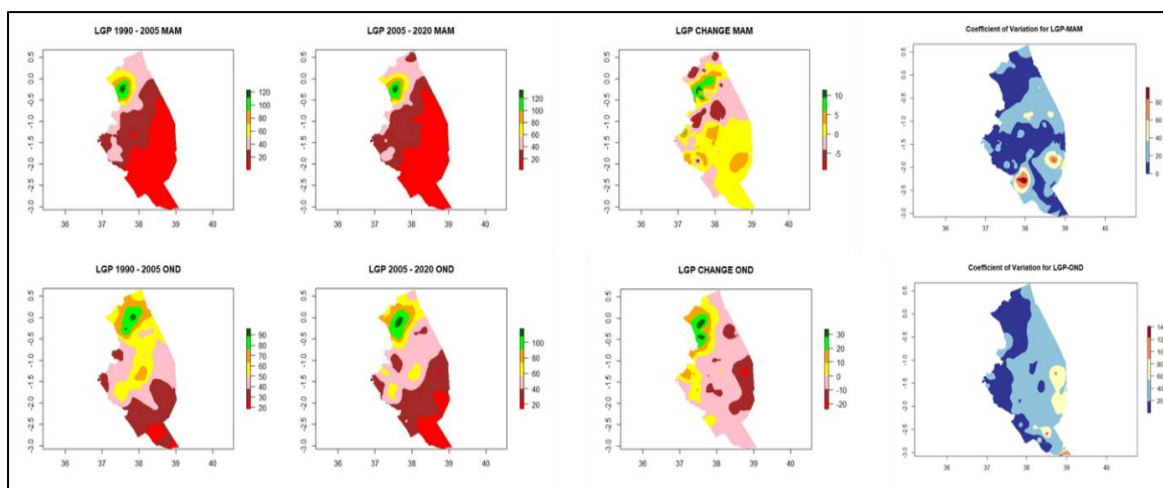
Figure 5.3 LGP for MAM and OND in 1990-2005 and 2006-2010

These changes in LGP impacts the range of crops that can be grown in these areas. With food security of subsistence farmers and farming systems highly depending on crop selection in each season due to changes and variability in LGP across the seasons and years as well as due to longer term trends(Vrieling et al., 2013). Moisture regimes were derived and used to represent the zones in moisture availability. Distinct changes were observed during MAM and OND seasons across the entire region in terms of seasonal variability as shown in Figure 5.4.
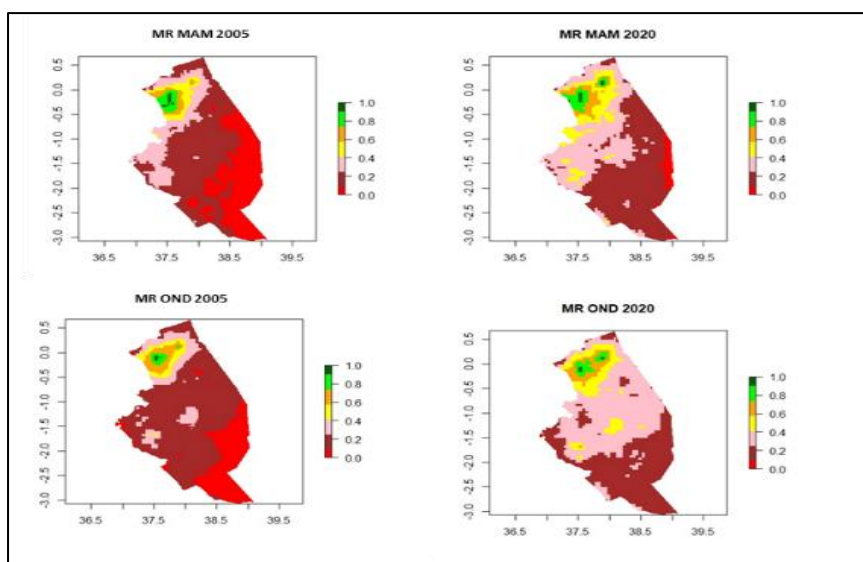
Figure 5.4 Moisture regimes for MAM and OND in 1990-2005 and 2006-2010

A threshold was applied on unbiased temperature data to remove values that fall below the minimum needed for crop growth (FAO, 1996). This was represented as thermal regimes computed by applying

a >5degrees Celsius threshold on daily unbiased temperature data (Figure 5.5). Most of the change in thermal regimes was observed in Machakos and from the highland's areas of Tharaka Nithi and Meru with the change pronounced in both MAM and OND.
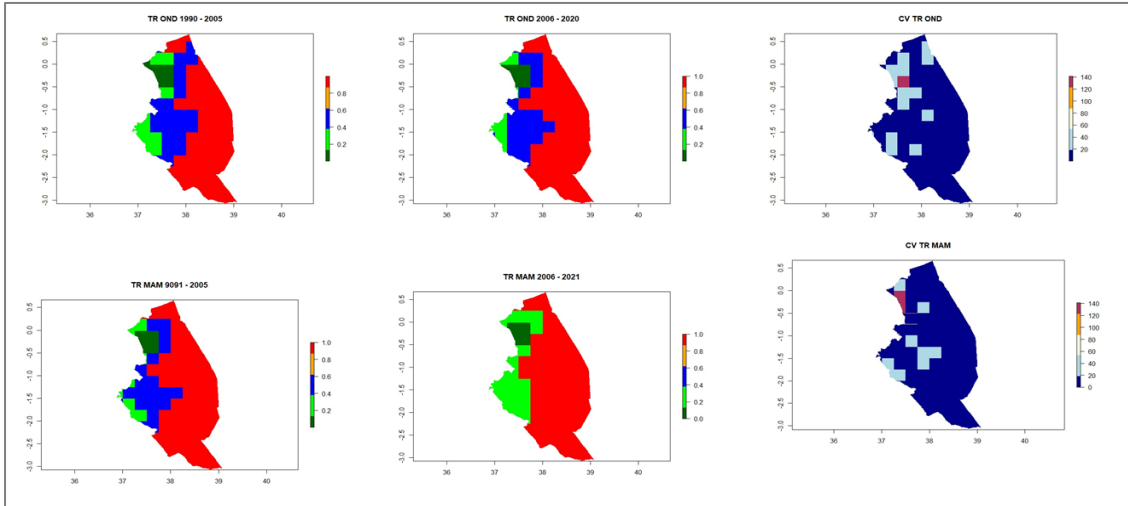
Figure 5.5 Thermal Regimes for MAM and OND in 1990-2005 and 2006-2010

To compute the climate regimes, all the inputs were first normalized using fuzzy logic before being combined to produce the climate regimes. The climate regimes consider the land surface water balances derived from moisture availability and evapotranspiration. Most of the change was observed from Machakos and in the highland's areas of Tharaka Nithi and Meru with the change pronounced in both MAM and OND as shown in Figure 5.6.
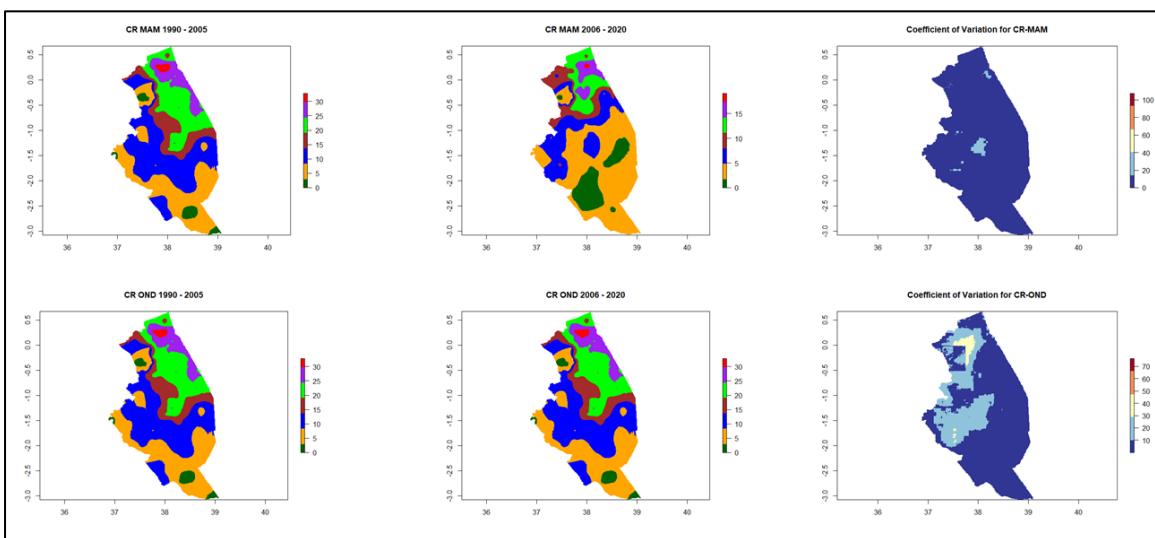
Figure 5.6 Climate Regimes for MAM and OND in 1990-2005 and 2006-2010

An aridity index was created to show how the climate affects agricultural productivity. Aridity index is a measurement of how dry the climate is and is based on rainfall and potential evapotranspiration (Greve et al., 2019). Utilized was Terra Climate's aridity index. The aridity index was calculated by dividing the average annual precipitation by the average annual PET. The values of the aridity index were divided into the following categories: hyper arid (0.05), arid (0.05-0.20), semi-arid (0.20-0.50), and dry sub-humid (0.50-0.65). The aridity index was then fuzzified and the variation from the seasonal average in the two epochs computed. Considerable change was observed in the aridity index especially in the central and eastern belts representing notable change between the two epochs during the MAM season. Aridity index is defined as a constraint to agriculture production and the observed change corresponds to the disturbances observed during the MAM season (see Figure 5.7).
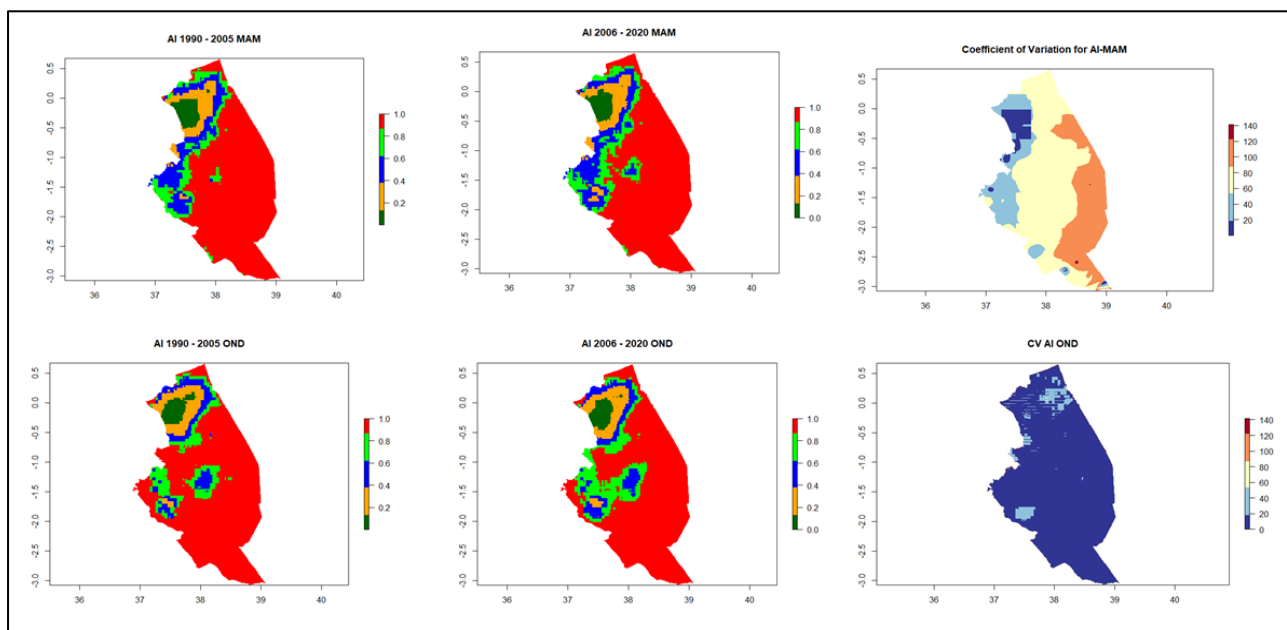
Figure 5.7 Aridity Index and change

5.1.4 Land inventory

The land inventory was derived from biophysical characteristics of the land which are static layers. These include slope, soil drainage, soil suitability for agricultural production and land productivity (FAO, 1996). Higher slopes represent access and use constraints, while soil drainage influences soil productivity as shown in Figure 5.8.
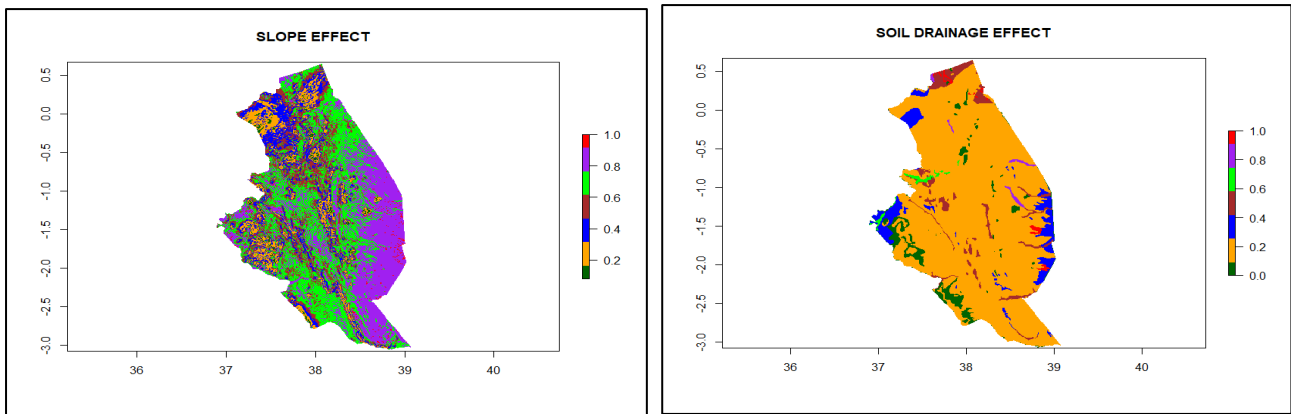
Figure 5.8 Fuzzified and reclassified slope and soil drainage maps

The land productivity was defined by the Dry Matter Productivity layers which detected slight changes in vegetation productivity around in the Meru areas close to Mt. Kenya, on the western parts of Tharaka Nithi and lower Kitui (see Figure 5.9).
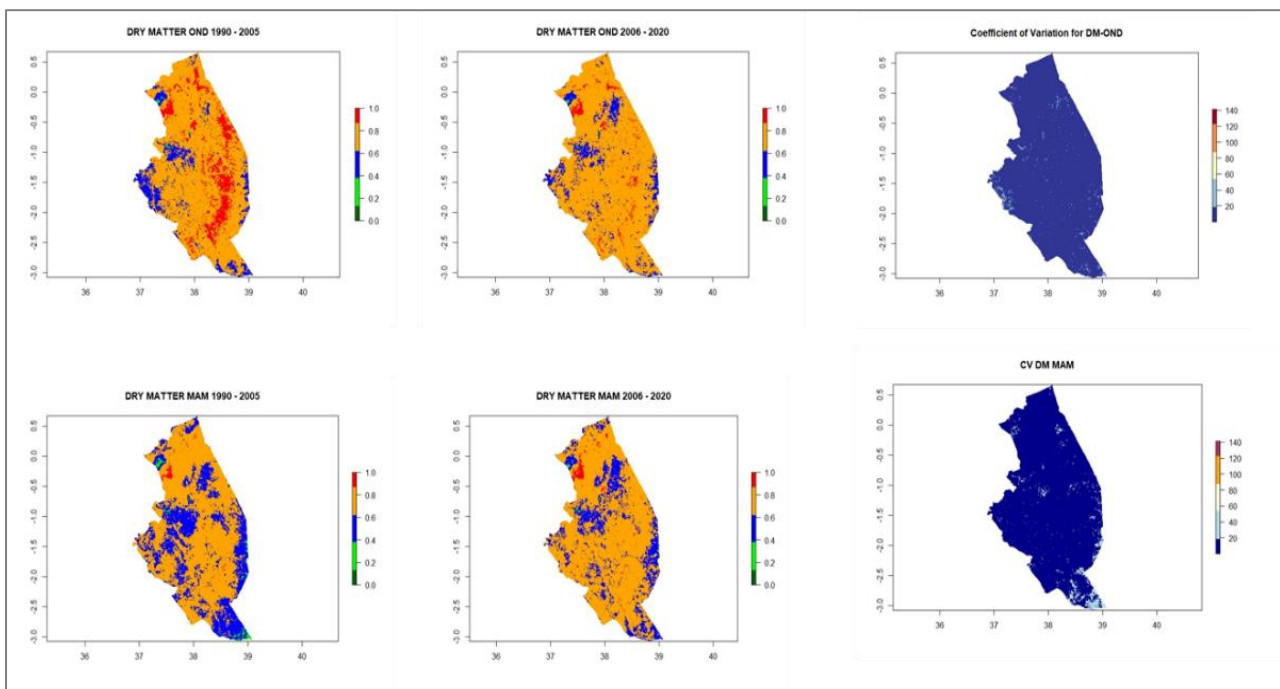
Figure 5.9 Dry matter productivity representing vegetation productivity.

The soil type, drainage capacity, elevation, depth, consistency was used in defining suitability for agricultural production (FAO, 1996; Jaetzold, *et al.,*1983*).* The soil and drainage suitability layers were represented without fuzzification (see Figure 5.10).

63
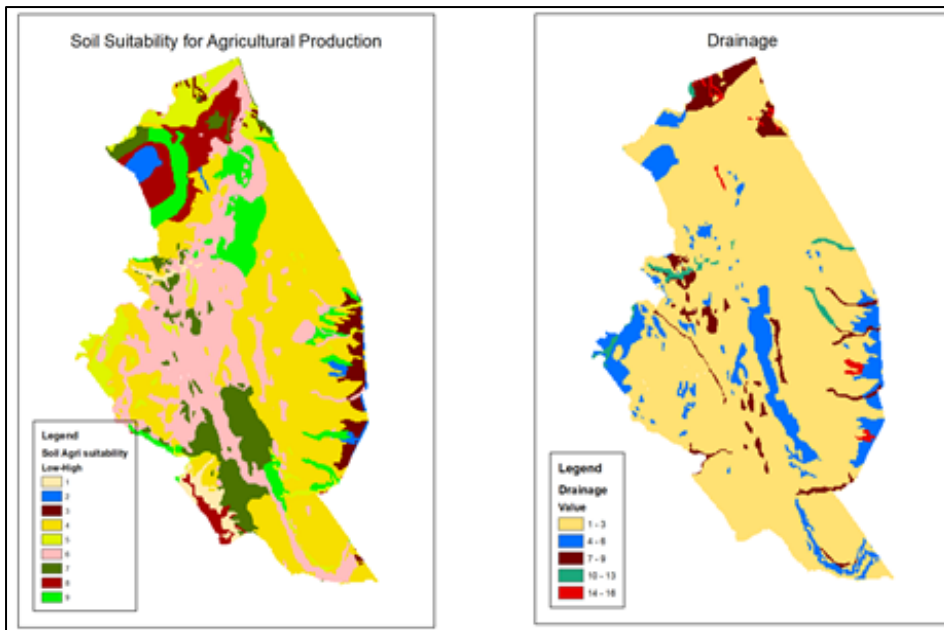
Figure 5.10 Soil suitability and soil drainage for agriculture production

The land inventory was derived by using the outlined biophysical or agro-edaphic parameters including slope constraints, dry matter productivity, soil suitability and drainage which were taken through an addition overlay of each other, after which the layers were smoothened by majority filter method in Quantum GIS (QGIS) to attain the desired output since they are categorical variables. The addition logic was a suppressing model, where agro-edaphic layers would give prominence to the climatic layers, but still contribute to generation of AEZ.

5.1.5 Deriving AEZ

The climate and land inventories were subjected to the fuzzy logic with inverse and direct relationships applied to produce the final agro-ecological zones. However, the fuzzification process, as with other methods such as the Principal Component Analysis (PCA), or the Multi-Criteria Decision Making (MCDM) work well with continuous data. When continuous and categorical data are used, additional weighting is required to ensure that the influence of each layer in the overall assessment was considered. Additional re-assignment and weighting was therefore done in QGIS as illustrated in Figure 5.11.

64
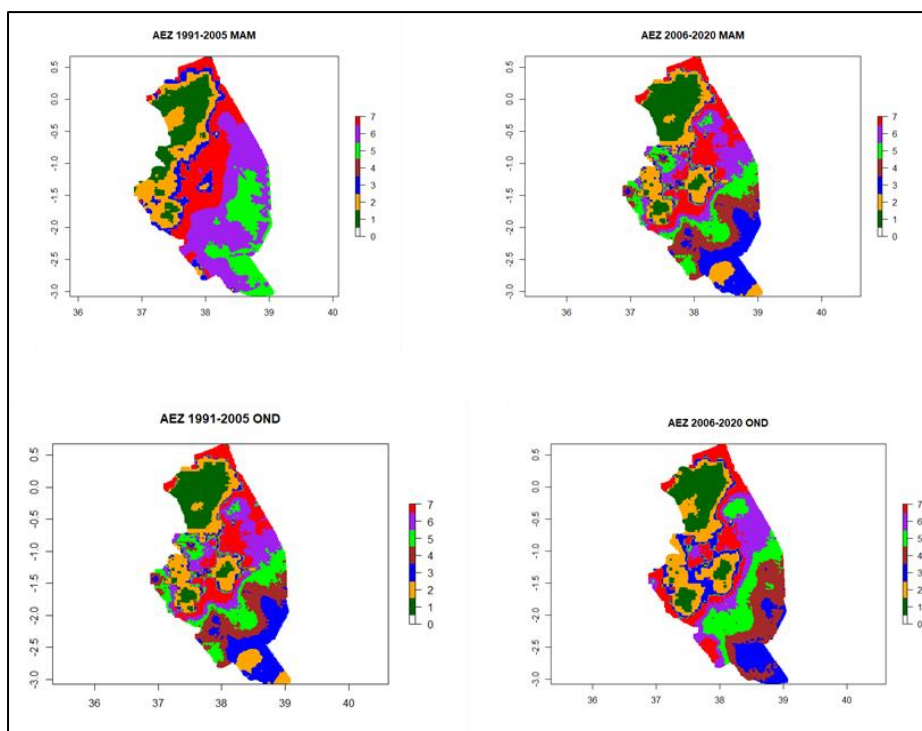
Figure 5.11 Agro-ecological zones for MAM and OND for 1990-2005 and 2005-2020

The resulting AEZ from the fuzzy classifier identified seven distinct agro-ecological zones representing different land potential, providing a better understanding of the micro-agro-ecology than has been previously defined as described in table 5.1.

Table 5.1 Definition of the AEZ Zones

Legend	AEZ No	AEZ No	Definition	GROWING PERIOD DAYS (LGP)	Description/Suitability
	1	0	Perhumid	>120	Forest(mountainous zone)
	2	i	Humid	80-120	Tea-dairy zone
	3	ii	Sub-Humid	65-79	Wheat, maize, beans, irish potatoes
	4	Iii	Semi-Humid	50-64	Beans, pulses, maize, wheat
	5	Iv	Transitional	40-49	Maize, sorghum/millet,
	6	v	Semi-Arid	25-39	Livestock , green grams sorghum/millet
	7	v	Arid	10-24	Rangeland
	7	Vii	Per-Arid	<10	Rangeland

65

To understand the change in the Agro ecologies, a difference image was derived for MAM and OND across the two evaluation time periods (1990-2005 and 2006-2020) (see Figure 5.13).
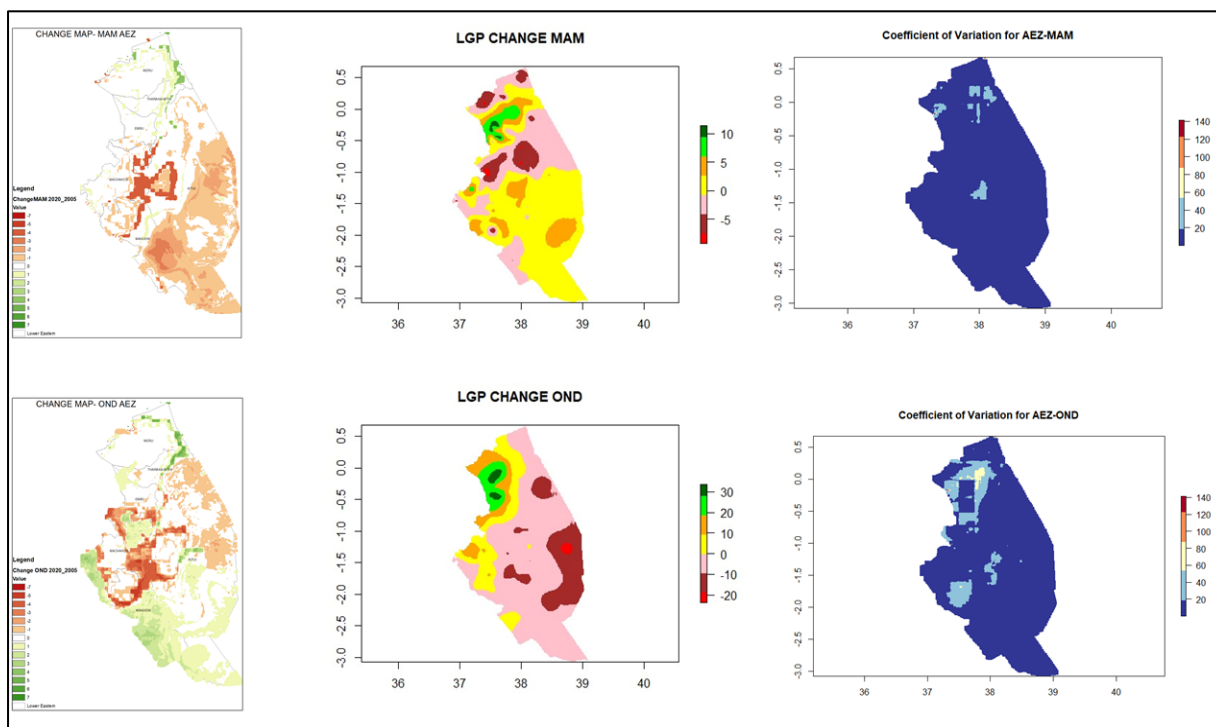
Figure 5.12 Changes in Agro Ecological Zones and corresponding change in the LGP

To understand the direction of change, a sampling of the variables across the agro-ecological zones was done and the change in AEZ represented together with the change in the LGP. The positive change means that category has moved to the next class, representing a worsening situation. For example, change from arid (6) to Per-arid (7) is negative. These negative changes in the AEZ, representing a decreasing potential for agricultural production, also correlate with the variations in the length of the growth season. However, some areas experienced an improvement in their agro ecologies. While these improvements are not significant as evidenced in the Coefficient of variation map, they however provide an insight on the possibilities in the diverging shifts in seasons and trends in both the Long and the Short rains. Specifically, there is an improvement in the Lower Midlands agro-ecology with a large part shifting from per-arid to Arid during the Long Rains (MAM) representing improving potential in the previously per-arid areas. Slight improvements in the AEZ and LGP were also observed the Mountain areas of Meru.

66

5.2 Opportunities for Optimizing Agriculture and Climate Adaptation in the Lower Eastern region in Kenya

5.2.1 Changing Agro-Ecological potential in a changing climate

To capture the microvariations, all layers were acquired at a scale of 1km or less where possible and resampled to the same scale. Fuzzy logic was used to normalize the outputs. Change was derived from the 2020 baseline assessments. From the assessment, the expected climate shifts and increase in precipitation was observed, with higher gains observed during OND than MAM. RCMRD (2018) assessed and found that future seasonal precipitation is possibly going to increase during MAM under all scenarios, with higher increase over eastern parts of Kenya as shown in Figure 5.13.
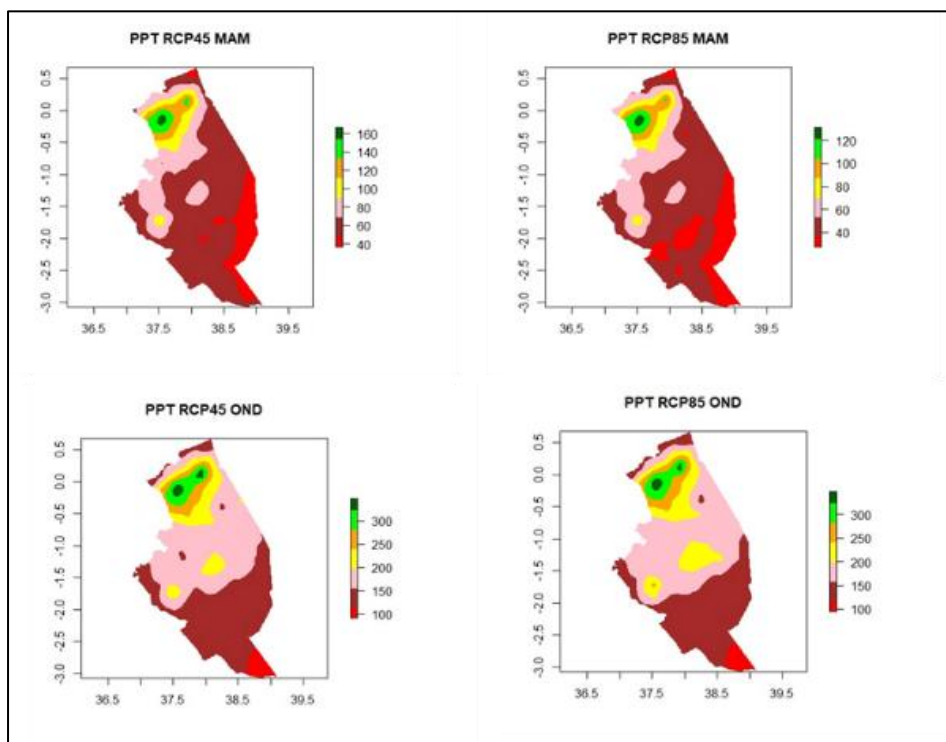
Figure 5.13 Precipitation range across MAM and OND for 2040 RCP's 4.5 and 8.5

Increasing temperature was observed across the region, with the higher increase observed in lower eastern part, but more pronounced in MAM than in OND (see Figure 5.14). This is consistent with estimates of increases in temperature that indicate a warmer future for practically all of Kenya.
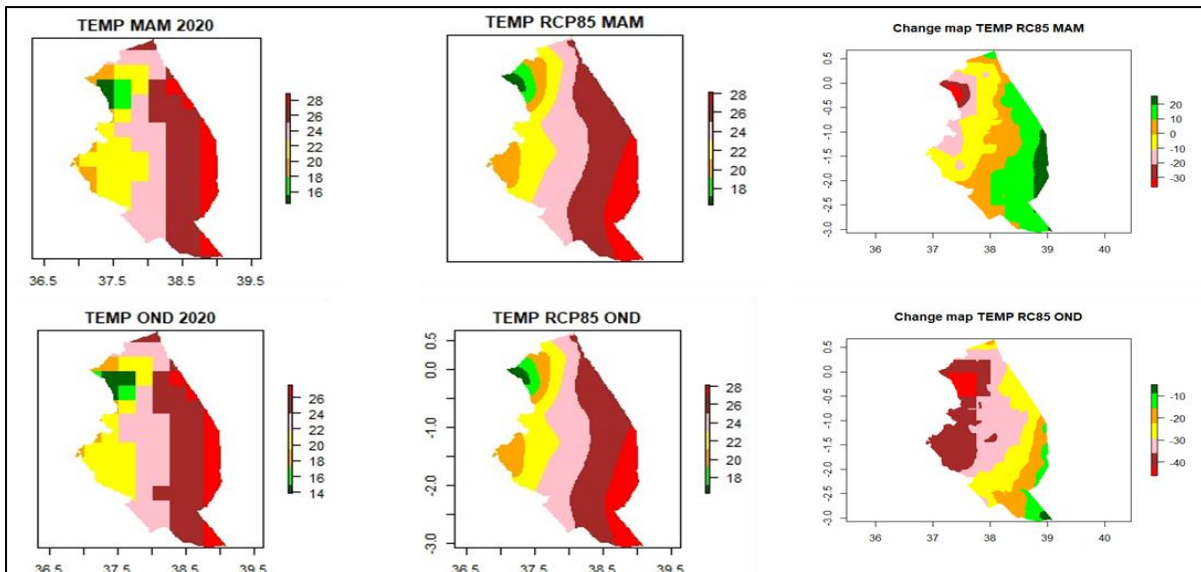
Figure 5.14 Thermal Regimes for MAM, OND in 2040 for RCPs 4.5 and 8.5

Similar trends in aridity index and temperature were observed. The addition of aridity index helped overcome data quality in assessment of change in temperature in RCP 4.5 MAM season. In the near future, the annual surface temperature is predicted to climb between 1.0 °C and 2.0 °C under the RCP4.5 scenario, whereas the RCP8.5 scenario predicts a rise between 1.5 °C and 2.5 °C (RCMRD, 2018).
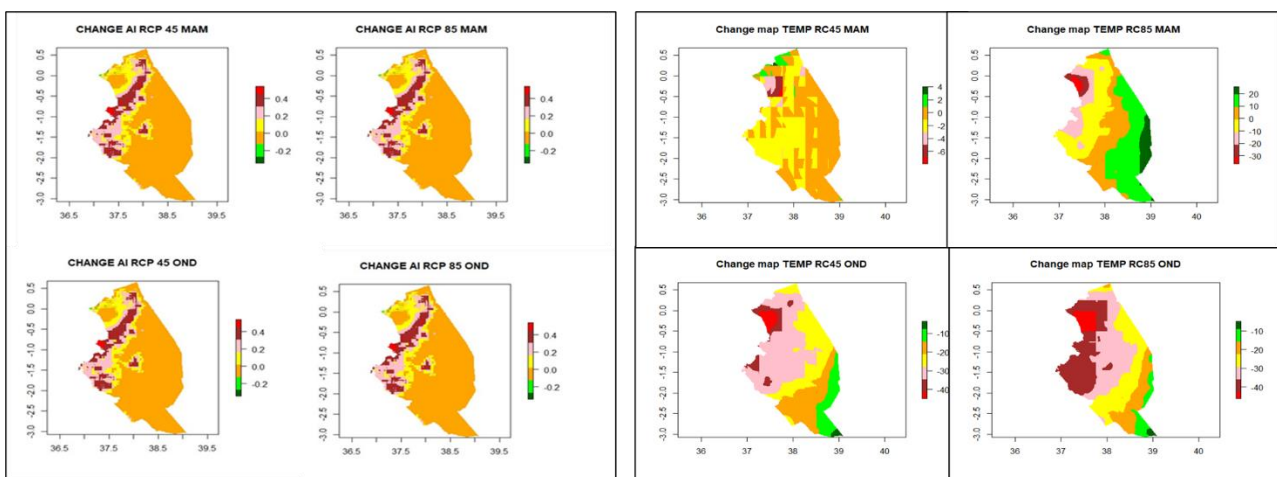
Figure 5.15 Changes in temperature and Aridity Index during MAM, OND in 2040 RCPs 4.5 and 8.5

Reductions in the aridity index of approx. 0.1 were notable in the Lower drylands of Makueni and Kitui. This correlates with the expected improvements in precipitation in the lowlands which would

reduce the aridity levels. Increasing aridity levels of approximately 0.1 to 0.4 were observed across Machakos, Embu, Tharaka Nithi and Meru (see Figure 5.15).

The temperature and precipitation data were used as an input to derive the Potential Evapotranspiration (PET), the LGP as well as the Moisture and aridity indexes. The projected climate outputs were compared with the baseline seasonal temperature, derived using the same methods. Agriculture is negatively impacted by an increase in PET because more water is wasted through evaporation and transpiration (Kogo et al., 2021).
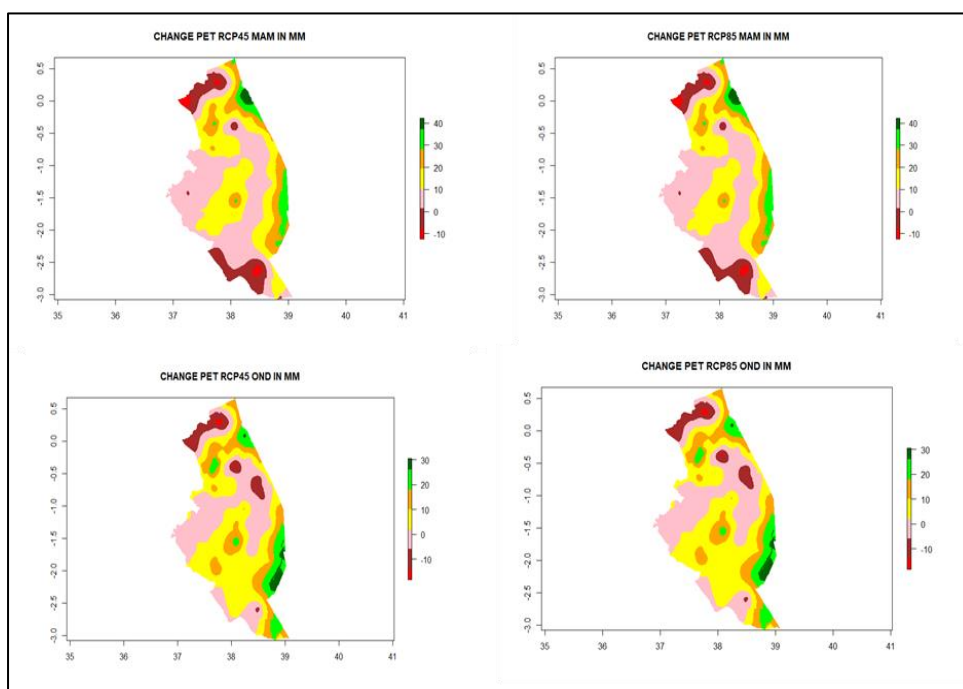
Figure 5.16. Potential Evapotranspiration and change across the seasons and Epochs.

Results show an increase in PET, with RCP 8.5 showing a more dramatic rise than RCP 4.5 (see Figure 5.16). The highest increases were observed in already constrained areas, such as Embu, Tharaka Nithi, North Meru and lower sides of Kitui. This increase agrees with other studies where the increase in PET offsets the increase in rainfall in ASALs especially (Adhikari et al., 2015; EroHerr et al., 2010). LGP was computed using baseline and future daily inputs and the seasonal change computed.
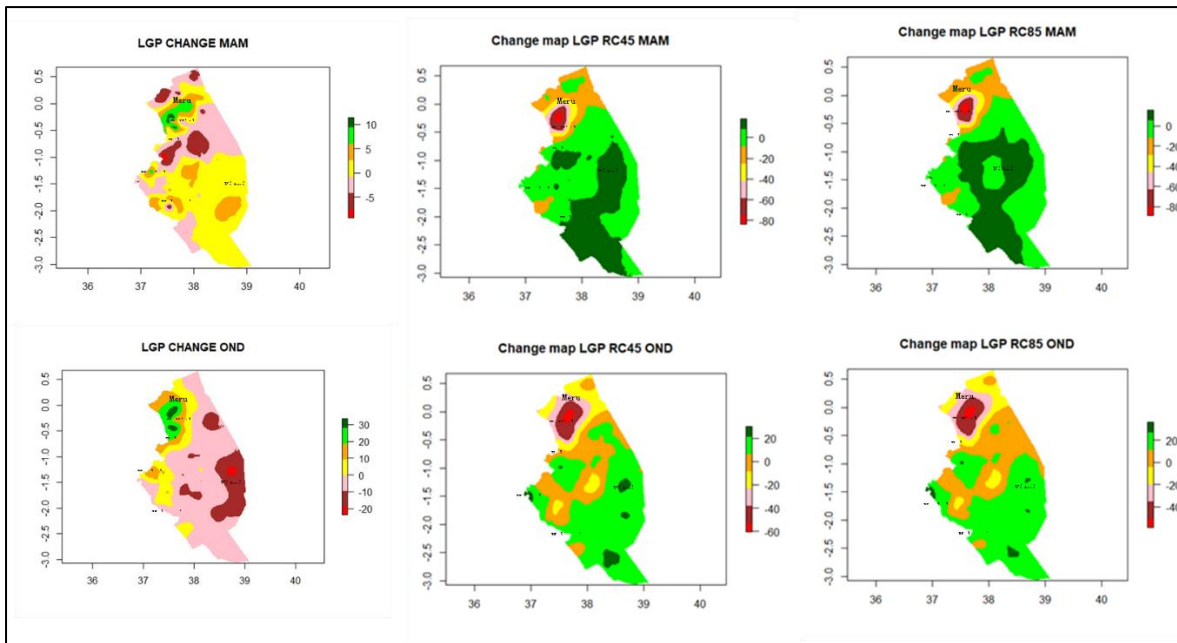
Figure 5.17 Changes in the LGP days during MAM, OND in 2040 RCPs 4.5 and 8.5

Highlands experience a significant decrease in LGP (-20-80) in RCP 4.5 in MAM while lowland drylands remain stable. Areas like Meru and Tharaka Nithi experience a negative change in LGP, this means that crops like tea/coffee might not be viable in future. Lowland drylands experience an increase of +20 in OND in all scenarios. LGP improve in lowlands drylands in future compared to bleak baselines (see Figure 5.17). Parts of the north arid areas of Meru also showed an increase in LGP. However, the main growing areas in Meru showed a reduction in the LGP of 1-10 days in MAM for RCP 4.5 and 8.5. OND projections for RCP 4.5 and 8.5 exhibited negative trends for the main growing areas in Meru. Higher increase in LGP OND over lower eastern areas of Kitui and Machakos, and in the upper parts of Machakos and Embu where a 1–20-day increase was observed in RCP 4.5. However, the highland areas experienced a reduction in LGP. Similar but more pronounced trends were observed in the RCP 8.5. These changes are anticipated to change the suitability of crops and similar changes in baseline LGP were observed in other studies (Vrieling et al., 2013).

Higher increases in effective moisture were observed in the eastern dryland regions, with the losses more pronounced in Machakos, Embu, Tharaka Nithi and Meru in OND (see Figure 5.18).

70
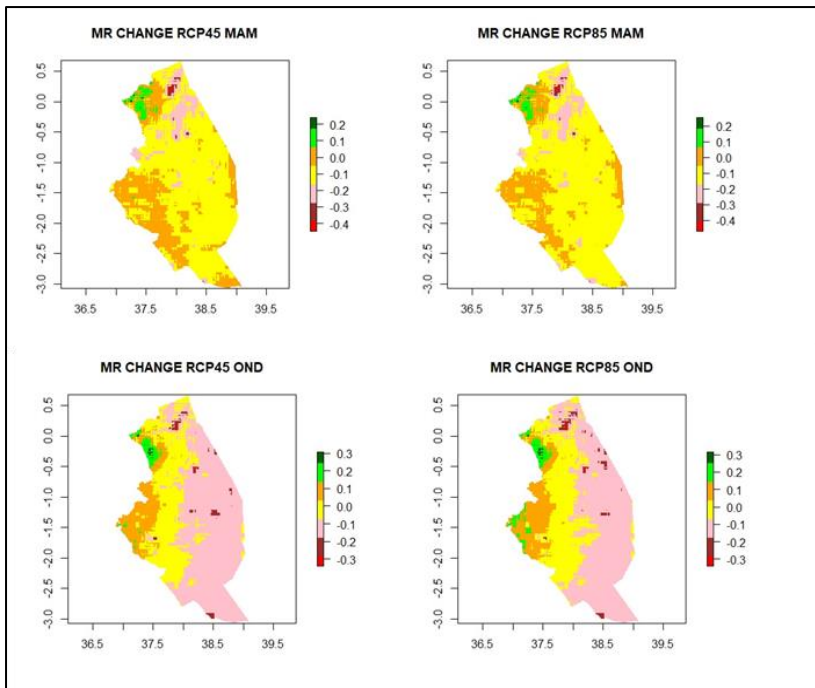
Figure 5.18 Changes in Moisture Index during MAM, OND in 2040 RCPs 4.5 and 8.5

Climate regimes were computed from PET, thermal regimes, moisture index and the LGP computed

by season. The inputs were first normalized using fuzzy logic before being combined to produce the

climate regimes (see Figure 5.19).
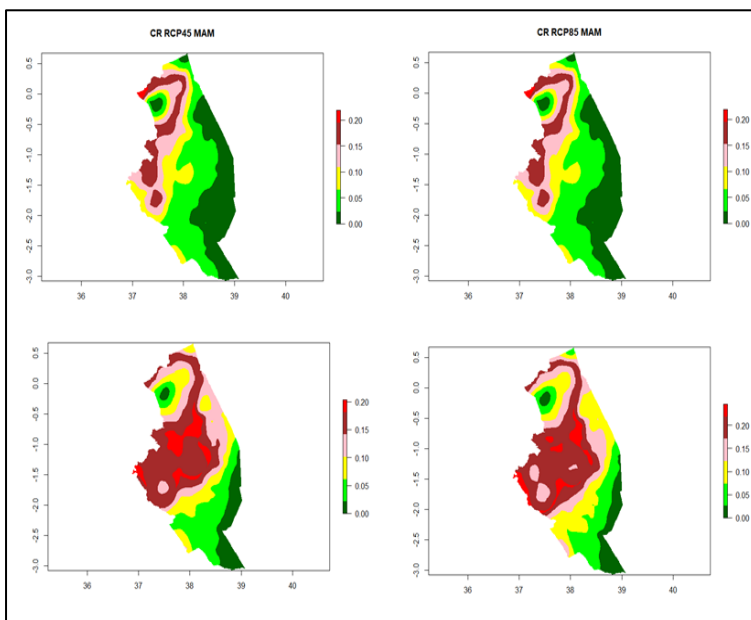
Figure 5.19 Climate Regimes for MAM, OND in 2040 for RCPs 4.5 and 8.5

Soil suitability and soil drainage derived from the soil and elevation data portray the biophysical

suitability for agricultural production (Figure 5.20).

71
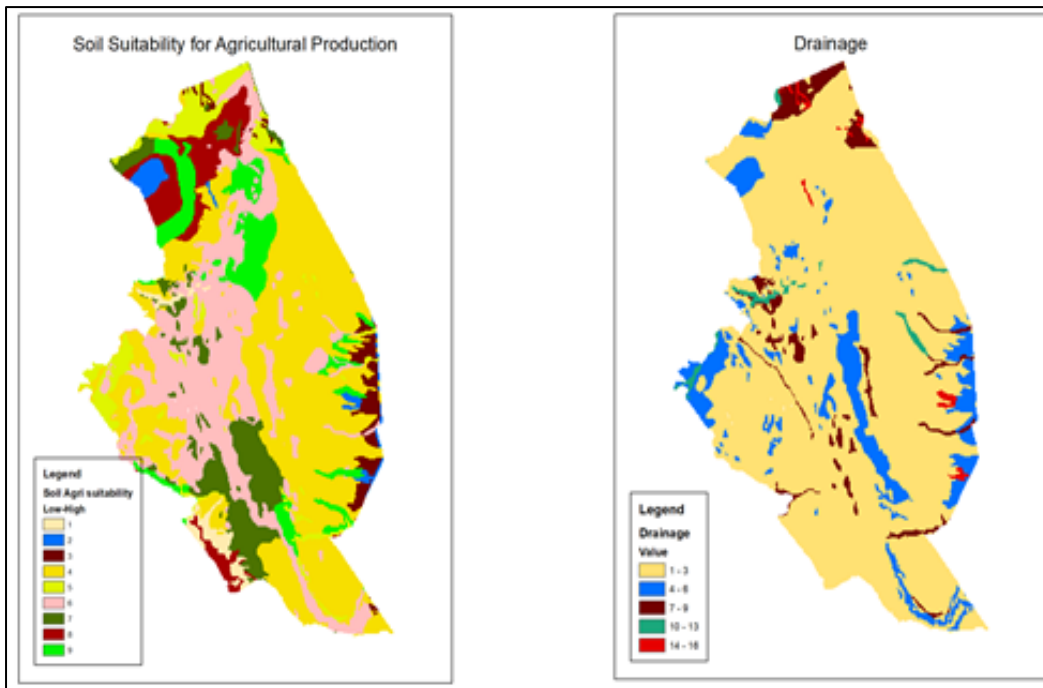
Figure 5.20 Soil suitability for agricultural production and drainage

Climate regimes and biophysical parameters were normalized using fuzzy logic and used as inputs to the definition of the AEZ. Linear and inverse relationships were applied based on the variable's contribution to agriculture potential. An inverse relationship applies in the interpretation of AEZ change maps. For example, a change from 7 (per-arid) to 6 (arid) represents improved potential. Around Machakos, Embu, Meru, and Tharaka Nithi, the agroecological potential suffered the greatest losses, which were more pronounced in RCP 4.5 MAM than in RCP 8.5 MAM (see Figure 5.21). Improvements in AEZ were more notable during the OND for both RCPs in the Lower Eastern Region, corresponding with the noted increase in precipitation and LGP.
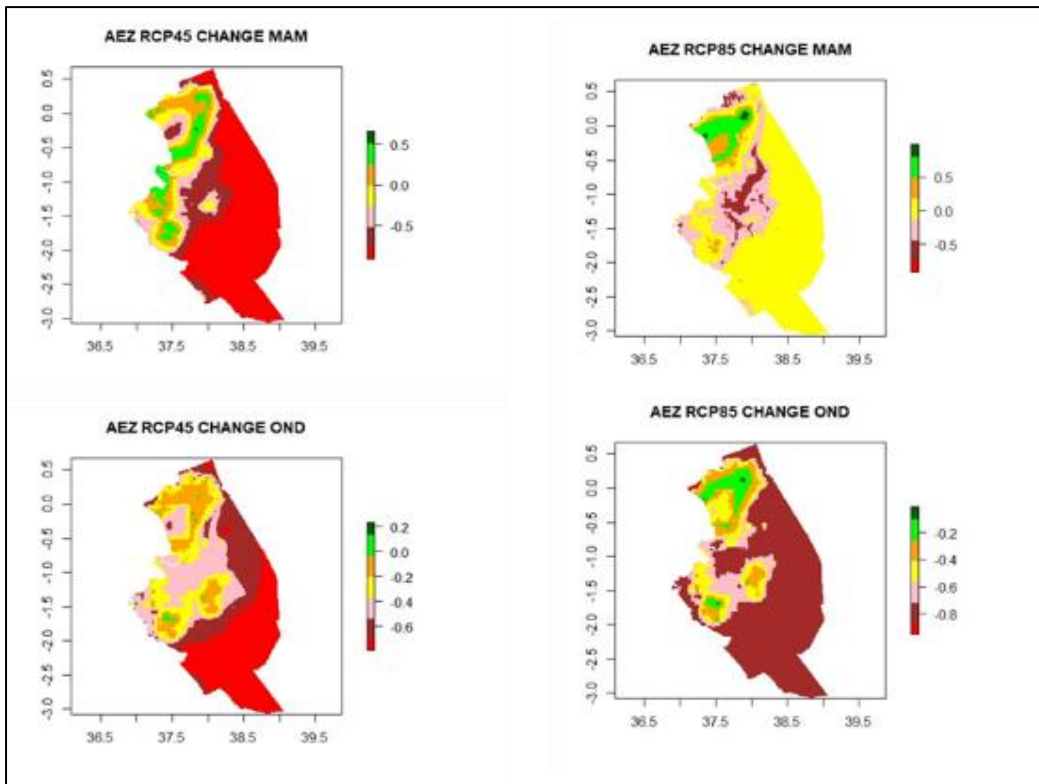
Figure 5.21 Agro-Ecological Zones and change maps from a 2020 baseline and RCP 4.5 2040

5.2.2 Defining the scope for field data collection

The data collection process encompassed a comprehensive scope of demographic, agricultural, and climate-related factors. Demographic information included gender, incomes, decision-making dynamics, farm size, and prevailing farm systems. The present cropping system was analyzed in terms of rainfed versus irrigated systems, as well as mixed systems categorized by land size, with attention to income diversity and production systems.

Understanding the drivers of vulnerability involved identifying groups most susceptible to food insecurity, considering factors such as land size, production trends, and coping strategies. Perceptions of climate change, including perceived positive and negative responses, were assessed alongside sources of information on climate forecasts and extension services. Participants' insights on investments to mitigate climate change impacts on their livelihoods are gathered, including barriers and opportunities. The intensity of the vulnerability was assessed ranging from low to remarkably high for several indicators such as season change, production change, increased prevalence of pests and

diseases, increased vulnerability to floods and droughts. Adaptation measures are explored in soil, water, and farming methods to inform strategies for building resilience in agricultural practices.

5.2.3 Confirming changes in length of growing period

In a survey conducted through consultations with 860 farmers representing the agro-ecologies and agroclimatic zones in the region, we sought to validate if the seasons are changing especially through a change in the length of the growing period and its impact on food production. From the data collected across all the microclimates, we confirmed that the length of the growing period is changing and becoming more erratic and is directly impacting food production . All counties experienced varying shifts in the length of the growing season with the highest shift being reported in Kitui, presumably due to user feedback bias as to the level of intensity as it was qualitative.

We sought to assess the changes in a more granular level by looking at the changes in each of the wards representing a microclimate where data was collected. All wards experienced a decrease in production as seen in the figure 5.22 below.

Ward	Intensity	Change
Mutongoni	1.784	NaN
Mutha	1.758	NaN
Mumoni	1.544	0.072
Kiima Kiu/Kalanzoni	1.314	0.049
Akachiu	1.307	0.127
Igambang`ombe	1.285	0.101
Muvau/Kikumini	1.131	-0.515
Nthawa	1.097	NaN
Nyaki east	1.088	NaN
Upper Kaewa-iveti	1.070	-0.451
Mwimbi	0.990	-0.175
Kiteta-Kisau	0.879	-0.180
Matungulu North	0.796	-0.095
Mulango	0.785	0.406
Tseikuru	0.723	0.121
Antubetwe kiongo	0.700	NaN
Muminji	0.508	NaN
Kivaa	0.450	NaN
Mitheru	0.000	NaN
Thangatha	0.000	NaN
Total	**1.705**	**0.248**

County	Intensity	Change
Kitui	2.176	0.611
Machakos	1.666	-0.662
Meru	1.664	0.068
Tharaka-Nithi	1.439	0.049
Makueni	1.136	0.050
Embu	0.969	NaN
Total	**1.705**	**0.248**

Figure 5.22 Validating changing seasons length and production

Further, food security was noted to be still a major concern in most of the households, despite diversification in farming systems and despite larger land holdings as shown in Figure 5.23.
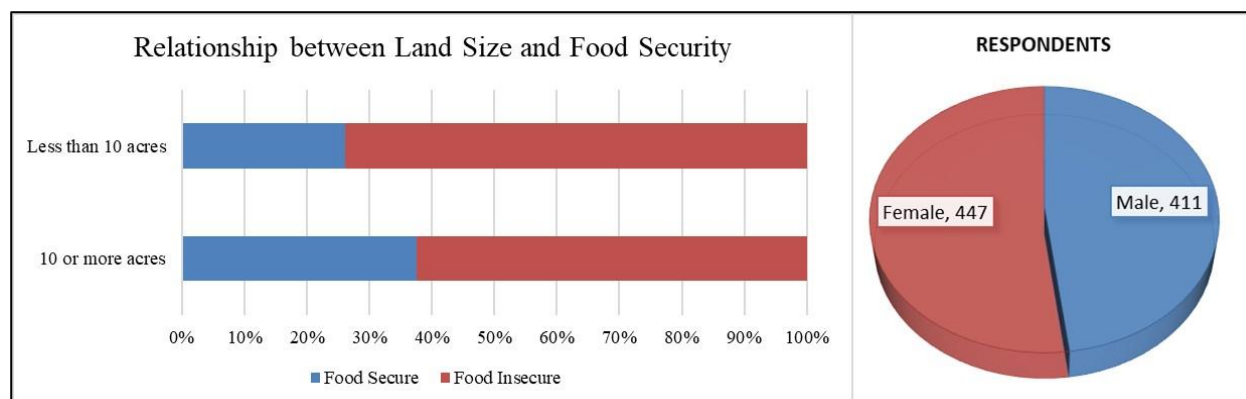
Figure 5.23 Relationship between land size and food security and demographics

Different adaptation measures were being adopted (see Figure 5.24). Most farmers adjusted their farming by adopting drought resistant crops, adjusting planting dates and diversifying livelihoods to include livestock keeping. Soil management focused on use of manure, retaining residue and zero tillage. Water harvesting and conservation methods were also used to manage water availability.
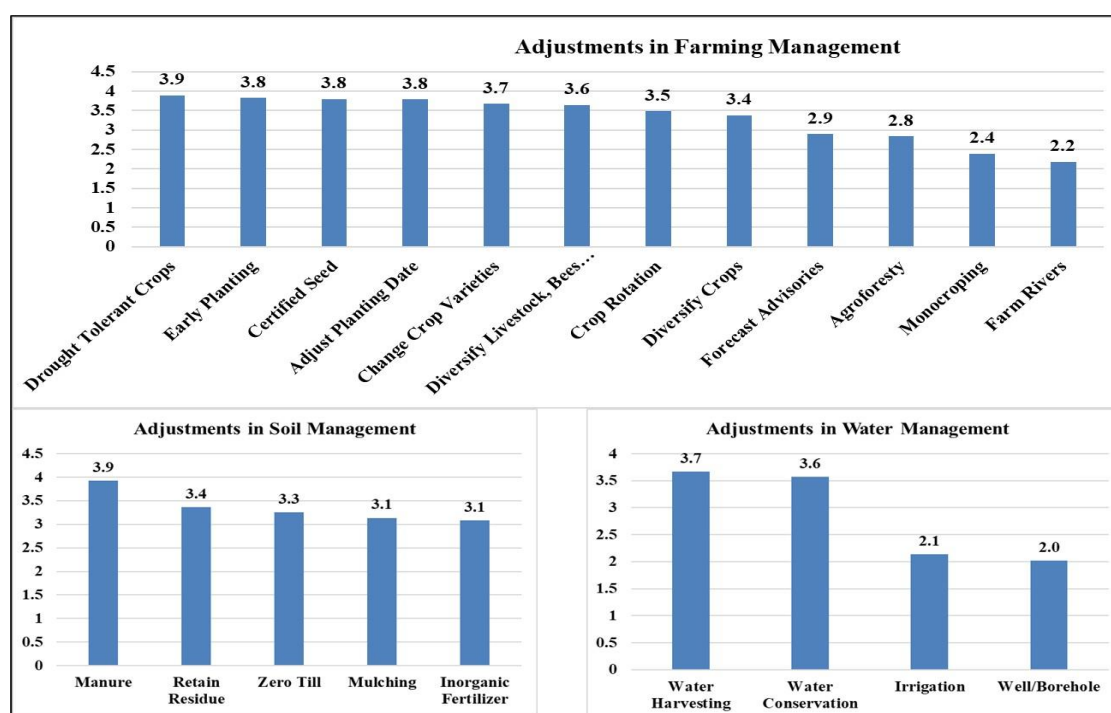
Figure 5.24 Farmers adaptation strategies for farming, soil, and water management

These adaptation mechanisms were enabled through farmers initiatives as well as government and donor investments in the region. Lack of capital, lack of storage facilities and challenges accessing extension and education were identified as key barriers (see Figure 5.25).
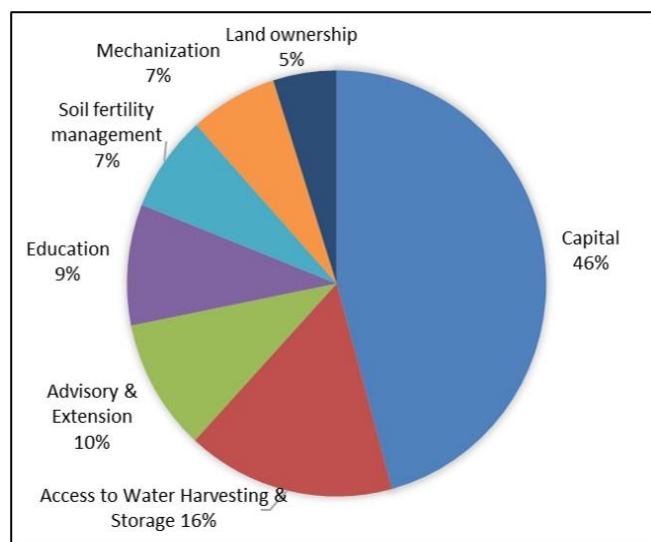
Figure 5.25 Adaptation Barriers

5.2.4   Opportunities for adapting and transitioning adaptation strategies

This section responds to the 3ʳᵈ research question on opportunities that observed changes presented in improving adaptation in the region's agricultural production systems.

5.2.4.1   Gender focused adaptation mechanisms

Gender influences the success of adaptation mechanisms. For example, the survey found that female headed households adapted by diversifying food crops, while male headed households adapted by diversifying cash crops with reported higher incomes (see Figure 5.26). Female headed households would be more interested in improving their food security first.

Analysis of Gender Vs. Income Sources Vs. Diversity of Crops				
Respondent	Decision Maker	Sources of Income	Diversity of Food Crops	Diversity of Cash Crops
Female	Female	2.47	3.62	1.73
Female	Male	2.16	3.20	1.30
Male	Female	2.44	3.40	1.70
Male	Male	2.48	3.17	1.94
	Median	2	3	1
	Minimum	1	0	0
	Maximum	5	7	5

Future adaptation mechanisms will need to be structured with the sensitivities of gender and population groups considered. For example, high yielding, drought resistant and early maturing food crops would be more appropriate for female headed households.

5.2.4.2   Agricultural zoning

From the survey, reported food insecurity in large (>5acres) points to challenges in land utilization and optimization of farming activities to increase return on investments. Agricultural zonation, where farmers, collectively plant specific suitable crops for their agro ecologies has been used to optimize production and accessibility to markets, improving the resilience of farmers.

5.2.4.3   Focused diversification of farming systems

The projected increase in rainfall and length of growing period in the lowland drylands (from per arid/arid to arid/semi-arid) presents an opportunity to shift purely rangeland areas to agro-pastoral production. RCMRD (2018) confirmed that higher runoff in OND was observed in lower dryland areas. This represents an opportunity for water harvesting for increasing agro-pastoral systems. In the midland areas of Embu, Tharaka Nithi and Meru, adaptation mechanisms would need to focus on the projected loss in agricultural potential to introduce production systems matching with the reduced potential.

5.2.4.4   Customizing adaptation based on vulnerabilities

An understanding of perceptions of drivers to vulnerability was found to be different between food secure and food insecure respondents. An assessment of the education levels of the respondents did not seem to affect their perceptions on their sensitivity to climate change. However, there were distinct variations in the definitions of the responses from food secure and insecure households (see Figure 5.27). For example, food secure households responded that they were more affected by farm destruction caused by floods and post-harvest losses than drought, poverty, and inflation. This would

mean that in food secure areas, management of post-harvest losses was more important as well as mitigation of flood related destruction.

Food Security	Secure	Insecure	Farmers perception on vulnerability drivers
Food crops Diversity	3.19	3.13	Food insecure persons have less food crops diversity by about 2%
Cash Crops Diversity	1.58	1.41	Food insecure persons have less Cash crops diversity by about 13%
No Positive Climate Change Outcome	0.40	0.46	Food insecure people find negative climate change to blame for their food insecurity
Impact on Production Trend	0.97	0.95	Food secure people are more impacted by climate change on their production.
Impact on Food Security	3.22	3.66	Food insecure people are more impacted by climate change
Season Change	4.90	4.88	Food secure people are more impacted by season change
Rain Time Change	5.12	5.12	Rain time change is insignificant to food security among respondents
Drought Crop Fail	4.83	4.87	Food insecure people are more susceptible to drought crop failure
Flood Farm Destruction	3.61	2.28	Food secure people were more affected by farm flood destruction
Post Harvest Loss	4.56	3.69	Food secure were more affected by post-harvest losses
Pests	4.68	4.76	Food insecure people were more affected by pests
Diseases	4.50	3.59	Food secure people were more affected by diseases
Poverty food shortage	4.57	4.95	Food insecure people are susceptible to poverty food shortages
Lack of Water	4.78	4.29	Food secure people identified lack of water as a significant climate change issue on their production
Soil Fertility Degradation	4.82	3.46	Food security people identified soil fertility degradation as an issue. *Probably food insecure people do not know how to assess soil degradation
Crop Viability	4.66	3.74	Food secure people identified climate change as a significant driver to reduced crop viability
Livestock Death	4.11	2.81	Food secure people are livelier diversified to livestock given the high impact they noted on livestock due to climate change
Inflation on Costs of Inputs	5.53	5.72	Food insecure people are highly vulnerable to inflation on cost of inputs

Figure 5.27Perceptions of Vulnerability

5.2.4.5 Converging technology and indigenous knowledge for adaptation

Most respondents accessed forecasts and using them to inform their farming activities. It is important to note that 27% of the farmers use indigenous knowledge of forecasts and seasons change to adapt their farming. The convergence of technological advances and indigenous knowledge can be harnessed

to increase access to information for optimizing adaptation. Further, education did not emerge as a considerable barrier to access to forecasts since TV and radios provided vernacular translations (see Figure 5.28).
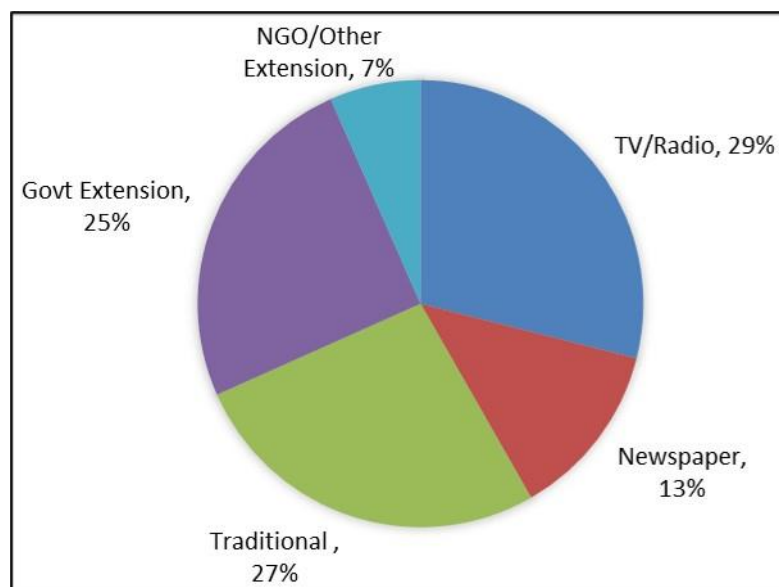
Figure 5.28 Access to information and forecasts

5.2.4.6 Innovations for de-risking agriculture and use of technologies

There is an increasing investment in de-risking agriculture in Kenya, with the government subsidized crop insurance extended to 33 counties covering high, medium and marginal production areas. Lowland drylands have especially benefited from higher subsidies from the government. The top barrier was cited as lack to capital and extension/education, as well as mechanization.

Opportunities for innovative financing of farmers is required, as well as education to ensure that there is a return on investment for the farmer. The increasing mobile and internet connectivity has made farmers more accessible. The African Union, through its digital Agriculture strategy has emphasized on the need for countries to register their farmers and develop agricultural data hubs that harness technological advances to deliver customized information, resources, and opportunities for farmers (African Union, 2020).

5.3 Discussion

30 years of data on Kenya's Lower Eastern Region's AEZs reveal a clear connection between climate shifts and agricultural challenges. This groundbreaking study employed a powerful approach, integrating various climate data points to paint a detailed picture. It analysed historical climate records (1990-2020) alongside future projections (2040) to understand how temperature, rainfall, potential evapotranspiration, growing season length, and aridity are changing. This data, along with land biophysical characteristics such as soil viability for agriculture production, was then used to create a map of AEZs.

What makes this study unique is its use of scalable cloud computing. Unlike traditional desktop processing with limited power, this approach harnessed the vast resources of cloud computing, allowing for a more robust and replicable analysis. This innovative method overcomes processing limitations and paves the way for future studies of this nature (Amani et al., 2020; Twagiramungu, 2022).

By delving into historical climate data for Kenya's Lower Eastern Region, the research pinpointed how key variables have shifted over two distinct wet seasons. Focusing on rainfall, temperature, potential evapotranspiration (PET), length of growing period (LGP), moisture index, aridity index, and thermal regimes, the study revealed significant trends. Notably, precipitation patterns changed, PET levels fluctuated, and LGP varied across different regions and seasons with a confluence in evidence from other research and projections (RCMRD, 2018).

These findings resonate with existing research that projects increased rainfall in specific areas of Kenya. This highlights the importance of a two-pronged approach in climate assessments, considering both observed trends and future projections to create a more complete picture. The observed changes in climate variables directly impact agricultural potential and productivity (Knox et al., 2012). For instance, increases in PET can lead to water loss through evaporation, potentially offsetting gains from increased precipitation. Changes in LGP affect the timing and suitability of crop cultivation,

particularly in regions experiencing shifts in growing seasons(Vrieling et al., 2013). Moreover, alterations in moisture availability and thermal regimes further influence agricultural practices and crop viability (Ochieng et al., 2016). These findings underscore the need for adaptive strategies to mitigate risks and optimize agricultural production in response to changing climate conditions.

The study's approach also integrated biophysical factors such as slope, soil drainage, soil suitability, and land productivity to assess agricultural suitability and land use constraints(FAO, 1996). By combining climate and land inventories using fuzzy logic which has been proved applicable to agricultural studies and use of disparate data formats, the study derived AEZs that provide valuable insights into micro-agroecological variations (Cassel-Gintz et al., 1997; Praseyto et al., 2013; Sharma et al., 2007)

The findings highlight opportunities for optimizing agriculture and climate adaptation in the Lower Eastern region of Kenya. These include recognizing gender-specific vulnerabilities and adapting strategies accordingly to enhance resilience and food security among different demographic groups, responding to the need for gendered resilience information delivery and adaptation mechanisms (Ngigi & Muange, 2022). Implementing agricultural zoning strategies based on AEZs can optimize crop selection and land use practices, improving resilience to climate variability(Kurukulasuriya & Mendelsohn, 2008; Ojwang et al., 2010).

Leveraging projected changes in rainfall and growing periods to diversify farming systems, including agro-pastoral production in lowland drylands, can enhance resilience and livelihoods (Silvestri et al., 2012).

Tailoring adaptation measures to address specific vulnerabilities and perceptions of different population groups can ensure effectiveness and inclusivity in climate resilience efforts (Obwocha et al., 2022). Integrating technological advancements with indigenous knowledge systems can enhance access to climate information and adaptation strategies, fostering community resilience. Investing in innovative financing mechanisms, digital agriculture platforms, and climate-smart technologies can

help de-risk agriculture and enhance adaptive capacity among farmers(Digital Economy for Africa Initiative, 2023).

While climate change occurs gradually, changes in seasonality can provide a good indication of the intensity of the variations and their influence on production systems. Combining continuous variables such as climate and categorical variables such as land biophysical parameters; adds significant value to understanding the agro-ecology as evidenced by the detail in the definition of the agro-ecological zones (Musafiri et al., 2022).

The study provides a use case for the value of blended data inputs into micro-assessments in terms of improving the quality of observations and detection of change. While in some cases, the intensity of the change was not clearly manifested, the outputs point to identification of hotspots that require further evaluation at localized scales to understand the climate-human interactions and structure appropriate responses and adaptation strategies.

Furthermore, even in "well-known" hotspots, such as parts of Northern Meru, Machakos, Kitui and Makueni, the varying degrees and intensities of change can inform a restructuring and review of priorities and the efficacy of existing adaptation structures. From the assessments, distinct losses and gains are being observed as both seasons change, presenting a changing potential that needs to be factored in, in the design and investments in climate adaptation and mitigation potentially responding more effectively to the diverse needs of farmers (Gebre et al., 2023; Manzi & Gweyi-onyango, 2020).

6 CONCLUSIONS, RECOMMENDATIONS AND CONTRIBUTION TO KNOWLEDGE

6.1 Conclusions

This research has successfully unveiled the dynamic landscape of changing and variable climate, as well as shedding light on the inversely shifting Agro-Ecological Zones (AEZ) in Kenya's Lower Eastern Region. The confirmed hypothesis underscores a pivotal moment for rethinking the conventional "business as usual" approach to climate investments and adaptation strategies. As COP27 sounded the alarm for transformative action, it is evident that the historical trajectory has not yielded commensurate gains in emission reduction, necessitating a change in basic assumptions in our approach.

The identified trend of decreasing agro-potential in traditionally labelled "food basket areas" and a simultaneous increase in low agro-potential regions, particularly in Arid and Semi-Arid Areas, calls for urgent action. The research proposes a groundbreaking method of prioritizing agriculture investments and adaptation strategies. By aligning these strategies with climate projections, we advocate for a forward-thinking workflow that can enhance the effectiveness of climate adaptation efforts and optimize Return on Investment (ROI).

Recognizing the pivotal role of Agro-Ecological zonation in the Farm Management Handbook, this study emphasizes the transformative potential of emerging technologies, data, and techniques. We envision a game-changing scenario where adaptation priorities and investments are redefined in terms of scale, timeliness, and customization, ensuring a more precise alignment with the evolving climate dynamics.

A key revelation from COP27 underscores the pressing need to rethink our trajectory in climate adaptation and investments. The African continent is increasingly turning towards farmer-centric digital systems, a strategic move to strengthen policy decisions and tailor services, investments, and interventions for farmers. Updated AEZ maps emerge as a critical input in this digital transition, yet

their true value lies in their adjustment based on future climate predictions and the anticipated changes in agro potential.

6.2 Recommendations

Considering the research findings, which provide compelling evidence of ongoing and future climate changes, the study proposes **<u>five key recommendations</u>** to elevate the country's responses and maximize returns on adaptation and resilience investments.

6.2.1 Future proof agriculture investments and adaptation priorities

Emerging tech innovations are allowing predicting the future with greater accuracy, with large volumes of historical data learning from past patterns to give a clearer picture of future climate and agriculture risks. Decisions are increasingly depending on early warning information. Adaptation and considerable shifts require time. In the face of climate change and other uncertainties, it is crucial for agricultural and resilience strategies to be forward-thinking and adaptable. This recommendation emphasizes the need to prioritize and allocate investments in agriculture and resilience based on future risk assessments. By considering future potential risks and vulnerabilities, policymakers can make informed decisions and ensure that resources are directed towards building a resilient and sustainable agricultural sector.

Specifically, by conducting comprehensive risk assessments and scenario planning, we can identify potential future risks and vulnerabilities in the agricultural sector. This includes not only analyzing climate variation projections but include other variables of production such as water availability, market dynamics, pest and disease outbreaks, an understanding of the broad range of potential risks to agriculture, policymakers can develop strategies and investments that address both current challenges and emerging threats.

IF the correct future risk adjusted investments are made, farmers are also aware of the anticipated future risks and opportunities, giving them adequate time to adjust or transform their practices resulting in greater gains in investments made, as well is greater resilience and capacities of farmers to cope

with a changing climate, as well as opportunities to cash in on emerging opportunities to utilize the changing climate to make better economic and farming decisions and investments.

Prioritizing investments in climate-smart agriculture is also crucial for future risk-adjusted planning. Climate-smart agricultural practices emphasize the integration of adaptation and mitigation strategies to enhance resilience and reduce greenhouse gas emissions. Such investments can strengthen the capacity of the agricultural sector to prevail against future climate uncertainties and ensure long-term food security.

Further, where farm size allows, promoting diversification of agricultural activities and supporting value addition can help reduce risks associated with market fluctuations and climate variability. Farmers can be advised to plant drought resistant crops, livestock breeds, and engage in other income generating activities. Additionally, the government should continue to invest in value addition infrastructure, such as processing facilities and storage systems, which can help farmers capture higher market value for their products, provide off-farm employment and reduce post-harvest losses.

Resilience-building should occur also at multiple scales, including farm-level, community-level, and national-level. Investments should be directed towards building resilient infrastructure, such as irrigation systems, early warning systems, and climate-resilient storage facilities. Additionally, supporting community-based organizations, cooperatives, and farmer networks can strengthen social capital and facilitate knowledge sharing and collective action in response to risks immediate and anticipated risks.

Additional investments should also be made in research and innovation. This includes funding scientific research on climate change impacts, emerging pests and diseases, and innovative farming technologies. By supporting innovation, policymakers can facilitate the development and adoption of innovative solutions that enhance agricultural resilience and productivity. Additionally, partnerships between research institutions, private sector entities, and farmers can promote the co-creation of knowledge and the translation of research findings into practical and context-specific interventions.

By prioritizing and investing in agriculture and resilience strategies that are future risk-adjusted, policymakers can proactively address emerging challenges and safeguard the livelihoods of farmers and rural communities both now and into the future.

6.2.2 Digitize and localize the farm management handbook

Cloud computing, automation methods, freely available medium resolution satellites provide an opportunity to develop and automate scalable and replicable methods for creating updated and detailed information to support decision making. The Farm management handbook needs to be digitized to ensure that agriculture and resilience priorities are based on the wealth of past, present and future "best available information."

By harnessing emerging technologies, such as artificial intelligence (AI) and machine learning, the farm management handbook can be continuously updated based on real-time data and insights. Additional information can be generated to add value from other automated systems that collect and analyze agricultural data, including climate patterns, soil conditions, pest and disease outbreaks, and market trends. This data-driven approach allows for more accurate and targeted updates to the handbook, ensuring that the information and recommendations provided are based on the most recent and relevant data available.

Digitizing the farm management handbook allows for real-time updates and revisions. With agricultural knowledge continually evolving, new research findings, innovative techniques, and changing climatic conditions can be incorporated to revise and update the handbook. This would ensure that farmers receive accurate and timely guidance that aligns with current updated analyses and the corresponding agricultural practices and adaptation strategies.

6.2.3 Localize advisories to be location specific, crop specific, and appropriate to regions and agro-climatic conditions.

By incorporating data on local agricultural practices, soil types, and weather patterns, the digital handbook can provide more targeted, localized and context-specific recommendations. Tailored

guidance enhances the effectiveness of the handbook and increases its relevance for farmers, enabling them to make informed decisions that suit their specific circumstances.Recommendation 3: Agro potential is changing inversely, reducing in high potential areas, and improving in low potential areas in Kenya

By understanding that viability for agriculture systems will shift, Kenya needs to adjust, and change the direction and trajectory of investments, and especially updating of e-extension and support to farmers to adjust accordingly. But also, develop mechanisms to match national recommendations to farmers existing adaptation mechanisms to create the right "fit." This recommendation highlights the need to recognize and respond to the changing agro potential by implementing targeted strategies to address the reduction in high potential areas and harness the improving potential in low potential areas in Kenya.

With the reduction in agro potential in high potential areas, it will be necessary to diversify agricultural practices to adapt to the changing conditions. Farmers and agricultural stakeholders should be encouraged explore alternative crops, farming systems, and agroecological approaches that are better suited to the emerging agro-climatic conditions. This may involve promoting climate-resilient crop varieties, agroforestry, conservation agriculture, and sustainable soil and water management practices. With such adjustments, farmers can mitigate risks, optimize resource use, and maintain productivity even in the face of reduced agro potential.

Technological advancements can contribute greatly to optimizing agricultural production in both low and high agro-potential areas. In high potential areas, precision agriculture technologies, such as remote sensing, geoinformation systems and data analytics, can construct advisories that help farmers make informed decisions regarding irrigation, fertilization, and pest management. In low potential areas, innovative approaches like hydroponics, vertical farming, and greenhouse farming can be explored to improve productivity and optimize resource use. Embracing digital technologies and

promoting innovation in agriculture can enhance the resilience and productivity of farming systems across diverse agro potential areas.

Water availability is a critical factor in agricultural production, particularly in areas experiencing agro potential changes. In high potential areas facing reduced agro potential, farmers and policymakers should focus on improving water resource management through efficient irrigation systems, water harvesting, and conservation practices. In low potential areas experiencing improving agro potential, efforts should be made to enhance water availability and accessibility through small-scale irrigation schemes, water storage facilities, and watershed management programs. Effective water resource management is critical in ensuring sustainable agricultural production in both high and low potential areas.

Enhancing the capacity and knowledge of farmers and agricultural stakeholders is essential to adapt to the changing agro potential. Training programs, extension services, and farmer-to-farmer knowledge sharing initiatives should be prioritized. Farmers need to be equipped with climate-smart agricultural practices, modern techniques, and information on market opportunities. Special attention should be given to empowering smallholder farmers, women, and youth in low potential areas, enabling them to harness the improving agro potential and contribute to local food production and livelihoods.

6.2.4 Localize adaptation mechanisms to suit gendered, socio-economic and indigenous preferences

Farmers always find ways to adopt. From this research, male and female headed households adapted differently. With male headed households prioritizing on cash crops with greater incomes realized, while female headed households prioritized food crops with relatively lower incomes realised. This is because, women, due to their nurturing nature, will focus on strengthening the household food security first. As we strive to promote sustainable agriculture and climate resilience, it is crucial to recognize and address the varying adaptation needs of different farming communities. This recommendation

emphasizes the importance of sensitivity to gender and indigenous adaptation in agricultural development strategies, policies, and programs.

Women play a significant role in agriculture, yet they often face distinct challenges as their immediate goal is always to feed their families first. Gender disparities in access to resources, autonomy in decision making, land ownership and information negatively impacts women's ability to adapt to changing environmental conditions. To address this, agricultural policies and programs should be gender-sensitive and promote gender equity in access to resources, technology, extension services, and market opportunities. Additionally, capacity-building initiatives should focus on empowering women farmers by enhancing their skills, knowledge, and leadership capabilities in climate-smart agriculture practices.

Indigenous communities possess a wealth of traditional knowledge and adaptation strategies that have been passed down through generations. This knowledge is significant in strengthening resilience and should be recognized and integrated into agricultural policies and practices. Governments and development organizations should engage with indigenous communities as partners, respecting their rights, traditional knowledge systems, and cultural practices. By collaborating with indigenous communities, we can develop context-specific adaptation strategies that preserve traditional agricultural practices while incorporating modern technologies and scientific insights.

Effective adaptation strategies require the active involvement of farmers themselves. Implementing participatory approaches that include farmers in decision-making processes, planning, and program design is essential. This ensures that their unique perspectives, needs, and priorities are considered. By engaging farmers in the design and implementation of adaptation programs, we can foster ownership, increase effectiveness, and promote sustainable agricultural practices that align with local contexts and realities.

Further, adequate data collection and research efforts will be needed to understand the specific challenges and adaptation needs of different farming communities. Governments, research institutions,

and development organizations should prioritize gender-disaggregated data collection and analysis to identify gender-specific vulnerabilities and opportunities for adaptation. Similarly, research should incorporate indigenous knowledge systems and collaborate with indigenous communities to develop robust and context-specific adaptation approaches.

By recognizing and addressing the varying adaptation needs of different farming communities, we can promote inclusivity, gender equity, and account for indigenous knowledge in agricultural adaption strategies. Sensitivity to gender and indigenous adaptation ensures that no farmer is left behind and paves the way for sustainable, resilient, and socially just agricultural systems. Embracing the diversity of farmers' experiences and empowering all stakeholders in adaptation efforts will contribute to more effective and impactful agricultural interventions in the face of climate change.

6.2.5 Utilize digital technologies to bridge the gap in government and private sector led farmer facing services.

Farmers were able to access digital information such as weather forecasts irrespective of their education background. Digital and broadband connectivity will play a key role in increasing access to information and services by farmers. In today's interconnected world, digital technologies have emerged as powerful tools that can revolutionize various sectors, including agriculture. Farmers, who form the backbone of our food production system, stand to benefit significantly from the integration of digital technologies into their daily practices. By leveraging these tools, governments and private sector entities can bridge the gap in delivering farmer-facing services, thereby empowering farmers with crucial information, resources, and support.

This recommendation emphasizes the importance of harnessing digital technologies to enhance agricultural services and create a more inclusive and efficient farming ecosystem.

Digital technologies enable the dissemination of timely and accurate information to farmers, which is crucial for making informed decisions. Governments and private sector organizations should collaborate to develop user-friendly mobile applications and SMS-based services that provide farmers

with real-time weather updates, market prices, pest, and disease alerts, farming best practices, and government schemes. This information empowers farmers to optimize their agricultural practices, improve productivity, and make informed choices based on market trends. Digital technologies can also enhance extension services, especially given the limitations facing extension officers who often are allocated large areas. By incorporating digital technologies into extension services, governments and private sector entities can overcome the limitations of traditional outreach methods. Digital technologies can also bridge the gap between farmers and markets, thereby improving access to better prices and reducing intermediaries. Digital applications can cut middlemen and connect farmers directly with buyers, agribusinesses, and value chain stakeholders resulting in better profits and returns. These platforms can provide information on demand, supply, price trends, and facilitate transparent transactions. Additionally, digital payment systems and logistics support can streamline the flow of agricultural produce, reducing post-harvest losses and improving overall profitability for farmers.

Further, digital technologies can enhance access to finance which is a significant challenge for many small-scale farmers. Digital technologies can facilitate customized financial services tailored to the specific needs of farmers, making credit, insurance, and savings products more accessible. Governments and financial institutions should collaborate to develop digital platforms that leverage data analytics, remote sensing, and machine learning algorithms to assess creditworthiness, provide weather-based insurance, and enable efficient disbursement of subsidies and financial support to farmers.

But, to fully harness the potential of digital technologies, it is essential to ensure that farmers have the necessary digital literacy skills. Governments, in collaboration with private sector entities, should launch training programs and capacity-building initiatives to enhance farmers' digital literacy. Furthermore, efforts should be made to bridge the digital divide by providing access to affordable

internet connectivity and devices in rural areas, ensuring that no farmer is left behind in benefiting from digital farmer-facing services.

In conclusion, digital technologies present immense opportunities for bridging the gap in delivering farmer-facing services. By embracing these technologies, governments and private sector entities can enhance information access, extension services, market linkages, financial services, and digital literacy among farmers. This transformation will empower farmers, improve agricultural productivity, foster sustainable practices, and ultimately contribute to strengthening rural households' incomes and their capacity to produce enough food.

6.3 Contribution to Knowledge

This section articulates the transformative contributions made by this research to the existing body of knowledge, particularly within the domain of technologies for climate and agriculture adaptation in Kenya's Lower Eastern Region. The study introduces innovative methodologies and forward-thinking paradigms, transcending conventional approaches and significantly enriching our perspectives on transforming climate adaptation. Three pivotal contributions are highlighted, each distinct yet collectively shaping a comprehensive advancement in the field.

Firstly, the research introduces a revised methodology that strategically harnesses satellite estimates. Departing from traditional approaches, this method enables the utilization of freely available satellite data, overcoming historical challenges of prohibitive costs, time intensiveness, and data limitations. By doing so, the study not only presents an efficient solution but also establishes a foundation for more frequent and cost-effective updates. This ensures the perpetual accuracy and relevance of Agro-Ecological Zone (AEZ) maps, thereby creating a sustainable framework for climate adaptation efforts.

Secondly, the research pioneers a scalable, reproducible cloud-based satellite-derived workflow specifically designed for mapping AEZ at a high granularity within Kenya's Lower Eastern Region. This workflow transcends regional boundaries, representing all of Kenya's AEZ. The innovation lies

in its ability to synthesize satellite data with ground information from field questionnaires, offering a nuanced understanding of the region's agro-ecological dynamics. The resultant micro-scale mapping enhances precision, providing a robust foundation for gender-sensitive adaptation mechanisms and investments.

Thirdly, the research introduces a novel approach that embraces a future risk-adjusted perspective in assessing agro-potential. This departure from historical baseline-driven methods underscores the study's commitment to a forward-thinking prioritization of resilience investments and interventions. Recognizing the dynamic nature of climate patterns, the research advocates for strategies informed by future projections rather than past conditions, especially crucial in areas with limited prior research, such as the Lower Eastern Region. Furthermore, the study explores innovative methods to adjust existing methodologies at the finest scale possible, ensuring their adaptability in the face of evolving climatic conditions. By assessing changes in AEZ due to climate change, the research contributes to the broader discourse on improving the accuracy of climate change impact assessments.

In a notable departure from existing research, the study shifts the narrative from focusing on negative consequences to <u>emphasizing emerging opportunities for adaptation</u>. By identifying shifts in seasons and production potential, particularly in lowland drylands and midland highland areas, the research outlines potential strategies for diversifying production systems and enhancing resilience. This positive perspective on opportunities provides a fresh outlook on how current and future adaptation and mitigation policies can be shaped.

In summation, **this research marks a significant advancement in the field by seamlessly combining technological innovation, methodological exploration, and a forward-thinking paradigm**. It offers a holistic and impactful contribution to the understanding and management of climate change impacts on agriculture in Kenya's Lower Eastern Region. The findings not only inform local policies and interventions but also provide valuable insights applicable to broader climate adaptation strategies in similar agro-ecological contexts.

7 REFERENCES

Adhikari, U., Nejadhashemi, A. P., & Woznicki, S. A. (2015). Climate change and eastern Africa: A review of impact on major crops. *Food and Energy Security*, *4*(2), 110–132. https://doi.org/10.1002/fes3.61

Amani, M., Ghorbanian, A., Ahmadi, S. A., Kakooei, M., Moghimi, A., Mirmazloumi, S. M., Moghaddam, S. H. A., Mahdavi, S., Ghahremanloo, M., Parsian, S., Wu, Q., & Brisco, B. (2020). Google Earth Engine Cloud Computing Platform for Remote Sensing Big Data Applications: A Comprehensive Review. *IEEE Journal of Selected Topics in Applied Earth Observations and Remote Sensing*, *13*(September), 5326–5350. https://doi.org/10.1109/JSTARS.2020.3021052

Antony, O. (2017). *Climate variability and change as stressors in a high potential agriculture zone in Kenya*.

Aravind, N. (2006). *Agro-climatical zoning using temporal satellite data and GIS*. *1*(2), 48–53.

Batjes, N. H., & Gicheru, P. (2004). *Soil data derived from SOTER for studies of carbon stocks and change in Kenya (Version 1.0) Global Environment Facility United Nations Environment Programme Netherlands Ministry of Housing, Spatial Planning and the Environment Kenya Agricultural Research Institute*.

Boitt, M., Pellikka, P. K. E., & Hills, T. (2016). *Modelling the Impacts of Climate Change on Agro-Ecological Zones – a Case Study of Taita Modelling the Impacts of Climate Change on Agro-Ecological Zones – a Case Study of*. *July 2014*.

Breisinger, C., Diao, X., Dorosh, P., Mbuthia, J., Omune, L., Oseko, E. O., Pradesha, A., Smart, J., & Thurlow, J. (2022). *Kenya : Impacts of the Ukraine and Global Crises on Poverty and Food Security*. *June*, 1–12.

Cairns, J. E., Sonder, K., Araus, J. L., Hellin, J., Thierfelder, C., Prasanna, B. M., & MacRobert, J. F. (2013). Adapting maize production to climate change in sub-Saharan Africa. *Food Security*, *5*(3), 345–360. https://doi.org/10.1007/s12571-013-0256-x

Cassel-Gintz, M. A., Lüdeke, M. K. B., Petschel-Held, G., Reusswig, F., Plöchl, M., Lammel, G., & Schellnhuber, H. J. (1997). Fuzzy logic based global assessment of the marginality of agricultural land use. *Climate Research*, *8*(2), 135–150. https://doi.org/10.3354/cr008135

DE4A (Digital Economy for Africa Initiative). (2023). *Digital Transformation Strategy for Africa*. https://www.worldbank.org/en/programs/all-africa-digital-transformation

Eichsteller, M., Njagi, T., & Nyukuri, E. (2022). The role of agriculture in poverty escapes in Kenya – Developing capabilities approach in the context of climate change. *World Development*, *149*, 105705. https://doi.org/10.1016/j.worlddev.2021.105705

Endris, H. S., Omondi, P., Jain, S., Lennard, C., Hewitson, B., Chang'a, L., Awange, J. L., Dosio, A., Ketiem, P., Nikulin, G., Panitz, H. J., Büchner, M., Stordal, F., & Tazalika, L. (2013). Assessment of the performance of CORDEX regional climate models in simulating East African rainfall. *Journal of Climate*, *26*(21), 8453–8475. https://doi.org/10.1175/JCLI-D-12-00708.1

EroHerr, M., Ringler, C., Steeg, J. Van De, Koo, J., & Notenbaert, A. (2010). Climate variability and climate change and their impacts on Kenya's agricultural sector. *ILRI, Nairobi. Kenya*, 1–56. https://doi.org/10.1038/ni.2833\rhttp://www.nature.com/ni/journal/v15/n4/abs/ni.2833.html#supplementary-information

FAO. (1996). *Agro Ecological Zonation Guidelines: Vol. FAO SOILS*. https://doi.org/10.1016/0009-2797(75)90001-0

FAO. (2010). *Analysis of Climate Change and Variability Risks in the Smallholder Sector: Case studies of the Laikipia and Narok Districts*.

FEWSNET. (2022). *Fewsnet Food Security Assessment*. https://fews.net/east-africa/kenya/food-security-outlook/february-2022#:~:text=In February 2022%2C the KFSSG's,percent increase since August 2021.

Gebre, G. G., Amekawa, Y., Fikadu, A. A., & Rahut, D. B. (2023). Farmers′ use of climate change adaptation strategies and their impacts on food security in Kenya. *Climate Risk Management*, *40*. https://doi.org/10.1016/j.crm.2023.100495

Gleixner, S., Demissie, T., & Diro, G. T. (2020). *Did ERA5 Improve Temperature and Precipitation Reanalysis over East Africa ?* 1–19. https://doi.org/10.3390/atmos11090996

Greve, P., Roderick, M. L., Ukkola, A. M., & Wada, Y. (2019). The aridity Index under global warming. *Environmental Research Letters*, *14*(12). https://doi.org/10.1088/1748-9326/ab5046

Herrick, J. E., Beh, A., Barrios, E., Bouvier, I., Coetzee, M., Dent, D., Elias, E., Hengl, T., Karl, J. W., Liniger, H., Matuszak, J., Neff, J. C., Ndungu, L. W., Obersteiner, M., Shepherd, K. D., Urama, K. C., Bosch, R., & Webb, N. P. (2016). The land-potential knowledge system (landpks): mobile apps and collaboration for optimizing climate change investments. *Ecosystem Health and Sustainability*, *2*(3). https://doi.org/10.1002/ehs2.1209

Holzkämper, A. (2017). Adapting Agricultural Production Systems to Climate Change—What's the Use of Models? *Agriculture*, *7*(10), 86. https://doi.org/10.3390/agriculture7100086

Indeje, M., Ogallo, L. J., Davies, G., Dilley, M., & Anyamba, A. (2005). Predictability of the Normalized Difference Vegetation Index in Kenya and Potential Applications as an Indicator of Rift Valley Fever Outbreaks in the Greater. *Journal of Climate*, *19*(1674). https://doi.org/10.3989/alqantara.2003.v24.i2.168

IPCC. (2007). IPCC, 2007: Climate Change 2007: Synthesis Report. In *Contribution of Working Groups, I, II and III to the Fourth Assessment Report of the Intergovernmental Panel on Climate Change [Core Writing Team, Pachauri, R.K and Reisinger, A. (eds.)].* https://doi.org/10.1256/004316502320517344

Jaetzold, R., & Schmidt, H. (1983). *Farm Management Handbook of Kenya (Vol.II, Part C): Natural Conditions and Farm Management Information, East Kenya*. Ministry of Agriculture.

Jatzold, R., & Kutsch, H. (1982). Agro-ecological zones of the tropics, with a sample from Kenya. *Tropenlandwirt*, *83*(April 1982), 15–34.

Jones, C. D., Hughes, J. K., Bellouin, N., Hardiman, S. C., Jones, G. S., Knight, J., Liddicoat, S., O'Connor, F. M., Andres, R. J., Bell, C., Boo, K. O., Bozzo, A., Butchart, N., Cadule, P., Corbin, K. D., Doutriaux-Boucher, M., Friedlingstein, P., Gornall, J., Gray, L., … Zerroukat, M. (2011). The HadGEM2-ES implementation of CMIP5 centennial simulations. *Geoscientific Model Development*, *4*(3), 543–570. https://doi.org/10.5194/gmd-4-543-2011

Kabubo-Mariara, J., & Kabara, M. (2015). *Environment for Development Centers Climate Change and Food Security in Kenya*. 1–36. https://doi.org/10.1007/978-90-481-9516-9

Kazembe, A., & Kenya, N. (2014). *DETERMINING THE ONSET AND CESSATION OF SEASONAL RAINS IN MALAWI Post Graduate Diploma (PGD) Research project submitted in Partial fulfilment for the Degree of Post Graduate Diploma in Meteorology*.

Kenduiywo, B. K., Ghosh, A., Hijmans, R., & Ndungu, L. (2020). Maize Yield Estimation in Kenya Using Modis. *ISPRS Annals of the Photogrammetry, Remote Sensing and Spatial Information Sciences*, *3*, 477–482.

KNBS. (2019). *2019 Kenya Population and Housing Census: Volume II i: Kenya National Bureau of Standards*.

Knox, J., Hess, T., Daccache, A., & Wheeler, T. (2012). Climate change impacts on crop productivity in Africa and South Asia. *Environmental Research Letters*, *7*(3). https://doi.org/10.1088/1748-9326/7/3/034032

Kogo, B. K., Kumar, L., Koech, R., Endris, H. S., Omondi, P., Jain, S., Lennard, C., Hewitson, B., Chang'a, L., Awange, J. L., Dosio, A., Ketiem, P., Nikulin, G., Panitz, H. J., Büchner, M., Stordal, F., Tazalika, L., Onyutha, C., Asiimwe, A., … Schirmbeck, J. (2021). Observed and future precipitation and evapotranspiration in water management zones of uganda: Cmip6 projections. *Land*, *23*(1), 1–15. https://doi.org/10.1007/s10668-020-00589-1

Kotir, J. H. (2011). Climate change and variability in Sub-Saharan Africa: A review of current and future trends and impacts on agriculture and food security. *Environment, Development and Sustainability*, *13*(3), 587–605. https://doi.org/10.1007/s10668-010-9278-0

Kurukulasuriya, P., & Mendelsohn, R. (2008). How Will Climate Change Shift Agro-Ecological Zones and Impact African Agriculture? *Policy Research Working Paper WPS/4717*, *September*, 1–31. hhttp://documents.worldbank.org/curated/en/603161468194653382/pdf/WPS4717.pdf

Lane, A., & Jarvis, A. (2007). Changes in Climate will modify the Geography of Crop Suitability: Agricultural Biodiversity can help with Adaptation. *SAT EJournal :An Open Access Journal Published by ICRISAT*, *4*(1), 1–12. https://doi.org/10.3914/ICRISAT.0094

Lane, Annie; Jarvis, A. (2007). Changes in Climate will modify the Geography of Crop Suitability: Agricultural Biodiversity can help with Adaptation. *SAT EJournal :An Open Access Journal Published by ICRISAT*. https://doi.org/10.3914/ICRISAT.0094

Lin, Y., Liu, A., Ma, E., & Zhang, F. (2013). Impacts of Future Climate Changes on Shifting Patterns of the Agro-Ecological Zones in China. *Advances in Meteorology*, *2013*, 1–9. https://doi.org/10.1155/2013/163248

Liu, C., White, M., & Newell, G. (2018). Detecting outliers in species distribution data. *Journal of Biogeography*, *45*(1), 164–176. https://doi.org/10.1111/jbi.13122

Liu, P. (2015). The future of food and agriculture: Trends and challenges. In *Food and Agriculture Organization of the United Nations*. http://www.fao.org/3/a-i6583e.pdf

Macharia, D., Kaijage, E., Kindberg, L., Koech, G., Ndungu, L., Wahome, A., & Mugo, R. (2020). Mapping Climate Vulnerability of River Basin Communities in Tanzania to Inform Resilience Interventions. *Sustainability*, *12*(10), 4102.

Manzi, H., & Gweyi-onyango, J. (2020). African Handbook of Climate Change Adaptation. *African Handbook of Climate Change Adaptation*, *February*. https://doi.org/10.1007/978-3-030-42091-8

Miller, S., Adams, E. C., Markert, K., Ndungu, L. W., Ellenberg, W. L., Mishra, V., & Anderson, E. R. (2019). Assessment of a spatially and temporally consistent MODIS derived NDVI product for application in index-based drought insurance. *AGUFM*, *2019*, GC51F--1132.

Mulinge, E., Gicheru, P., Muriithi, F., & Kihiu, E. (2015). Economics of Land Degradation and Improvement in Kenya. *Economics of Land Degradation and Improvement - A Global Assessment for Sustainable Development*, *April*, 1–686. https://doi.org/10.1007/978-3-319-19168-3

Muok, B., Ochieng, A. A., Kungu, K. J., Tonui, C., & Wakhungu, P. J. W. (2012). *Case Study on Climate Compatible Development (CCD) in Agriculture for Food Security in Kenya Prepared by : Technical Guidance and Support : African Centre for Technology studies (ACTS) Project : Advancing Climate Compatible Development for Food Securi*. *November*.

Musafiri, C. M., Kiboi, M., Macharia, J., Ng'etich, O. K., Kosgei, D. K., Mulianga, B., Okoti, M., & Ngetich, F. K. (2022). Smallholders' adaptation to climate change in Western Kenya: Considering socioeconomic, institutional and biophysical determinants. *Environmental Challenges*, *7*. https://doi.org/10.1016/j.envc.2022.100489

Muthoni, F. K., Odongo, V. O., Ochieng, J., Mugalavai, E. M., Mourice, S. K., Hoesche-Zeledon, I., Mwila, M., & Bekunda, M. (2019). Long-term spatial-temporal trends and variability of rainfall over Eastern and Southern Africa. *Theoretical and Applied Climatology*, *137*(3–4), 1869–1882. https://doi.org/10.1007/s00704-018-2712-1

Nakalembe, C., Becker-Reshef, I., Bonifacio, R., Hu, G., Humber, M. L., Justice, C. J., Keniston, J., Mwangi, K., Rembold, F., Shukla, S., Urbano, F., Whitcraft, A. K., Li, Y., Zappacosta, M., Jarvis, I., & Sanchez, A. (2021). A review of satellite-based global agricultural monitoring systems available for Africa. *Global Food Security*, *29*, 100543. https://doi.org/10.1016/j.gfs.2021.100543

Nakalembe, C. L., Becker-Reshef, I., Justice, C. J., Dempewolf, J., Ndungu, L. W., Mwangi, K., Dienya, T., Owor, M., Mtalo, M., & Justice, C. O. (2019). Leveraging Earth Observation for agriculture monitoring in Eastern Africa. *AGUFM*, *2019*, GC51F--1139.

Ndungu, L. W., Oware, A. M., Otieno, S. O., Wahome, A. M., Mugo, R., & Adams, E. C. (2019). Application of MODIS NDVI for Monitoring Kenyan Rangelands through a Web Based Decision Support Tool. *Frontiers in Environmental Science*, *7*, 187.

Ngigi, M. W., & Muange, E. N. (2022). Access to climate information services and climate-smart agriculture in Kenya: a gender-based analysis. *Climatic Change*, *174*(3–4). https://doi.org/10.1007/s10584-022-03445-5

Obwocha, E. B., Ramisch, J. J., Duguma, L., & Orero, L. (2022). The Relationship between Climate Change, Variability, and Food Security: Understanding the Impacts and Building Resilient Food Systems in West Pokot County, Kenya. *Sustainability (Switzerland)*, *14*(2). https://doi.org/10.3390/su14020765

Ochieng, J., Kirimi, L., & Mathenge, M. (2016). Effects of climate variability and change on agricultural production: The case of small scale farmers in Kenya. *NJAS - Wageningen Journal of Life Sciences*, *77*(2016), 71–78. https://doi.org/10.1016/j.njas.2016.03.005

Ojwang, G., Agatsiva, J., & Situma, C. (2010). *Analysis of Climate Change and Variability Risks in the Smallholder Sector. Case studies of the Laikipia and Narok Districts representing major agro-ecological zones in Kenya . Ministry of Environment and Natural Resources Working Paper.*

Patel, N. R. (2007). *Remote Sensing and Gis Application in Change*. *35*(4), 3–5.

Praseyto, S. Y. J., S., B. H., Hartomo, K. D., Paseleng, M., & Nuswantoro, B. (2013). Geographic Information System of Critical Level of Land Degradation (Critical Land) Based on Agro-ecological Zone (AEZ) in Agricultural Areas with Recombination Method of Fuzzy Logic and Scoring. *International Journal of Computer Science Issues*, *10*(6), 217–221.

R. Quiroz, Zorogastúa, P., Baigorria, G., Barreda, C., Valdivia, R., Cruz, M., & J. Reinoso. (2000). *Toward A Dynamic Definition of Agroecological Zones Using Modern Information Technology Tools, CIP program report 1999-2000.* 361–370.

Ratcheva, Vesselina., Zahidi, Saadia., [et al.], Pal, K. Kali., Piaget, Kim., Baller, Silja., & World Economic Forum. (2022). *Global gender gap report 2022 : insight report.*

RCMRD. (2018). *Downscaling climate data and run off projections for KIWASH project counties Deliverable : Technical Report.*

Rios, P. (2015). Assessment Of Impacts of Climate Change and Variability on Food Security in West Pokot County, Kenya. *Biomass Chem Eng*, *49*(23–6).

Sagero, P. O., Shisanya, C. A., & Makokha, G. L. (2021). *Projected Changes in Rainfall and Temperature Extremes Over Kenya.*

Schlenker, W., Lobell, B. D., Bryan, E., Ringler, C., Okoba, B., Roncoli, C., Silvestri, S., Herrero, M., Nhemachena, C., Rashid, H., Narayanan, K., Sahu, S. K., Mertz, O., Mbow, C., Reenberg, A., Diouf, A., Below, T., Artner, A., Siebert, R., … Program, S. (2010). Determinants of African farmers' strategies for adapting to climate change: Multinomial choice analysis. *Environmental Management*, *114*(1), 83–104. http://10.0.72.88/cs/v110/i7/1240-1250%5Cnhttp://ezproxy.unal.edu.co/login?url=http://search.ebscohost.com/login.aspx?direct=true&db=a9h&AN=114335616&lang=es&site=eds-live%0Ahttp://stacks.iop.org/1748-9326/5/i=1/a=014010

Seo, S. N. (2014). Evaluation of the Agro-Ecological Zone methods for the study of climate change with micro farming decisions in sub-Saharan Africa. *European Journal of Agronomy*, *52*, 157–165. https://doi.org/10.1016/j.eja.2013.09.014

Sharma, D. K., Jana, R. K., & Gaur, A. (2007). Fuzzy goal programming for agricultural land allocation problems. *Yugoslav Journal of Operations Research*, *17*(1), 31–42. https://doi.org/10.2298/YJOR0701031S

Shukla, S., Macharia, D., Husak, G. J., Landsfeld, M., Nakalembe, C. L., Blakeley, S. L., Adams, E. C., & Way-Henthorne, J. (2021). Enhancing Access and Usage of Earth Observations in Environmental Decision-Making in Eastern and Southern Africa Through Capacity Building. *Frontiers in Sustainable Food Systems*, *5*(April). https://doi.org/10.3389/fsufs.2021.504063

Silvestri, S., Bryan, E., Ringler, C., Herrero, M., & Okoba, B. (2012). Climate change perception and adaptation of agro-pastoral communities in Kenya. *Regional Environmental Change*, *12*(4), 791–802. https://doi.org/10.1007/s10113-012-0293-6

Stige, L. C., Stave, J., Chan, K.-S., Ciannelli, L., Pettorelli, N., Glantz, M., Herren, H. R., & Stenseth, N. C. (2006). The effect of climate variation on agro-pastoral production in Africa. *Proceedings of the National Academy of Sciences*, *103*(9), 3049–3053. https://doi.org/10.1073/pnas.0600057103

Twagiramungu, J. R. (2022). *Transformation of organizations through cloud technologies-challenges & benefits. Case study in Rwanda.*

Vermeulen, S., Aggarwal, P., Campbell, B., Davey, E., Grainger-Jones, E., & Yao, X. (2014). *Climate change, food security and small-scale producers*.

Vrieling, A., De Leeuw, J., & Said, M. Y. (2013). Length of growing period over africa: Variability and trends from 30 years of NDVI time series. *Remote Sensing*, *5*(2), 982–1000. https://doi.org/10.3390/rs5020982

8 APPENDICES

8.1 APPENDIX 1A -DATA COLLECTION TOOLS

8.1.1 The data collection form on kobo toolbox

Revised data collection form on Farmers Adaptation to Climate Change in Meru Embu Tharaka Kitui Makueni and Machakos

Data Collector Name

- ◯ Annrita Gitonga- Tharaka Mwimbi
- ◯ Magdalene Neema- Tharaka Igambangombe
- ◯ Beatrice Ndegi- Embu Nthawa
- ◯ Evanson Ngondi- Embu Muminji
- ◯ Joseph Ngugi- Meru Akachiu
- ◯ Gerald Kinyua- Antubetwe Kiongo
- ◯ Meru-Nyaki East
- ◯ Benard Makala - Machakos Upper Kaewa
- ◯ Elizabeth Mulika - Makueni Kiteta Kisau
- ◯ Eunice Sila- Makueni Muvau Kikumini
- ◯ Francis John- Makueni Kalanzoni
- ◯ Musau- Machakos North Matungulu
- ◯ Nicholas Kimeu - Machakos Kivaa
- ◯ Francis Sila- Kitui Mumoni
- ◯ John Kiilu- Kitui Mulango
- ◯ Purity Mukithi- Kitui Mutonguni
- ◯ Shadrack Mbuvi- Kitui Mutha
- ◯ Stella Mueni- Kitui Tseikuru

county

- ◯ Embu
- ◯ Meru
- ◯ Tharaka-Nithi
- ◯ Kitui
- ◯ Machakos
- ◯ Makueni

subcounty

ward

Record your current location

_____

latitude (x.y °)

_____

longitude (x.y °)

_____

altitude (m)

_____

accuracy (m)

_____

103
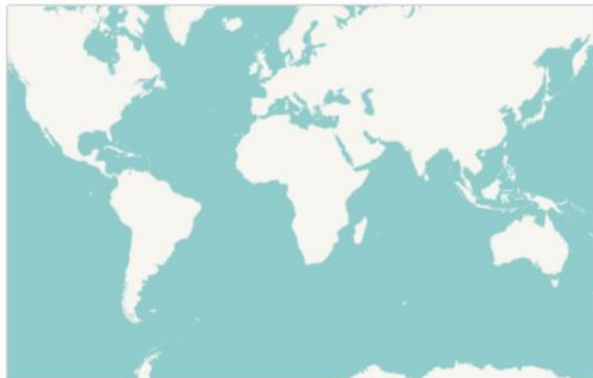
What is your name (Farmer)

_____

What is your Phone Number (Farmer)

The phone number will ONLY BE USED if verification or follow-up required?

_____

Gender

○ Male

○ Female

Age

○ 15-25

○ 26-35

○ 36-50

○ 51-65

○ >65

Education level

○ No formal education

○ Primary

○ Secondary

○ College/Tertiary

○ University

DEMOGRAPHICS

Number of People Living in Household

○ <3

○ 3-7

○ >7

What are your sources of income

☐ Crop farming

☐ Livestock farming

☐ Bee keeping

☐ Fishing

☐ off-farm employment

☐ government employment

☐ Pension

☐ Business

☐ Other (Please specify)

Please specify other sources of income

_____

Do you generally have enough food to sustain you till the next harvest?

○ Yes

○ No

○ Most of the time

○ I Dont Know

Where else do you get money or save to strengthen your farming activities or buy food?

☐ Relatives/siblings

☐ Table banking/ village savings groups

☐ microfinance/microcredit organizations

☐ digital loans like Mpesa, Mshwari, Tala etc

☐ Banks

☐ None

Do you farm using irrigation or you depend on rainfall for farming?

☐ Rainfed

☐ Irrigated

☐ Irrigated and Rainfed

What is the area of farm under irrigation?

_____

105

What are the main food crops that you grow in your farm?

- [ ] Maize
- [ ] Beans
- [ ] Rice
- [ ] Wheat
- [ ] Sorghum/Millet
- [ ] Greengrams
- [ ] Pigeon peas/ Cowpeas
- [ ] Cassava
- [ ] Sweet potatoes
- [ ] Other (please specify)

Please specify other food crops grown

_____

What are the main CASH crops & FRUIT TREES that you grow in your farm?

- [ ] Coffee
- [ ] Macadamia
- [ ] Avocadoes
- [ ] Oranges
- [ ] Bananas
- [ ] Mangoes
- [ ] Pawpaw
- [ ] Miraa
- [ ] Other (please specify)

Please specify other CASH crops & FRUIT TREES grown

a crop produced for its commercial value rather than for use by the grower

_____

What is the size (TOTAL estimate of acres) of farm where farming of food crops and cash crops is done (Own, rented etc)

_____

CLIMATE VULNERABILITY

106

How long have you lived here (Number of years)

◯ 5-10

◯ 10-20

◯ 20-30

◯ 30-40

◯ >50

What changes in rainfall, temperature and the growing season, have you observed in the time you have lived here?
Explain to the respondent that these changes in rainfall, temperature, growing season represent Climate Variability/Change

☐ Increased temperature

☐ Increased rain

☐ Increased Length of the growing/cropping season

☐ REDUCED temperatures

☐ ERRATIC rain

☐ REDUCED length of the growing/cropping season

How has your production changed in the years you have lived here?

◯ Increased

◯ Decreased

◯ Same

Have these changes in rainfall and temperature(climate variability/change) affected food production for your household ?

changes in rainfall and temperature over time

◯ Greatly Affected

◯ Slightly Affected

◯ Not affected

What has been the IMPACT of following factors of negative climate change and socio-economic factors on your FARM? 7=Extremely severe(Disastrous), 6=Very Severe(Critical),, 5=Severe, 4=Significant,3=Somewhat significant., 2=Irrelevant, 1=I don't know/Not Applicable	7	6	5	4	3	2	1
Abrupt changes in season	◯	◯	◯	◯	◯	◯	◯
Changes in timing of rain	◯	◯	◯	◯	◯	◯	◯
Increase frequency of drought and crop failure	◯	◯	◯	◯	◯	◯	◯
Increased frequency of floods and farm destructions	◯	◯	◯	◯	◯	◯	◯
Post harvest losses	◯	◯	◯	◯	◯	◯	◯

Pest invasion	○	○	○	○	○	○	○
Prevalence of crop and livestock diseases	○	○	○	○	○	○	○
Poverty and Food shortages	○	○	○	○	○	○	○
Lack of portable water	○	○	○	○	○	○	○
Erosion, soil fertility reduction, land degradation	○	○	○	○	○	○	○
Some crops are no longer viable (crop fails)	○	○	○	○	○	○	○
Frequent death of livestock	○	○	○	○	○	○	○
Rising cost of farming ie cost of seeds, fertilizer etc	○	○	○	○	○	○	○

In some cases, positive outcomes of climate change such as more stable rainfall during the growing season have been experienced. What have you observed to be the main opportunities (positive impacts) of these long term changes in the climate?

☐ Flood water for irrigation and water harvesting

☐ Improved ground water yields (more available water in shallow wells, boreholes)

☐ Ability to grow new/ other crop varieties

☐ No positive effect felt

☐ Other

Specify other positive outcomes from the changing climate

_____

From what source do you get forecasts that inform how you manage your farming activities i.e. when to plant?

☐ Radio

☐ Newspapers

☐ TV

☐ Traditional forecasters

☐ Government extension agents

☐ Local elders/religious elders

☐ NGO extension agents/ officers

☐ None- I do not receive any information

If forecasts about a coming rainy season could be provided reliably, what type of forecast information will be MOST USEFUL to you?

○ Forecasts about when rains are expected to fall in your area

○ Forecasts about when rains are expected to END in your area

○ Forecasts about whether the AMOUNT of rainfall will be above average, normal or below average

○ Forecasts about the distribution of the rainfall during the season

» FARMERS ADAPTATION STRATEGIES

How have you been adjusting your CROPS FARMING STRATEGIES with climate change ? 5=Very Large Extent, 4=Large Extent, 3=Moderate Extent, 2=LESS Extent, 1=Not at All	5	4	3	2	1
Changing planting dates	◯	◯	◯	◯	◯
Changing crop varieties	◯	◯	◯	◯	◯
Planting drought-tolerant varieties	◯	◯	◯	◯	◯
Crop diversification	◯	◯	◯	◯	◯
Use of Certified Seed	◯	◯	◯	◯	◯
Crop Rotation	◯	◯	◯	◯	◯
Monocropping	◯	◯	◯	◯	◯
Early Planting	◯	◯	◯	◯	◯
Agroforestry	◯	◯	◯	◯	◯
Using forecasts and advisories	◯	◯	◯	◯	◯
Farming near rivers	◯	◯	◯	◯	◯
Keeping animals ie livestock, bees	◯	◯	◯	◯	◯

How have you been adjusting your SOIL CONSERVATION strategies with climate change ? 5=Very Large Extent, 4=Large Extent, 3=Moderate Extent, 2=LESS Extent, 1=Not at All	5	4	3	2	1
Using conservation Agriculture ie zero tillage	◯	◯	◯	◯	◯
Mulching	◯	◯	◯	◯	◯
Retaining crop residues	◯	◯	◯	◯	◯
Use of Organic fertilizers i.e manure	◯	◯	◯	◯	◯
Use of inorganic fertilizers	◯	◯	◯	◯	◯

How have you been adjusting your WATER CONSERVATION strategies with climate change ? 5=Very Large Extent, 4=Large Extent, 3=Moderate Extent, 2=LESS Extent, 1=Not at All	5	4	3	2	1
Water Harvesting	◯	◯	◯	◯	◯
Water Conservation	◯	◯	◯	◯	◯
Use of Irrigation System	◯	◯	◯	◯	◯
Digging Well/Borehole	◯	◯	◯	◯	◯

Who makes most farm decisions i.e. what to farm, sell farm produce, change planted crops?

◯ Respondent

◯ Other Family Member

What is the gender of other family member

◯ Male

◯ Female

What form of support do you recieve to help you cope with climate change and to strengthen agriculture and food security?

☐ Financial support (cash, credit)

☐ Material Support (Food, access to machinery/planters,harvesters, tanks etc)

☐ Extension services (advisory, forecasts etc)

☐ subsidized farm inputs (seeds, fertilizer)

☐ livestock /beekeeping/ fisheries support

☐ Irrigation support

☐ No support

What are the terms that come with the support offered?

☐ Loan to be paid back

☐ Buy farm machinery on credit

☐ Buy improved inputs(seeds, animals, fertilizers, pesticides) on subsidized prices

☐ Crop/livestock insurance

☐ Buy tanks and other water preservation measures

☐ None

What are the THREE main barrier/challenge that hinders/stops you from improving your farming ways to increase your productivity?

_____

1st choice

◯ Education level   ◯ Challenges in accessing information

◯ Limited access to credit   ◯ Lack of extension services   ◯ Inadequate capital

◯ Land ownership   ◯ Infertile soil   ◯ Lack of enough labour

◯ Lack of access to water for irrigation/other farm activities

110

2nd choice

○ Education level   ○ Challenges in accessing information
○ Limited access to credit   ○ Lack of extension services   ○ Inadequate capital
○ Land ownership   ○ Infertile soil   ○ Lack of enough labour
○ Lack of access to water for irrigation/other farm activities

3rd choice

○ Education level   ○ Challenges in accessing information
○ Limited access to credit   ○ Lack of extension services   ○ Inadequate capital
○ Land ownership   ○ Infertile soil   ○ Lack of enough labour
○ Lack of access to water for irrigation/other farm activities

111

8.2 APPENDIX 2A - STATISTICAL ANALYSES CODES

8.2.1 Statistical analysis

Loading...

Final_AEZ_Analytics.ipynb_

CodeTextConnect
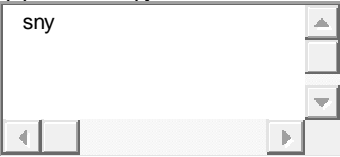
Making the necessary library installation including pandas, plotly, plotly express, seaborn
They are used for reading data as dataframe, for data visualisation and neat visualisation respective

Double-click (or enter) to edit
CodeText

```
[ ]
!pip install pandas
!pip install seaborn
!pip install plotly.express
!pip install numpy
```

sny

Importing the imported libraries for use

```
[ ]
import pandas as pd
import plotly.express as px
import numpy as np
import plotly.express as px
import seaborn as sns
import matplotlib.pyplot as plt
```

```
[ ]
from google.colab import drive
drive.mount('/content/drive')
root_dir = "/content/drive/MyDrive"
```

Reading the CSV data as a dataframe using pandas library in python

```
[ ]
Rainfall_Sensor_1990_2020 = pd.read_csv('/content/drive/MyDrive/csv/DailyPPT_csv_exports_ALL_1990-
2021_REGIONAL_COL_DATA.csv')
Rainfall_Station_1990_2020 = pd.read_csv('/content/drive/MyDrive/csv/Rainfall_Station_Regional_1991_2020_Transposed.csv')
Temperature_Sensor_1990_2020 = pd.read_csv('/content/drive/MyDrive/csv/DailyTemp_csv_exports_ALL_1990-
2021_REGIONAL_COL_DATA.csv')
Temperature_Station_1990_2020 = pd.read_csv('/content/drive/MyDrive/csv/Temperature_Station_Regional_1991_2020_Transposed.csv')
# Temperature_Sensor_1990_2020.head()
# Temperature_Station_1990_2020.head()
# Rainfall_Sensor_1990_2020
Rainfall_Sensor_1990_2020.tail()
Rainfall_Station_1990_2020
# Temperature_Sensor_1990_2020.head()
```

```
[ ]
Temperature_Station_1990_2020.head()

date_temp = Temperature_Station_1990_2020[['ID']].astype(str)
```

```
date_temp.head()


# type(Temperature_Station_1990_2020)
```

```
[ ]
rain_date = Rainfall_Station_1990_2020[['ID']].astype(str)
rain_date

from datetime import datetime

regional_date3 = pd.DataFrame(columns=['Year','Month','Day'])

for data in range(len(rain_date)):
 # print(ppt_llpg_fitered.iloc[data,0])
 date_coverted = datetime.strptime((rain_date.iloc[data,0]),'%Y%m%d')
 Year = date_coverted.date().year
 Month = date_coverted.date().month
 Day = date_coverted.date().day

 # print(date_coverted)

 regional_date3 = regional_date3.append({'Year':Year,'Month':Month,'Day':Day}, ignore_index=True)


regional_date3

regional_date3['ID2']=rain_date['ID']
regional_date3
```

```
[ ]
regional_date3
Rainfall_Station_1990_2020.head()
Rainfall_Station_1990_2020['ID2']=regional_date3['ID2']

concat_rain_station = pd.merge(Rainfall_Station_1990_2020,regional_date3,on='ID2')
concat_rain_station.head()
```

```
[ ]
from datetime import datetime
regional_date2 = pd.DataFrame(columns=['Year','Month','Day'])
for data in range(len(date_temp)):
 # print(ppt_llpg_fitered.iloc[data,0])
 date_coverted = datetime.strptime((date_temp.iloc[data,0]),'%Y%m%d')
 Year = date_coverted.date().year
 Month = date_coverted.date().month
 Day = date_coverted.date().day

 # print(date_coverted)
 regional_date2 = regional_date2.append({'Year':Year,'Month':Month,'Day':Day}, ignore_index=True)
regional_date2['ID2']=date_temp['ID']
regional_date2
```

```
[ ]
# regional_date2['ID'].astype(int)
```

```
[ ]
regional_date2
Temperature_Station_1990_2020.head()
Temperature_Station_1990_2020['ID2']=regional_date2['ID2']

concat_temp_station = pd.merge(Temperature_Station_1990_2020,regional_date2,on='ID2')
concat_temp_station.head()
```

```
[ ]
concat_rain_station
# concat_temp_station
```

```
# concat_rain_station[(concat_rain_station['Year'] >= 1991) & (concat_rain_station['Year'] <= 2005) & (concat_rain_station['Month'] >= 3)
& (concat_rain_station['Month'] <= 5) ]
```

[ ]
"""
Filtering by years and months to identify the MAM and OND LGP values

"""

"""
Filtering by seasons including OND and MAM for both epochs and findingh their LPG per season in each location.

"""

"""
Finding the LPG (MAM & OND) 1991 - 2005
"""
```
SELECTED1990_2005_MAM = concat_temp_station[(concat_temp_station['Year'] >= 1991) & (concat_temp_station['Year'] <= 2005) & (concat_temp_station['Month'] >= 3) & (concat_temp_station['Month'] <= 5) ]
SELECTED1990_2005_MAM
SELECTED1990_2005_OND = concat_temp_station[(concat_temp_station['Year'] >= 1991) & (concat_temp_station['Year'] <= 2005) & (concat_temp_station['Month'] >= 10) & (concat_temp_station['Month'] <= 12) ]
SELECTED1990_2005_OND
```

"""
Finding the LPG (MAM & OND) 2006 - 2021
"""

```
SELECTED2006_2020_OND = concat_temp_station[(concat_temp_station['Year'] >= 2006) & (concat_temp_station['Year'] <= 2020) & (concat_temp_station['Month'] >= 10) & (concat_temp_station['Month'] <= 12) ]

SELECTED2006_2020_MAM = concat_temp_station[(concat_temp_station['Year'] >= 2006) & (concat_temp_station['Year'] <= 2020) & (concat_temp_station['Month'] >= 3) & (concat_temp_station['Month'] <= 5) ]
SELECTED2006_2020_MAM.head()
```

"""
Rearranging the LPGs to plottabel both spatially and as charts and maps and getting the sum of OND days per season
"""

```
SELECTED_2006_2020_MAM_T_temp = SELECTED2006_2020_MAM.drop(['Year', 'Month'], axis=1).T.mean(axis = 1).to_frame().rename(columns = {0:'Sum'}).reset_index()

SELECTED_2006_2020_OND_T_temp = SELECTED2006_2020_OND.drop(['Year', 'Month'], axis=1).T.mean(axis = 1).to_frame().rename(columns = {0:'Sum'}).reset_index()

SELECTED_1990_2005_OND_T_temp = SELECTED1990_2005_OND.drop(['Year', 'Month'], axis=1).T.mean(axis = 1).to_frame().rename(columns = {0:'Sum'}).reset_index()

SELECTED_1990_2005_MAM_T_temp = SELECTED1990_2005_MAM.drop(['Year', 'Month'], axis=1).T.mean(axis = 1).to_frame().rename(columns = {0:'Sum'}).reset_index()


SELECTED_1990_2005_MAM_T_temp.tail()


SELECTED_2006_2020_MAM_T_temp.to_csv('SELECTED_2006_2020_MAM_T_temp.csv', index=True, encoding='utf-8')
SELECTED_2006_2020_OND_T_temp.to_csv('SELECTED_2006_2020_OND_T_temp.csv', index=True, encoding='utf-8')
SELECTED_1990_2005_OND_T_temp.to_csv('SELECTED_1990_2005_OND_T_temp.csv', index=True, encoding='utf-8')
SELECTED_1990_2005_MAM_T_temp.to_csv('SELECTED_1990_2005_MAM_T_temp.csv', index=True, encoding='utf-8')
```

[ ]
"""
Filtering by years and months to identify the MAM and OND LGP values

"""
"""
Filtering by seasons including OND and MAM for both epochs and findingh their LPG per season in each location.

"""

"""
Finding the LPG (MAM & OND) 1991 - 2005
"""
```
SELECTED1990_2005_MAM = concat_rain_station[(concat_rain_station['Year'] >= 1991) & (concat_rain_station['Year'] <= 2005) & (concat_rain_station['Month'] >= 3) & (concat_rain_station['Month'] <= 5) ]
```

```
SELECTED1990_2005_MAM
SELECTED1990_2005_OND = concat_rain_station[(concat_rain_station['Year'] >= 1991) & (concat_rain_station['Year'] <= 2005) & (concat_rain_station['Month'] >= 10) & (concat_rain_station['Month'] <= 12) ]
SELECTED1990_2005_OND

"""
Finding the LPG (MAM & OND) 2006 - 2021
"""

SELECTED2006_2020_OND = concat_rain_station[(concat_rain_station['Year'] >= 2006) & (concat_rain_station['Year'] <= 2020) & (concat_rain_station['Month'] >= 10) & (concat_rain_station['Month'] <= 12) ]

SELECTED2006_2020_MAM = concat_rain_station[(concat_rain_station['Year'] >= 2006) & (concat_rain_station['Year'] <= 2020) & (concat_rain_station['Month'] >= 3) & (concat_rain_station['Month'] <= 5) ]
SELECTED2006_2020_MAM.head()

"""
Rearranging the LPGs to plottabel both spatially and as charts and maps and getting the sum of OND days per season
"""

SELECTED_2006_2020_MAM_T_rain = SELECTED2006_2020_MAM.drop(['Year', 'Month'], axis=1).T.mean(axis = 1).to_frame().rename(columns = {0:'Sum'}).reset_index()

SELECTED_2006_2020_OND_T_rain = SELECTED2006_2020_OND.drop(['Year', 'Month'], axis=1).T.mean(axis = 1).to_frame().rename(columns = {0:'Sum'}).reset_index()

SELECTED_1990_2005_OND_T_rain = SELECTED1990_2005_OND.drop(['Year', 'Month'], axis=1).T.mean(axis = 1).to_frame().rename(columns = {0:'Sum'}).reset_index()

SELECTED_1990_2005_MAM_T_rain = SELECTED1990_2005_MAM.drop(['Year', 'Month'], axis=1).T.mean(axis = 1).to_frame().rename(columns = {0:'Sum'}).reset_index()


SELECTED_1990_2005_MAM_T_rain.tail()


SELECTED_2006_2020_MAM_T_rain.to_csv('SELECTED_2006_2020_MAM_T_rain.csv', index=True, encoding='utf-8')
SELECTED_2006_2020_OND_T_rain.to_csv('SELECTED_2006_2020_OND_T_rain.csv', index=True, encoding='utf-8')
SELECTED_1990_2005_OND_T_rain.to_csv('SELECTED_1990_2005_OND_T_rain.csv', index=True, encoding='utf-8')
SELECTED_1990_2005_MAM_T_rain.to_csv('SELECTED_1990_2005_MAM_T_rain.csv', index=True, encoding='utf-8')
```

Transpose the sensor dataset (temperature and rainfall), to be in the same format with station datasets. using a function for the two dataframes. This will nessesitate plotting of the data in line graph, as seen in the next section.

```
[ ]
# Rainfall_Sensor_1990_2020.head()
Temperature_Sensor_1990_2020
```

```
[ ]

def transpose(df):
  df2=df.T
  header=df2.iloc[0]
  df2=df2[1:]
  df2.columns=header
  df2.head()
  return df2

Rainfall_Sensor_1990_2020_T = Rainfall_Sensor_1990_2020.set_index('ID').T

Temperature_Sensor_1990_2020_T = Temperature_Sensor_1990_2020.set_index('Place').T

Rainfall_Sensor_1990_2020_T
Temperature_Sensor_1990_2020_T
```

Code that finds outlier in the datasets, however, we have to plot them first using box plots

```
[ ]
def find_outliers_IQR(df):

  q1=df.quantile(0.25)

  q3=df.quantile(0.75)
```

```python
    IQR=q3-q1

    outliers = df[((df<(q1-1.5*IQR)) | (df>(q3+1.5*IQR)))]

    return outliers

outliers = find_outliers_IQR(Rainfall_Station_1990_2020['AthiRiver'])
print(outliers)
0       7.678
25      4.429
49      8.771
82     19.547
83     30.033
          ...
10925   3.337
10933  13.746
10935   6.865
10943   3.579
10956  11.411
Name: AthiRiver, Length: 1857, dtype: float64
```

```python
[ ]
Rainfall_Station_1990_2020.head()
Rainfall_Sensor_1990_2020_T.tail()
# Merged_Rainfall = pd.merge(Rainfall_Station_1990_2020, Rainfall_Sensor_1990_2020_T, how='outer')
# Merged_Rainfall.head()
```

Plotting Rainfall(sensor data) against Rainfall(Station data) , first you cast all the column inputs as integers in order for them to plot as numbers

```python
[ ]
Rainfall_Sensor_1990_2020_T
Temperature_Sensor_1990_2020_T


# Rainfall_Station_1990_2020 = Rainfall_Station_1990_2020.astype({col:int for col in Rainfall_Station_1990_2020})
# Rainfall_Sensor_1990_2020_T = Rainfall_Sensor_1990_2020_T.astype({col:int for col in Rainfall_Sensor_1990_2020_T})
# for col in Rainfall_Sensor_1990_2020_T.columns:
#     print(col)
```

```python
[ ]
"""

MACHAKOS COUNTY

"""


# px.scatter(x=Rainfall_Station_1990_2020['Mutituni'], y=Rainfall_Sensor_1990_2020_T['Mutituni'], trendline="ols", title='Athi River')
from scipy import stats
def r2(x, y):
    return stats.pearsonr(x, y)[0] ** 2



fig, axes = plt.subplots(10, 4, figsize=(40, 70))

# fig.suptitle('Station data against sensor data for Rainfall amounts (mm)')
# fig.tight_layout()
plt.rcParams["figure.autolayout"] = True
fig.subplots_adjust(hspace=0.125, wspace=0.125)


sns.regplot(ax=axes[0, 0], x=Rainfall_Station_1990_2020['AthiRiver'], y=Rainfall_Sensor_1990_2020_T['AthiRiver'], color='r')
sns.regplot(ax=axes[0, 1], x=Rainfall_Station_1990_2020['Ekalakala'], y=Rainfall_Sensor_1990_2020_T['Ekalakala'], color='b')
sns.regplot(ax=axes[0, 2], x=Rainfall_Station_1990_2020['Ikombe'], y=Rainfall_Sensor_1990_2020_T['Ikombe'], color='r')
sns.regplot(ax=axes[0, 3], x=Rainfall_Station_1990_2020['Kalama'], y=Rainfall_Sensor_1990_2020_T['Kalama'], color='b')
sns.regplot(ax=axes[1, 0], x=Rainfall_Station_1990_2020['KangundoCentral'], y=Rainfall_Sensor_1990_2020_T['KangundoCentral'], color='r')
sns.regplot(ax=axes[1, 1], x=Rainfall_Station_1990_2020['KangundoEast'], y=Rainfall_Sensor_1990_2020_T['KangundoEast'], color='b')
sns.regplot(ax=axes[1, 2], x=Rainfall_Station_1990_2020['KangundoNorth'], y=Rainfall_Sensor_1990_2020_T['KangundoNorth'],color='r')
sns.regplot(ax=axes[1, 3], x=Rainfall_Station_1990_2020['KangundoWest'], y=Rainfall_Sensor_1990_2020_T['KangundoWest'], color='b')


sns.regplot(ax=axes[2, 0], x=Rainfall_Station_1990_2020['Katangi'], y=Rainfall_Sensor_1990_2020_T['Katangi'], color='r')
```

```
sns.regplot(ax=axes[2, 1], x=Rainfall_Station_1990_2020['KathianiCentral'], y=Rainfall_Sensor_1990_2020_T['KathianiCentral'], color='b')
sns.regplot(ax=axes[2, 2], x=Rainfall_Station_1990_2020['Kibauni'], y=Rainfall_Sensor_1990_2020_T['Kibauni'], color='r')
sns.regplot(ax=axes[2, 3], x=Rainfall_Station_1990_2020['Kinanie'], y=Rainfall_Sensor_1990_2020_T['Kinanie'], color='b')

sns.regplot(ax=axes[3, 0], x=Rainfall_Station_1990_2020['Kithimani'], y=Rainfall_Sensor_1990_2020_T['Kithimani'], color='r')
sns.regplot(ax=axes[3, 1], x=Rainfall_Station_1990_2020['Kivaa'], y=Rainfall_Sensor_1990_2020_T['Kivaa'], color='b')
sns.regplot(ax=axes[3, 2], x=Rainfall_Station_1990_2020['Kola'], y=Rainfall_Sensor_1990_2020_T['Kola'], color='r')
sns.regplot(ax=axes[3, 3], x=Rainfall_Station_1990_2020['Kyeleni'], y=Rainfall_Sensor_1990_2020_T['Kyeleni'], color='b')

sns.regplot(ax=axes[4, 0], x=Rainfall_Station_1990_2020['LowerKaewaKaani'], y=Rainfall_Sensor_1990_2020_T['LowerKaewaKaani'], color='r')
sns.regplot(ax=axes[4, 1], x=Rainfall_Station_1990_2020['MachakosCentral'], y=Rainfall_Sensor_1990_2020_T['MachakosCentral'], color='b')
sns.regplot(ax=axes[4, 2], x=Rainfall_Station_1990_2020['MakutanoMwala'], y=Rainfall_Sensor_1990_2020_T['MakutanoMwala'], color='r')
sns.regplot(ax=axes[4, 3], x=Rainfall_Station_1990_2020['Masii'], y=Rainfall_Sensor_1990_2020_T['Masii'], color='b')

sns.regplot(ax=axes[5, 0], x=Rainfall_Station_1990_2020['MasingaCentral'], y=Rainfall_Sensor_1990_2020_T['MasingaCentral'],color='r')
sns.regplot(ax=axes[5, 1], x=Rainfall_Station_1990_2020['MatunguluEast'], y=Rainfall_Sensor_1990_2020_T['MatunguluNorth'], color='b')
sns.regplot(ax=axes[5, 2], x=Rainfall_Station_1990_2020['MatunguluWest'], y=Rainfall_Sensor_1990_2020_T['MatunguluWest'], color='r')
sns.regplot(ax=axes[5, 3], x=Rainfall_Station_1990_2020['Matuu'], y=Rainfall_Sensor_1990_2020_T['Matuu'], color='b')

sns.regplot(ax=axes[6, 0], x=Rainfall_Station_1990_2020['Mbiuni'], y=Rainfall_Sensor_1990_2020_T['Mbiuni'], color='r')
sns.regplot(ax=axes[6, 1], x=Rainfall_Station_1990_2020['Mitaboni'], y=Rainfall_Sensor_1990_2020_T['Mitaboni'], color='b')
sns.regplot(ax=axes[6, 2], x=Rainfall_Station_1990_2020['Mua'], y=Rainfall_Sensor_1990_2020_T['Mua'], color='r')
sns.regplot(ax=axes[6, 3], x=Rainfall_Station_1990_2020['MumbuniNorth'], y=Rainfall_Sensor_1990_2020_T['MumbuniNorth'], color='b')

sns.regplot(ax=axes[7, 0], x=Rainfall_Station_1990_2020['Muthesya'], y=Rainfall_Sensor_1990_2020_T['Muthesya'], color='r')
sns.regplot(ax=axes[7, 1], x=Rainfall_Station_1990_2020['Muthetheni'], y=Rainfall_Sensor_1990_2020_T['Muthetheni'], color='b')
sns.regplot(ax=axes[7, 2], x=Rainfall_Station_1990_2020['Muthwani'], y=Rainfall_Sensor_1990_2020_T['Muthwani'], color='r')
sns.regplot(ax=axes[7, 3], x=Rainfall_Station_1990_2020['Mutituni'], y=Rainfall_Sensor_1990_2020_T['Mutituni'], color='b')

sns.regplot(ax=axes[8, 0], x=Rainfall_Station_1990_2020['MuvutiKiimaKimwe'], y=Rainfall_Sensor_1990_2020_T['MuvutiKiimaKimwe'], color='r')
sns.regplot(ax=axes[8, 1], x=Rainfall_Station_1990_2020['Ndalani'], y=Rainfall_Sensor_1990_2020_T['Ndalani'], color='b')
sns.regplot(ax=axes[8, 2], x=Rainfall_Station_1990_2020['Ndithini'], y=Rainfall_Sensor_1990_2020_T['Ndithini'], color='r')
sns.regplot(ax=axes[8, 3], x=Rainfall_Station_1990_2020['SyokimauMulolongo'], y=Rainfall_Sensor_1990_2020_T['SyokimauMulolongo'], color='b')

sns.regplot(ax=axes[9, 0], x=Rainfall_Station_1990_2020['Tala'], y=Rainfall_Sensor_1990_2020_T['Tala'], color='r')
sns.regplot(ax=axes[9, 1], x=Rainfall_Station_1990_2020['UpperKaewaIveti'], y=Rainfall_Sensor_1990_2020_T['UpperKaewaIveti'], color='b')
sns.regplot(ax=axes[9, 2], x=Rainfall_Station_1990_2020['Wamunyu'], y=Rainfall_Sensor_1990_2020_T['Wamunyu'], color='r')
sns.regplot(ax=axes[9, 3], x=Rainfall_Station_1990_2020['Wamunyu'], y=Rainfall_Sensor_1990_2020_T['Wamunyu'], color='b')

"""
rainfall plots for all the stations in Machakos County. The plots are Station data against sensor data"""
```

```
[ ]
"""
Plots of other counties
Embu Plots

Makima
Mwea
Mavuria
Kiambere
MbetiSouth
Muminji
Nthawa
MbetiNorth
Kithimu
Kirimari
Evurore
KagaariSouth
GaturiSouth
KyeniSouth
CentralWard
GaturiNorth
RuguruNgandori
Nginda
KagaariNorth
"""
```

```python
fig, axes = plt.subplots(3,4, figsize=(35, 20))

# fig.suptitle('Station data against sensor data for Rainfall amounts (mm)')
# fig.tight_layout()
plt.rcParams["figure.autolayout"] = True
fig.subplots_adjust(hspace=0.125, wspace=0.125)


sns.regplot(ax=axes[0, 0], x=Rainfall_Station_1990_2020['KagaariNorth'], y=Rainfall_Sensor_1990_2020_T['KagaariNorth'], color='r')
sns.regplot(ax=axes[0, 1], x=Rainfall_Station_1990_2020['Nginda'], y=Rainfall_Sensor_1990_2020_T['Nginda'], color='b')
sns.regplot(ax=axes[0, 2], x=Rainfall_Station_1990_2020['RuguruNgandori'], y=Rainfall_Sensor_1990_2020_T['RuguruNgandori'], color='r'
)
sns.regplot(ax=axes[0, 3], x=Rainfall_Station_1990_2020['GaturiNorth'], y=Rainfall_Sensor_1990_2020_T['GaturiNorth'], color='b')
sns.regplot(ax=axes[1, 0], x=Rainfall_Station_1990_2020['CentralWard'], y=Rainfall_Sensor_1990_2020_T['CentralWard'], color='r')
sns.regplot(ax=axes[1, 1], x=Rainfall_Station_1990_2020['KyeniSouth'], y=Rainfall_Sensor_1990_2020_T['KyeniSouth'], color='b')
sns.regplot(ax=axes[1, 2], x=Rainfall_Station_1990_2020['GaturiSouth'], y=Rainfall_Sensor_1990_2020_T['GaturiSouth'],color='r')
sns.regplot(ax=axes[1, 3], x=Rainfall_Station_1990_2020['KagaariSouth'], y=Rainfall_Sensor_1990_2020_T['KagaariSouth'], color='b')


sns.regplot(ax=axes[2, 0], x=Rainfall_Station_1990_2020['Evurore'], y=Rainfall_Sensor_1990_2020_T['Evurore'], color='r')
sns.regplot(ax=axes[2, 1], x=Rainfall_Station_1990_2020['Kirimari'], y=Rainfall_Sensor_1990_2020_T['Kirimari'], color='b')
sns.regplot(ax=axes[2, 2], x=Rainfall_Station_1990_2020['Nthawa'], y=Rainfall_Sensor_1990_2020_T['Nthawa'], color='r')
sns.regplot(ax=axes[2, 3], x=Rainfall_Station_1990_2020['MbetiNorth'], y=Rainfall_Sensor_1990_2020_T['MbetiNorth'], color='b')
```

```
[ ]
"""
Kitui Plots

Athi
Ikutha
Kanziko
Mutha
Mutomo
Kanyangi
IkangaKyatune
VooKyamatu
Kisasi
Mbitini
Mulango
Chuluni
ZombeMwitika
Nzambani
KyangwithyaWest
Township
KwavonzaYatta
KyangwithyaEast
Matinyani
KwaMutongaKithumula
EndauMalalani
MutitoKaliku
Miambani
Kauwi
Mutonguni
Nguutani
Migwani
Nuu
Mui
Central
KyomeThaana
Kivou
KiomoKyethani
Nguni
Waita
Mumoni
Ngomeni
Kyuso
Tharaka
Tseikuru
"""

fig, axes = plt.subplots(3,4, figsize=(35, 20))

# fig.suptitle('Station data against sensor data for Rainfall amounts (mm)')
# fig.tight_layout()
plt.rcParams["figure.autolayout"] = True
```

```
fig.subplots_adjust(hspace=0.125, wspace=0.125)

sns.regplot(ax=axes[0, 0], x=Rainfall_Station_1990_2020['Tseikuru'], y=Rainfall_Sensor_1990_2020_T['Tseikuru'], color='r')
sns.regplot(ax=axes[0, 1], x=Rainfall_Station_1990_2020['Tharaka'], y=Rainfall_Sensor_1990_2020_T['Tharaka'], color='b')
sns.regplot(ax=axes[0, 2], x=Rainfall_Station_1990_2020['Kyuso'], y=Rainfall_Sensor_1990_2020_T['Kyuso'], color='r')
sns.regplot(ax=axes[0, 3], x=Rainfall_Station_1990_2020['Ngomeni'], y=Rainfall_Sensor_1990_2020_T['Ngomeni'], color='b')
sns.regplot(ax=axes[1, 0], x=Rainfall_Station_1990_2020['Mumoni'], y=Rainfall_Sensor_1990_2020_T['Mumoni'], color='r')
sns.regplot(ax=axes[1, 1], x=Rainfall_Station_1990_2020['Waita'], y=Rainfall_Sensor_1990_2020_T['Waita'], color='b')
sns.regplot(ax=axes[1, 2], x=Rainfall_Station_1990_2020['Nguni'], y=Rainfall_Sensor_1990_2020_T['Nguni'],color='r')
sns.regplot(ax=axes[1, 3], x=Rainfall_Station_1990_2020['KiomoKyethani'], y=Rainfall_Sensor_1990_2020_T['KiomoKyethani'], color='b')


sns.regplot(ax=axes[2, 0], x=Rainfall_Station_1990_2020['Kivou'], y=Rainfall_Sensor_1990_2020_T['Kivou'], color='r')
sns.regplot(ax=axes[2, 1], x=Rainfall_Station_1990_2020['KyomeThaana'], y=Rainfall_Sensor_1990_2020_T['KyomeThaana'], color='b')
sns.regplot(ax=axes[2, 2], x=Rainfall_Station_1990_2020['Central'], y=Rainfall_Sensor_1990_2020_T['Central'], color='r')
sns.regplot(ax=axes[2, 3], x=Rainfall_Station_1990_2020['Migwani'], y=Rainfall_Sensor_1990_2020_T['Migwani'], color='b')
```

```
[ ]
"""
MAKUENI

Thange
Masongaleni
Nguumo
KikumbulyuSouth
KikumbulyuNorth
Makindu
NguuMasumba
EmaliMulala
KitiseKithuki
Kathonzweni
Mbitini
Kasikeu
NzauiKililiKalamba
MuvauKikuumini
Mavindini
Mukaa
Ilima
Wote
Kilungu
KiimaKiuKalanzoni
Ukia
Kee
KithungoKitundu
Kalawa
WaiaKako
Mbooni
KitetaKisau
Tulimani

"""


fig, axes = plt.subplots(3,4, figsize=(35, 20))

# fig.suptitle('Station data against sensor data for Rainfall amounts (mm)')
# fig.tight_layout()
plt.rcParams["figure.autolayout"] = True
fig.subplots_adjust(hspace=0.125, wspace=0.125)

sns.regplot(ax=axes[0, 0], x=Rainfall_Station_1990_2020['Tulimani'], y=Rainfall_Sensor_1990_2020_T['Tulimani'], color='r')
sns.regplot(ax=axes[0, 1], x=Rainfall_Station_1990_2020['KitetaKisau'], y=Rainfall_Sensor_1990_2020_T['KitetaKisau'], color='b')
sns.regplot(ax=axes[0, 2], x=Rainfall_Station_1990_2020['Mbooni'], y=Rainfall_Sensor_1990_2020_T['Mbooni'], color='r')
sns.regplot(ax=axes[0, 3], x=Rainfall_Station_1990_2020['WaiaKako'], y=Rainfall_Sensor_1990_2020_T['WaiaKako'], color='b')
sns.regplot(ax=axes[1, 0], x=Rainfall_Station_1990_2020['Kalawa'], y=Rainfall_Sensor_1990_2020_T['Kalawa'], color='r')
sns.regplot(ax=axes[1, 1], x=Rainfall_Station_1990_2020['KithungoKitundu'], y=Rainfall_Sensor_1990_2020_T['KithungoKitundu'], color=
'b')
sns.regplot(ax=axes[1, 2], x=Rainfall_Station_1990_2020['Kee'], y=Rainfall_Sensor_1990_2020_T['Kee'],color='r')
sns.regplot(ax=axes[1, 3], x=Rainfall_Station_1990_2020['Ukia'], y=Rainfall_Sensor_1990_2020_T['Ukia'], color='b')


sns.regplot(ax=axes[2, 0], x=Rainfall_Station_1990_2020['KiimaKiuKalanzoni'], y=Rainfall_Sensor_1990_2020_T['KiimaKiuKalanzoni'], c
olor='r')
sns.regplot(ax=axes[2, 1], x=Rainfall_Station_1990_2020['Kilungu'], y=Rainfall_Sensor_1990_2020_T['Kilungu'], color='b')
sns.regplot(ax=axes[2, 2], x=Rainfall_Station_1990_2020['Wote'], y=Rainfall_Sensor_1990_2020_T['Wote'], color='r')
```

```
sns.regplot(ax=axes[2, 3], x=Rainfall_Station_1990_2020['Ilima'], y=Rainfall_Sensor_1990_2020_T['Ilima'], color='b')
```

```
[ ]
for col in Rainfall_Station_1990_2020.columns:
    print(col)
ID
CentralWard
Evurore
GaturiNorth
GaturiSouth
KagaariNorth
KagaariSouth
Kiambere
Kirimari
Kithimu
KyeniNorth
KyeniSouth
Makima
Mavuria
MbetiNorth
MbetiSouth
Muminji
Mwea
Nginda
Nthawa
RuguruNgandori
Athi
Central
Chuluni
EndauMalalani
IkangaKyatune
Ikutha
Kanyangi
Kanziko
Kauwi
KiomoKyethani
Kisasi
Kivou
KwaMutongaKithumula
KwavonzaYatta
KyangwithyaEast
KyangwithyaWest
KyomeThaana
Kyuso
Matinyani
Mbitini_x
Miambani
Migwani
Mui
Mulango
Mumoni
Mutha
MutitoKaliku
Mutomo
Mutonguni
Ngomeni
Nguni
Nguutani
Nuu
Nzambani
Tharaka
Township
Tseikuru
VooKyamatu
Waita
ZombeMwitika
AthiRiver
Ekalakala
Ikombe
Kalama
KangundoCentral
KangundoEast
KangundoNorth
KangundoWest
```

Katangi
KathianiCentral
Kibauni
Kinanie
Kithimani
Kivaa
Kola
Kyeleni
LowerKaewaKaani
MachakosCentral
MakutanoMwala
Masii
MasingaCentral
MatunguluEast
MatunguluNorth
MatunguluWest
Matuu
Mbiuni
Mitaboni
Mua
MumbuniNorth
Muthesya
Muthetheni
Muthwani
Mutituni
MuvutiKiimaKimwe
Ndalani
Ndithini
SyokimauMulolongo
Tala
unknown7
UpperKaewaIveti
Wamunyu
EmaliMulala
Ilima
IvingoniNzambani
Kalawa
Kasikeu
Kathonzweni
Kee
KiimaKiuKalanzoni
KikumbulyuNorth
KikumbulyuSouth
Kilungu
KitetaKisau
KithungoKitundu
KitiseKithuki
Makindu
Masongaleni
Mavindini
Mbitini_y
Mbooni
MtitoAndei
Mukaa
MuvauKikuumini
NguuMasumba
Nguumo
NzauiKililiKalamba
Thange
Tulimani
Ukia
WaiaKako
Wote
AbogetaEast
AbogetaWest
AbothuguchiCentral
AbothuguchiWest
Akachiu_x
AkirangOndu
Akithii
Amwathi
Antuambui
AntubetweKiongo
AthiruGaiti
AthiruRuujine

```
Athwana
IgembeEast
IgojiEast
IgojiWest
Kangeta
Kanuni
Karama
Kiagu
Kianjai
Kibirichia
KiegoiAntubochiu
Kiguchwa
KiiruaNaari
Kisima
Maua
Mbeu
Mikinduri
Mitunguu
Municipality
Muthara
Mwanganthia
Naathu
Njia
Nkomo
Nkuene
NtimaEast
NtimaWest
Ntunene
NyakiEast
NyakiWest
RuiriRwarera
Thangatha
Timau
unknown5
Akachiu_y
Chiakariga
Chogoria
Ganga
Gatunga
IgambangOmbe
Karingani
Magumoni
Mariani
Mitheru
Mugwe
Mukothima
Muthambi
Mwimbi
Nkondi
ID2
```

```python
[ ]
# """
# MERU COUNTY
# SouthImenti
# CentralImenti
# unknown5
# NorthImenti
# Buuri
# IgembeSouth
# TiganiaWest
# TiganiaEast
# IgembeCentral
# IgembeNorth

# AthiruGaiti
# AthiruRuujine
# Athwana
# IgembeEast
# IgojiEast
# IgojiWest
# """

# fig, axes = plt.subplots(2,4, figsize=(35, 20))
```

```python
# # fig.suptitle('Station data against sensor data for Rainfall amounts (mm)')
# # fig.tight_layout()
# plt.rcParams["figure.autolayout"] = True
# fig.subplots_adjust(hspace=0.125, wspace=0.125)

# sns.regplot(ax=axes[0, 0], x=Rainfall_Station_1990_2020['IgembeEast'], y=Rainfall_Sensor_1990_2020_T['IgembeEast'], color='r')
# sns.regplot(ax=axes[0, 1], x=Rainfall_Station_1990_2020['IgojiWest'], y=Rainfall_Sensor_1990_2020_T['IgojiWest'], color='b')
# sns.regplot(ax=axes[0, 2], x=Rainfall_Station_1990_2020['Athwana'], y=Rainfall_Sensor_1990_2020_T['Athwana'], color='r')
# sns.regplot(ax=axes[0, 3], x=Rainfall_Station_1990_2020['AthiruRuujine'], y=Rainfall_Sensor_1990_2020_T['AthiruRuujine'], color='b')
# sns.regplot(ax=axes[1, 0], x=Rainfall_Station_1990_2020['AthiruGaiti'], y=Rainfall_Sensor_1990_2020_T['AthiruGaiti'], color='r')
# sns.regplot(ax=axes[1, 1], x=Rainfall_Station_1990_2020['TiganiaWest'], y=Rainfall_Sensor_1990_2020_T['TiganiaWest'], color='b')
# sns.regplot(ax=axes[1, 2], x=Rainfall_Station_1990_2020['TiganiaEast'], y=Rainfall_Sensor_1990_2020_T['TiganiaEast'],color='r')
# sns.regplot(ax=axes[1, 3], x=Rainfall_Station_1990_2020['IgembeCentral'], y=Rainfall_Sensor_1990_2020_T['IgembeCentral'], color='b')

import plotly.express as px

# df = px.data.tips()
# fig = px.scatter(df, x=Rainfall_Station_1990_2020['IgembeEast'], y=Rainfall_Sensor_1990_2020_T['IgembeEast'], trendline="ols")
# fig.show()
```

```python
[ ]
"""
THARAKA_NITHI

IgambangOmbe
Mariani
KyeniNorth
Magumoni
Mugwe
Chiakariga
Karingani
Mitheru
Muthambi
Ganga
Mwimbi
Chogoria
Gatunga
Nkondi
Mukothima

"""

fig, axes = plt.subplots(3,4, figsize=(35, 20))

# fig.suptitle('Station data against sensor data for Rainfall amounts (mm)')
# fig.tight_layout()
plt.rcParams["figure.autolayout"] = True
fig.subplots_adjust(hspace=0.125, wspace=0.125)

sns.regplot(ax=axes[0, 0], x=Rainfall_Station_1990_2020['Mukothima'], y=Rainfall_Sensor_1990_2020_T['Mukothima'], color='r')
sns.regplot(ax=axes[0, 1], x=Rainfall_Station_1990_2020['Nkondi'], y=Rainfall_Sensor_1990_2020_T['Nkondi'], color='b')
sns.regplot(ax=axes[0, 2], x=Rainfall_Station_1990_2020['Gatunga'], y=Rainfall_Sensor_1990_2020_T['Gatunga'], color='r')
sns.regplot(ax=axes[0, 3], x=Rainfall_Station_1990_2020['Mariani'], y=Rainfall_Sensor_1990_2020_T['Mariani'], color='b')
sns.regplot(ax=axes[1, 0], x=Rainfall_Station_1990_2020['Chogoria'], y=Rainfall_Sensor_1990_2020_T['Chogoria'], color='r')
sns.regplot(ax=axes[1, 1], x=Rainfall_Station_1990_2020['Mwimbi'], y=Rainfall_Sensor_1990_2020_T['Mwimbi'], color='b')
sns.regplot(ax=axes[1, 2], x=Rainfall_Station_1990_2020['Ganga'], y=Rainfall_Sensor_1990_2020_T['Ganga'],color='r')
sns.regplot(ax=axes[1, 3], x=Rainfall_Station_1990_2020['Muthambi'], y=Rainfall_Sensor_1990_2020_T['Muthambi'], color='b')


sns.regplot(ax=axes[2, 0], x=Rainfall_Station_1990_2020['Mitheru'], y=Rainfall_Sensor_1990_2020_T['Mitheru'], color='r')

sns.regplot(ax=axes[2, 1], x=Rainfall_Station_1990_2020['Karingani'], y=Rainfall_Sensor_1990_2020_T['Karingani'], color='b')
sns.regplot(ax=axes[2, 2], x=Rainfall_Station_1990_2020['Chiakariga'], y=Rainfall_Sensor_1990_2020_T['Chiakariga'], color='r')
sns.regplot(ax=axes[2, 3], x=Rainfall_Station_1990_2020['Mugwe'], y=Rainfall_Sensor_1990_2020_T['Mugwe'], color='b')
```

Accuracy assessment table for each station of observed rainfall against station data

```python
[ ]
Rainfall_Station_1990_2020['AthiRiver']
0      7.678
1      0.000
2      0.006
3      0.001
```

```
4        0.000
         ...
10953    0.000
10954    0.000
10955    0.000
10956    11.411
10957    1.491
Name: AthiRiver, Length: 10958, dtype: float64
```

```
[ ]
from sklearn.metrics import confusion_matrix

# confusion_matrix(Rainfall_Station_1990_2020['AthiRiver'], Rainfall_Sensor_1990_2020_T['AthiRiver'])
y_pred = Rainfall_Sensor_1990_2020_T['AthiRiver']

y_act = Rainfall_Station_1990_2020['AthiRiver']
# df_confusion = pd.crosstab(y_pred, y_act, rownames=['Actual'], colnames=['Predicted'], margins=True)
confusion_matrix = pd.crosstab(y_pred, y_act, rownames=['Actual'], colnames=['Predicted'])
print(confusion_matrix)

# sns.regplot(ax=axes[0, 0], x=Rainfall_Station_1990_2020['AthiRiver'], y=Rainfall_Sensor_1990_2020_T['AthiRiver'], color='r')
# sns.regplot(ax=axes[0, 1], x=Rainfall_Station_1990_2020['Ekalakala'], y=Rainfall_Sensor_1990_2020_T['Ekalakala'], color='b')
# sns.regplot(ax=axes[0, 2], x=Rainfall_Station_1990_2020['Ikombe'], y=Rainfall_Sensor_1990_2020_T['Ikombe'], color='r')
# sns.regplot(ax=axes[0, 3], x=Rainfall_Station_1990_2020['Kalama'], y=Rainfall_Sensor_1990_2020_T['Kalama'], color='b')
# sns.regplot(ax=axes[1, 0], x=Rainfall_Station_1990_2020['KangundoCentral'], y=Rainfall_Sensor_1990_2020_T['KangundoCentral'], color='r')
# sns.regplot(ax=axes[1, 1], x=Rainfall_Station_1990_2020['KangundoEast'], y=Rainfall_Sensor_1990_2020_T['KangundoEast'], color='b')
# sns.regplot(ax=axes[1, 2], x=Rainfall_Station_1990_2020['KangundoNorth'], y=Rainfall_Sensor_1990_2020_T['KangundoNorth'],color='r')
# sns.regplot(ax=axes[1, 3], x=Rainfall_Station_1990_2020['KangundoWest'], y=Rainfall_Sensor_1990_2020_T['KangundoWest'], color='b')
Empty DataFrame
Columns: []
Index: []
```

Plotting line of best fit for any of the station data. The station rainfall against sensor based data.

```
[ ]
from scipy.stats import linregress

from sklearn.metrics import r2_score
linregress(Rainfall_Station_1990_2020['AthiRiver'], Rainfall_Sensor_1990_2020_T['AthiRiver'])
pearsons_coefficient = np.corrcoef(Rainfall_Station_1990_2020['AthiRiver'], Rainfall_Sensor_1990_2020_T['AthiRiver'])
sns.heatmap(pearsons_coefficient, annot=True)
print(linregress(Rainfall_Station_1990_2020['AthiRiver'], Rainfall_Sensor_1990_2020_T['AthiRiver']))
print(linregress(Rainfall_Station_1990_2020['AthiRiver'], Rainfall_Sensor_1990_2020_T['AthiRiver']))
print(linregress(Rainfall_Station_1990_2020['Ekalakala'], Rainfall_Sensor_1990_2020_T['Ekalakala']))
```

Plotting confusion matrix of rainfall dataset

```
[ ]
Temperature_Sensor_1990_2020_T = Temperature_Sensor_1990_2020_T.head().reset_index()
Temperature_Station_1990_2020 = Temperature_Station_1990_2020.head()
```

Repeating the process above for temperature data, with scatter plots, and producing line of best fit First by making sure that both the datasets are equal in terms of length. Station data was observed to have fewer columns than sensor's data. This was done through merging of both dataframes and then dropping the null values.

```
[ ]
Temperature_Station_1990_2020.head()
Temperature_Sensor_1990_2020_T.head()
```

```
[ ]
# Temperature_Sensor_1990_2020_T = Temperature_Sensor_1990_2020_T.reset_index(drop=True)
# Temperature_Sensor_1990_2020_T.head()


Temperature_Sensor_1990_2020_T.rename(columns = {'index':'Date'}, inplace = True)
Temperature_Station_1990_2020.rename(columns = {'ID':'Date'}, inplace = True)
Temperature_Station_1990_2020.head()
# Temperature_Sensor_1990_2020_T.drop([0,1], axis=0, inplace=True)
Temperature_Station_1990_2020.tail()
# Temperature_Sensor_1990_2020_T.tail()
# df.drop([5,6], axis=0, inplace=True)
```

```python
# Temperature_Sensor_1990_2020_T.drop('Date', inplace=True, axis=1)
# Temperature_Sensor_1990_2020_T.head()
# Temperature_Sensor_1990_2020_T.drop(['Place', 'Date', 'Date', 'level_0'], axis=1)
# Temperature_Station_1990_2020.head()
```

```python
Temperature_Sensor= pd.read_csv('/content/drive/MyDrive/csv/DailyTemp_csv_exports_ALL_1990-2021_REGIONAL_COL_DATA.csv')
Temperature_Station = pd.read_csv('/content/drive/MyDrive/csv/Temperature_Station_Regional_1991_2020_Transposed.csv')
Temperature_Station.head()
Temperature_Sensor.head()
Temperature_Sensor_T = Temperature_Sensor.set_index('Place').T.reset_index()
Temperature_Sensor_T.head()
```

```python
from google.colab import drive
drive.mount('/content/drive')
Mounted at /content/drive
```

```python
""" printing the column heads for temeprature data for refernce"""
print(Temperature_Sensor_T.columns)
print(Temperature_Station.columns)
```

```python
Temperature_Sensor_T.rename(columns = {'index':'Date'}, inplace = True)
Temperature_Station.rename(columns = {'ID':'Date'}, inplace = True)
Temperature_Station_1990_2020.head()
```

```python
"""
Station data was inadequate as it covered up to July 2020, while sensor data covered up to December.
To plot correlation plots, equal length of data is needed, thus merging of dataframes to eliminate the
null values, and have an equal length of data
"""
Temperature_Sensor_T['Date']=Temperature_Sensor_T['Date'].astype(int)

Temperature_Station['Date']=Temperature_Station['Date'].astype(int)


Merged_data_Sensor_Station = pd.merge(Temperature_Sensor_T, Temperature_Station, on="Date")
Merged_data_Sensor_Station.tail()
print(Merged_data_Sensor_Station.columns)
Merged_data_Sensor_Station.tail()
```

```python
Temperature_Sensor_1990_2020_T.rename(columns = {'index':'Date'}, inplace = True)
Temperature_Station_1990_2020.rename(columns = {'ID':'Date'}, inplace = True)
Temperature_Station_1990_2020.head()

print(Merged_data_Sensor_Station.columns)
```

```python
fig, axes = plt.subplots(10, 4, figsize=(40, 90))

# fig.suptitle('Station data against sensor data for Rainfall amounts (mm)')
# fig.tight_layout()
plt.rcParams["figure.autolayout"] = True
fig.subplots_adjust(hspace=0.125, wspace=0.125)


"""transforming kelvin temperature to degree celcius before plotting by subtracting 271.15 """
sns.regplot(ax=axes[0, 0], x=(Merged_data_Sensor_Station['AthiRiver_x'] -
272.15), y=Merged_data_Sensor_Station['AthiRiver_y'], color='r', truncate=False)
sns.regplot(ax=axes[0, 1], x=Merged_data_Sensor_Station['Ekalakala_x']-
272.15, y=Merged_data_Sensor_Station['Ekalakala_y'], color='b',ci=68, truncate=False)
sns.regplot(ax=axes[0, 2], x=Merged_data_Sensor_Station['Ikombe_x']-
272.15, y=Merged_data_Sensor_Station['Ikombe_y'], color='r', ci=68, truncate=False)
sns.regplot(ax=axes[0, 3], x=Merged_data_Sensor_Station['Kalama_x']-
272.15, y=Merged_data_Sensor_Station['Kalama_y'], color='b', ci=68, truncate=False)
sns.regplot(ax=axes[1, 0], x=Merged_data_Sensor_Station['KangundoCentral_x']-
272.15, y=Merged_data_Sensor_Station['KangundoCentral_y'], color='r', ci=68, truncate=False)
sns.regplot(ax=axes[1, 1], x=Merged_data_Sensor_Station['KangundoEast_x']-
```

```python
272.15, y=Merged_data_Sensor_Station['KangundoEast_y'], color='b', ci=68, truncate=False)
sns.regplot(ax=axes[1, 2], x=Merged_data_Sensor_Station['KangundoNorth_x']-
272.15, y=Merged_data_Sensor_Station['KangundoNorth_y'],color='r', ci=68, truncate=False)
sns.regplot(ax=axes[1, 3], x=Merged_data_Sensor_Station['KangundoWest_x']-
272.15, y=Merged_data_Sensor_Station['KangundoWest_y'], color='b', ci=68, truncate=False)


sns.regplot(ax=axes[2, 0], x=(Merged_data_Sensor_Station['Katangi_x'] -
272.15), y=Merged_data_Sensor_Station['AthiRiver_y'], color='r', truncate=False)
sns.regplot(ax=axes[2, 1], x=Merged_data_Sensor_Station['KathianiCentral_x']-
272.15, y=Merged_data_Sensor_Station['Ekalakala_y'], color='b',ci=68, truncate=False)
sns.regplot(ax=axes[2, 2], x=Merged_data_Sensor_Station['Kibauni_x']-
272.15, y=Merged_data_Sensor_Station['Ikombe_y'], color='r', ci=68, truncate=False)
sns.regplot(ax=axes[2, 3], x=Merged_data_Sensor_Station['Kinanie_x']-272.15, y=Merged_data_Sensor_Station['Kalama_y'],
        color='b', ci=68, truncate=False)

sns.regplot(ax=axes[3, 0], x=Merged_data_Sensor_Station['Kithimani_x']-
272.15, y=Merged_data_Sensor_Station['KangundoCentral_y'], color='r', ci=68, truncate=False)
sns.regplot(ax=axes[3, 1], x=Merged_data_Sensor_Station['Kivaa_x']-
272.15, y=Merged_data_Sensor_Station['KangundoEast_y'], color='b', ci=68, truncate=False)
sns.regplot(ax=axes[3, 2], x=Merged_data_Sensor_Station['Kola_x']-
272.15, y=Merged_data_Sensor_Station['KangundoNorth_y'],color='r', ci=68, truncate=False)
sns.regplot(ax=axes[3, 3], x=Merged_data_Sensor_Station['Kyeleni_x']-
272.15, y=Merged_data_Sensor_Station['KangundoWest_y'], color='b', ci=68, truncate=False)

"""
 'LowerKaewaKaani_x', 'MachakosCentral_x', 'MakutanoMwala_x', 'Masii_x',

    'MasingaCentral_x', 'MatunguluEast_x', 'MatunguluNorth_x',
    'MatunguluWest_x',

    'Matuu_x', 'Mbiuni_x', 'Mitaboni_x', 'Mua_x',


    'MumbuniNorth_x', 'Muthesya_x', 'Muthetheni_x', 'Muthwani_x',


    'Mutituni_x', 'MuvutiKiimaKimwe_x', 'Ndalani_x', 'Ndithini_x',
    'SyokimauMulolongo_x', 'Tala_x', 'unknown7_x', 'UpperKaewaIveti_x',
    'Wamunyu_x' """



sns.regplot(ax=axes[4, 0], x=Merged_data_Sensor_Station['LowerKaewaKaani_x']-
272.15, y=Merged_data_Sensor_Station['LowerKaewaKaani_y'], color='r', ci=68, truncate=False)
sns.regplot(ax=axes[4, 1], x=Merged_data_Sensor_Station['MachakosCentral_x']-
272.15, y=Merged_data_Sensor_Station['MachakosCentral_y'], color='b', ci=68, truncate=False)
sns.regplot(ax=axes[4, 2], x=Merged_data_Sensor_Station['MakutanoMwala_x']-
272.15, y=Merged_data_Sensor_Station['MakutanoMwala_y'],color='r', ci=68, truncate=False)
sns.regplot(ax=axes[4, 3], x=Merged_data_Sensor_Station['Masii_x']-
272.15, y=Merged_data_Sensor_Station['Masii_y'], color='b', ci=68, truncate=False)


sns.regplot(ax=axes[5, 0], x=Merged_data_Sensor_Station['MasingaCentral_x']-
272.15, y=Merged_data_Sensor_Station['MasingaCentral_y'], color='r', ci=68, truncate=False)
sns.regplot(ax=axes[5, 1], x=Merged_data_Sensor_Station['MatunguluEast_x']-
272.15, y=Merged_data_Sensor_Station['MatunguluEast_y'], color='b', ci=68, truncate=False)
sns.regplot(ax=axes[5, 2], x=Merged_data_Sensor_Station['MatunguluNorth_x']-
272.15, y=Merged_data_Sensor_Station['MatunguluNorth_y'],color='r', ci=68, truncate=False)
sns.regplot(ax=axes[5, 3], x=Merged_data_Sensor_Station['MatunguluWest_x']-
272.15, y=Merged_data_Sensor_Station['MatunguluWest_y'], color='b', ci=68, truncate=False)

sns.regplot(ax=axes[6, 0], x=Merged_data_Sensor_Station['Matuu_x']-
272.15, y=Merged_data_Sensor_Station['Matuu_y'], color='r', ci=68, truncate=False)
sns.regplot(ax=axes[6, 1], x=Merged_data_Sensor_Station['Mbiuni_x']-
272.15, y=Merged_data_Sensor_Station['Mbiuni_y'], color='b', ci=68, truncate=False)
sns.regplot(ax=axes[6, 2], x=Merged_data_Sensor_Station['Mitaboni_x']-
272.15, y=Merged_data_Sensor_Station['Mitaboni_y'],color='r', ci=68, truncate=False)
sns.regplot(ax=axes[6, 3], x=Merged_data_Sensor_Station['Mua_x']-
272.15, y=Merged_data_Sensor_Station['Mua_y'], color='b', ci=68, truncate=False)

sns.regplot(ax=axes[7, 0], x=Merged_data_Sensor_Station['MumbuniNorth_x']-
272.15, y=Merged_data_Sensor_Station['MumbuniNorth_y'], color='r', ci=68, truncate=False)
sns.regplot(ax=axes[7, 1], x=Merged_data_Sensor_Station['Muthesya_x']-
```

```python
                272.15, y=Merged_data_Sensor_Station['Muthesya_y'], color='b', ci=68, truncate=False)
sns.regplot(ax=axes[7, 2], x=Merged_data_Sensor_Station['Muthetheni_x']-
272.15, y=Merged_data_Sensor_Station['Muthetheni_y'],color='r', ci=68, truncate=False)
sns.regplot(ax=axes[7, 3], x=Merged_data_Sensor_Station['Muthwani_x']-
272.15, y=Merged_data_Sensor_Station['Muthwani_y'], color='b', ci=68, truncate=False)

sns.regplot(ax=axes[8, 0], x=Merged_data_Sensor_Station['Mutituni_x']-
272.15, y=Merged_data_Sensor_Station['Mutituni_y'], color='r', ci=68, truncate=False)
sns.regplot(ax=axes[8, 1], x=Merged_data_Sensor_Station['MuvutiKiimaKimwe_x']-
272.15, y=Merged_data_Sensor_Station['MuvutiKiimaKimwe_y'], color='b', ci=68, truncate=False)
sns.regplot(ax=axes[8, 2], x=Merged_data_Sensor_Station['Ndalani_x']-
272.15, y=Merged_data_Sensor_Station['Ndalani_y'],color='r', ci=68, truncate=False)
sns.regplot(ax=axes[8, 3], x=Merged_data_Sensor_Station['Ndithini_x']-
272.15, y=Merged_data_Sensor_Station['Ndithini_y'], color='b', ci=68, truncate=False)

sns.regplot(ax=axes[9, 0], x=Merged_data_Sensor_Station['SyokimauMulolongo_x']-
272.15, y=Merged_data_Sensor_Station['SyokimauMulolongo_y'], color='r', ci=68, truncate=False)
sns.regplot(ax=axes[9, 1], x=Merged_data_Sensor_Station['Tala_x']-
272.15, y=Merged_data_Sensor_Station['Tala_y'], color='b', ci=68, truncate=False)
sns.regplot(ax=axes[9, 2], x=Merged_data_Sensor_Station['UpperKaewaIveti_x']-
272.15, y=Merged_data_Sensor_Station['UpperKaewaIveti_y'],color='r', ci=68, truncate=False)
sns.regplot(ax=axes[9, 3], x=Merged_data_Sensor_Station['Wamunyu_x']-
272.15, y=Merged_data_Sensor_Station['Wamunyu_y'], color='b', ci=68, truncate=False)


[ ]
"""
Plots of other counties
Embu Plots

Makima
Mwea
Mavuria
Kiambere
MbetiSouth
Muminji
Nthawa
MbetiNorth
Kithimu
Kirimari
Evurore
KagaariSouth
GaturiSouth
KyeniSouth
CentralWard
GaturiNorth
RuguruNgandori
Nginda
KagaariNorth
"""


fig, axes = plt.subplots(3,4, figsize=(35, 20))

# fig.suptitle('Station data against sensor data for Rainfall amounts (mm)')
# fig.tight_layout()
plt.rcParams["figure.autolayout"] = True
fig.subplots_adjust(hspace=0.125, wspace=0.125)


sns.regplot(ax=axes[0, 0], x=Merged_data_Sensor_Station['KagaariNorth_x'], y=Merged_data_Sensor_Station['KagaariNorth_y'], color='r')
sns.regplot(ax=axes[0, 1], x=Merged_data_Sensor_Station['Nginda_x'], y=Merged_data_Sensor_Station['Nginda_y'], color='b')
sns.regplot(ax=axes[0, 2], x=Merged_data_Sensor_Station['RuguruNgandori_x'], y=Merged_data_Sensor_Station['RuguruNgandori_y'], color='r')
sns.regplot(ax=axes[0, 3], x=Merged_data_Sensor_Station['GaturiNorth_x'], y=Merged_data_Sensor_Station['GaturiNorth_y'], color='b')
sns.regplot(ax=axes[1, 0], x=Merged_data_Sensor_Station['CentralWard_x'], y=Merged_data_Sensor_Station['CentralWard_y'], color='r')
sns.regplot(ax=axes[1, 1], x=Merged_data_Sensor_Station['KyeniSouth_x'], y=Merged_data_Sensor_Station['KyeniSouth_y'], color='b')
sns.regplot(ax=axes[1, 2], x=Merged_data_Sensor_Station['GaturiSouth_x'], y=Merged_data_Sensor_Station['GaturiSouth_y'],color='r')
sns.regplot(ax=axes[1, 3], x=Merged_data_Sensor_Station['KagaariSouth_x'], y=Merged_data_Sensor_Station['KagaariSouth_y'], color='b')


sns.regplot(ax=axes[2, 0], x=Merged_data_Sensor_Station['Evurore_x'], y=Merged_data_Sensor_Station['Evurore_y'], color='r')
sns.regplot(ax=axes[2, 1], x=Merged_data_Sensor_Station['Kirimari_x'], y=Merged_data_Sensor_Station['Kirimari_y'], color='b')
```

```python
sns.regplot(ax=axes[2, 2], x=Merged_data_Sensor_Station['Nthawa_x'], y=Merged_data_Sensor_Station['Nthawa_y'], color='r')
sns.regplot(ax=axes[2, 3], x=Merged_data_Sensor_Station['MbetiNorth_x'], y=Merged_data_Sensor_Station['MbetiNorth_y'], color='b')
```

```python
[ ]
"""
Kitui temperature Plots
"""

fig, axes = plt.subplots(3,4, figsize=(35, 20))

# fig.suptitle('Station data against sensor data for Rainfall amounts (mm)')
# fig.tight_layout()
plt.rcParams["figure.autolayout"] = True
fig.subplots_adjust(hspace=0.125, wspace=0.125)

sns.regplot(ax=axes[0, 0], x=Merged_data_Sensor_Station['Tseikuru_x'], y=Merged_data_Sensor_Station['Tseikuru_y'], color='r')
sns.regplot(ax=axes[0, 1], x=Merged_data_Sensor_Station['Tharaka_x'], y=Merged_data_Sensor_Station['Tharaka_y'], color='b')
sns.regplot(ax=axes[0, 2], x=Merged_data_Sensor_Station['Kyuso_x'], y=Merged_data_Sensor_Station['Kyuso_y'], color='r')
sns.regplot(ax=axes[0, 3], x=Merged_data_Sensor_Station['Ngomeni_x'], y=Merged_data_Sensor_Station['Ngomeni_y'], color='b')
sns.regplot(ax=axes[1, 0], x=Merged_data_Sensor_Station['Mumoni_x'], y=Merged_data_Sensor_Station['Mumoni_y'], color='r')
sns.regplot(ax=axes[1, 1], x=Merged_data_Sensor_Station['Waita_x'], y=Merged_data_Sensor_Station['Waita_y'], color='b')
sns.regplot(ax=axes[1, 2], x=Merged_data_Sensor_Station['Nguni_x'], y=Merged_data_Sensor_Station['Nguni_y'],color='r')
sns.regplot(ax=axes[1, 3], x=Merged_data_Sensor_Station['KiomoKyethani_x'], y=Merged_data_Sensor_Station['KiomoKyethani_y'], color='b')


sns.regplot(ax=axes[2, 0], x=Merged_data_Sensor_Station['Kivou_x'], y=Merged_data_Sensor_Station['Kivou_y'], color='r')
sns.regplot(ax=axes[2, 1], x=Merged_data_Sensor_Station['KyomeThaana_x'], y=Merged_data_Sensor_Station['KyomeThaana_y'], color='b')
sns.regplot(ax=axes[2, 2], x=Merged_data_Sensor_Station['Central_x'], y=Merged_data_Sensor_Station['Central_y'], color='r')
sns.regplot(ax=axes[2, 3], x=Merged_data_Sensor_Station['Migwani_x'], y=Merged_data_Sensor_Station['Migwani_y'], color='b')
```

```python
[ ]
"""
THARAKA_NITHI Temperaryre plots
"""

fig, axes = plt.subplots(3,4, figsize=(35, 20))

# fig.suptitle('Station data against sensor data for Rainfall amounts (mm)')
# fig.tight_layout()
plt.rcParams["figure.autolayout"] = True
fig.subplots_adjust(hspace=0.125, wspace=0.125)

sns.regplot(ax=axes[0, 0], x=Merged_data_Sensor_Station['Mukothima_x'], y=Merged_data_Sensor_Station['Mukothima_y'], color='r')
sns.regplot(ax=axes[0, 1], x=Merged_data_Sensor_Station['Nkondi_x'], y=Merged_data_Sensor_Station['Nkondi_y'], color='b')
sns.regplot(ax=axes[0, 2], x=Merged_data_Sensor_Station['Gatunga_x'], y=Merged_data_Sensor_Station['Gatunga_y'], color='r')
sns.regplot(ax=axes[0, 3], x=Merged_data_Sensor_Station['Mariani_x'], y=Merged_data_Sensor_Station['Mariani_y'], color='b')
sns.regplot(ax=axes[1, 0], x=Merged_data_Sensor_Station['Chogoria_x'], y=Merged_data_Sensor_Station['Chogoria_y'], color='r')
sns.regplot(ax=axes[1, 1], x=Merged_data_Sensor_Station['Mwimbi_x'], y=Merged_data_Sensor_Station['Mwimbi_y'], color='b')
sns.regplot(ax=axes[1, 2], x=Merged_data_Sensor_Station['Ganga_x'], y=Merged_data_Sensor_Station['Ganga_y'],color='r')
sns.regplot(ax=axes[1, 3], x=Merged_data_Sensor_Station['Muthambi_x'], y=Merged_data_Sensor_Station['Muthambi_y'], color='b')


sns.regplot(ax=axes[2, 0], x=Merged_data_Sensor_Station['Mitheru_x'], y=Merged_data_Sensor_Station['Mitheru_y'], color='r')

sns.regplot(ax=axes[2, 1], x=Merged_data_Sensor_Station['Karingani_x'], y=Merged_data_Sensor_Station['Karingani_y'], color='b')
sns.regplot(ax=axes[2, 2], x=Merged_data_Sensor_Station['Chiakariga_x'], y=Merged_data_Sensor_Station['Chiakariga_y'], color='r')
sns.regplot(ax=axes[2, 3], x=Merged_data_Sensor_Station['Mugwe_x'], y=Merged_data_Sensor_Station['Mugwe_y'], color='b')
```

Computing standard error based on each station and sensor data, plus their correlation matrix. There is a high correlation between the two datasets (tempertaure sensors and temperature station).

```python
[ ]
from scipy.stats import linregress

from sklearn.metrics import r2_score

linregress(Merged_data_Sensor_Station['AthiRiver_x'], Merged_data_Sensor_Station['AthiRiver_y'])
pearsons_coefficient = np.corrcoef(Merged_data_Sensor_Station['AthiRiver_x'], Merged_data_Sensor_Station['AthiRiver_y'])
pearsons_coefficient2 = np.corrcoef(Merged_data_Sensor_Station['Ekalakala_x'], Merged_data_Sensor_Station['Ekalakala_x'])
sns.heatmap(pearsons_coefficient, annot=True)

print(linregress((Merged_data_Sensor_Station['AthiRiver_x'] -272.15), Merged_data_Sensor_Station['AthiRiver_y']))
print(linregress((Merged_data_Sensor_Station['Ekalakala_x'] -272.15), Merged_data_Sensor_Station['Ekalakala_y']))
```

```
print(linregress((Merged_data_Sensor_Station['Ikombe_x'] -272.15), Merged_data_Sensor_Station['Ikombe_y']))
# sns.heatmap(pearsons_coefficient2, annot=True)
```

Getting the Tavg finding the average between the Min temperature and max temperature.

```
[ ]
Min_Temp = pd.read_csv('/content/drive/MyDrive/AEZ_MACHAKOS_CSV/machakos-tmax_stations.csv')
Min_Temp.head()
Max_Temp = pd.read_csv('/content/drive/MyDrive/AEZ_MACHAKOS_CSV/machakos-tmin-stations.csv')
print(Max_Temp.size)
print(Min_Temp.size)

# concatenate dataframe

Cont_Temp = pd.concat([Max_Temp, Min_Temp])
Cont_Temp.mean()

Blended_Temp = pd.DataFrame(Cont_Temp.mean()).reset_index().drop(1, )

Blended_Temp.rename(columns={'index' :'Place', 0 : 'Temperature'},inplace=True)

Blended_Temp.head()
Temp_mean = Blended_Temp.drop([0, ])
```

Plotting temperature mean plots based on the averaged min and max temperatures

```
[ ]
import seaborn as sn
fig = px.line(Temp_mean, x="Place", y="Temperature")
fig.show()
```

```
[ ]
"""
Plotting LGP since we had all the dataset processed earlier from codes going down
"""
LGP_90_MAM = pd.read_csv('/content/drive/MyDrive/csv/SELECTED_1990_2005_MAM_T_PET.csv')
LGP_90_MAM.head()

import seaborn as sn
fig = px.line(LGP_90_MAM, x="index", y="Sum")
fig.show()
```

```
[ ]
LGP_90_OND = pd.read_csv('/content/drive/MyDrive/csv/SELECTED_1990_2005_OND_T_LPG.csv')
LGP_90_OND.head()

import seaborn as sn
fig = px.line(LGP_90_OND, x="index", y="Sum")
fig.show()
```

```
[ ]
LGP_20_MAM = pd.read_csv('/content/drive/MyDrive/csv/SELECTED_2006_2020_MAM_T_LPG.csv')
LGP_90_MAM.head()

import seaborn as sn
fig = px.line(LGP_90_OND, x="index", y="Sum")
fig.show()
```

```
[ ]
LGP_20_OND = pd.read_csv('/content/drive/MyDrive/csv/SELECTED_2006_2020_OND_T_LPG.csv')
LGP_90_OND.head()

import seaborn as sn
fig = px.line(LGP_90_OND, x="index", y="Sum")
fig.show()
```

```
[ ]
PET_90_MAM = pd.read_csv('/content/drive/MyDrive/csv/SELECTED_1990_2005_MAM_T_PET.csv')
PET_90_MAM .head()

import seaborn as sn
fig = px.line(PET_90_MAM, x="index", y="Sum")
fig.show()
```

```
[ ]
```

```python
PET_90_OND = pd.read_csv('/content/drive/MyDrive/csv/SELECTED_1990_2005_OND_T_PET.csv')
PET_90_OND .head()

import seaborn as sn
fig = px.line(PET_90_OND, x="index", y="Sum")
fig.show()
```

```python
[ ]
PET_20_MAM = pd.read_csv('/content/drive/MyDrive/csv/SELECTED_2006_2020_MAM_T_PET.csv')
PET_90_MAM .head()

import seaborn as sn
fig = px.line(PET_90_MAM, x="index", y="Sum")
fig.show()
```

```python
[ ]
PET_20_OND = pd.read_csv('/content/drive/MyDrive/csv/SELECTED_2006_2020_OND_T_PET.csv')
PET_90_OND .head()

import seaborn as sn
fig = px.line(PET_90_OND, x="index", y="Sum")
fig.show()
```

The codes going down might be obsolete since they focused on computing LGP. We already computed LGP initially so their usage migh be limited from here. The graph abaove can show the avaerage temeperature, but its output is not so needed.

Processing dataframe and preparing it to be ingested in the R function for computation of daily PET using methods available.

```python
[ ]
Temperature_Sensor.head()
```

```python
[ ]
Temperature_Sensor.head()
```

```python
[ ]


""" Saving the locations as a separate dataframe for later use in merging to the final datasets for processing of PET in R """


Positions = Temperature_Sensor[['Place','Latitude','Longitude']]
Positions.head()

Positions.rename(columns = {'Place':'index'}, inplace = True)

Positions.head()
```

```python
[ ]
"""
setting the new dataframe in a manner that can be used in formating the index column to Year, Month and Day to be used in PET computation in R

"""
Temperature_Sensor_T_PET = Temperature_Sensor.drop(['Latitude', 'Longitude'], axis=1, inplace=False)
Temperature_Sensor_T_PET_T = Temperature_Sensor_T_PET.set_index('Place').T.reset_index()
Temperature_Sensor_T_PET_T.head()
```

```python
[ ]
"""
Processing the LGP for the entire study area. Start by transposing the Temperature and Rainfall sensor data extracted.
After transposing, change the data format to years and months alone
"""


Temperature_Regional = (pd.read_csv('/content/drive/MyDrive/CSV_FINAL_2022_08_31/DailyTemp_csv_exports_ALL_1990-
2021_REGIONAL_FOR_LGP.csv')).set_index('ID').T.reset_index()

Rainfall_Regional = (pd.read_csv('/content/drive/MyDrive/CSV_FINAL_2022_08_31/DailyTemp_csv_exports_ALL_1990-
2021_REGIONAL_FOR_LGP.csv')).set_index('ID').T.reset_index()
date_col = Rainfall_Regional['index'].to_frame()
```

```
    date_col
    # Temperature_Regional
    # Rainfall_Regional.head()
```

```
[ ]
from datetime import datetime

regional_date = pd.DataFrame(columns=['Year','Month','Day'])

for data in range(len(date_col)):
 # print(ppt_llpg_fitered.iloc[data,0])
 date_coverted = datetime.strptime((date_col.iloc[data,0]),'%Y%m%d')
 Year = date_coverted.date().year
 Month = date_coverted.date().month
 Day = date_coverted.date().day

 # print(date_coverted)

 regional_date = regional_date.append({'Year':Year,'Month':Month,'Day':Day}, ignore_index=True)


regional_date
```

```
[ ]
Temperature_Regional
# Rainfall_Regional

regional_date.to_csv('regional_date.csv', index=True, encoding='utf-8')
```

```
[ ]
Rainfall_Regional.head()

Rainfall_Regional.to_csv('Rainfall_Regional_dateset.csv', index=True, encoding='utf-8')
```

```
[ ]
"""
Converting the date column to year, month and day. Later the Dataframe will
 be merged with the other dataframe for processing purposes
"""
import datetime
from datetime import datetime
Temperature_Sensor_T_PET_T.head()

Just_Temp_Data = pd.DataFrame(columns=['Date','Year', 'Month', 'Day', 'index'])
```

```
[ ]
print(',-1.5'*156)
```

```
[ ]
# Temperature_Sensor_T_PET_T.head()
Just_Temp_Data.head()
```

```
[ ]
Positions.head()
```

```
[ ]
"""
Merging the various dataframes with date, year adn day columns for processing thereafter
"""

Merged_Temp_Sensor_Station_4PET = pd.merge(Temperature_Sensor_T_PET_T, Just_Temp_Data, on="index")
Merged_Temp_Sensor_Station_4PET.head()

Merged_Temp_Transposed = Merged_Temp_Sensor_Station_4PET.set_index('index').T.reset_index()
Merged_Positions_Temp_Transposed = pd.merge(Merged_Temp_Transposed, Positions, on = "index")
Merged_Positions_Temp_Transposed.head()
# print(Merged_Positions_Temp_Transposed.columns)
Merged_Positions_Temp_Transposed.tail()
# print(Merged_Positions_Temp_Transposed['index'])
Merged_Temp_Sensor_Station_4PET.head()
# Merged_Temp_Transposed.tail()
# print(Merged_Temp_Transposed['index'])
```

```python
"""
 saving the prepared dataframe as a csv and using it in R for PET analysis
"""

Merged_Temp_Sensor_Station_4PET.to_csv('Merged_Temp_Sensor_Station_4PET.csv', index=True, encoding='utf-8')
```

```python
[ ]
"""
using the daily PET to compute LGP for various years in each station

"""

Daily_PET = pd.read_csv('/content/drive/MyDrive/AEZ_MACHAKOS_CSV/DAILY_PET_DATA_COMPUTED_With_ROWS.csv')
Daily_PET
```

```python
[ ]
"""
Computing the value of LGP per year based on the Rainfall Data. Rainfall data that is more than 0.5 PET should be considered as a day that c
rops could germinate, as some
mositure was left in the soil. This starts by reading the daily PET that was computed in R using the thornthwite function, with Tavg and latitu
de as the input of the model

"""

Compututed_daily_PET = pd.read_csv('/content/drive/MyDrive/AEZ_MACHAKOS_CSV/DAILY_PET_DATA_COMPUTED_With_ROW
S_FORLGP.csv')
Compututed_daily_PET.head()
Compututed_daily_PPT = pd.read_csv('/content/drive/MyDrive/AEZ_MACHAKOS_CSV/Rainfall_Sensor_1990_2020_Transposed_ROWS
_forLGP_2.csv')
Compututed_daily_PPT.head()

"""
Comparing the values of daily precipitation and the values of daily PET
where PPT >= 0.5PET
"""

Compututed_daily_PPT.head()
# Compututed_daily_PET.head()


columns = Compututed_daily_PPT[['Year','Month']]
columns

Compututed_daily_PET
```

```python
[ ]
"""
Comparing the dataframes of PET and daily Rainfall to analys LPG. The resultant dataframe was transformed to a bolean dataframe, where t
he days that
PPT was greater than PET, the value is 1, while the reverse was made to be 0. This is to necessitate the possibility of creating a pivot table of
sum of days that
of LPG

"""
```

```python
[ ]
import pandas as pd
import numpy as np



final_df = pd.DataFrame()




Compututed_daily_PPT.head()
Compututed_daily_PET.head()

for column, col in range(len(Compututed_daily_PPT.iloc[: 2:42]), len(Compututed_daily_PET.iloc[: 2:42])):
  df = column  >= col/2

  print(df)
```

```
    final_df = final_df.append(df)
final_df.head()
```

[ ]
```
Compututed_daily_PPT
```

[ ]
```
Compututed_daily_PPT
Compututed_daily_PET

Compututed_daily_PPT.eq(Compututed_daily_PET/2)

df_new = (Compututed_daily_PPT.iloc[:, 0:43]).ge(Compututed_daily_PET.iloc[:, 0:43]/2)
df_new


Compututed_daily_PET.iloc[:, 0:43]/2
```

[ ]
```python
Regional_PET = pd.read_csv('/content/drive/MyDrive/CSV_FINAL_2022_08_31/PET_REGIONAL.csv')
Regional_PET


"""

Filtering by years and months to identify the MAM and OND LGP values

"""


"""

Filtering by seasons including OND and MAM for both epochs and findingh their LPG  per season in each location.

"""


"""
Finding the LPG (MAM & OND) 1991 - 2005
"""
SELECTED1990_2005_MAM = Regional_PET[(Regional_PET['Year'] >= 1991) & (Regional_PET['Year'] <= 2005) & (Regional_PET['Month'] >= 3) & (Regional_PET['Month'] <= 5) ]
SELECTED1990_2005_MAM
SELECTED1990_2005_OND = Regional_PET[(Regional_PET['Year'] >= 1991) & (Regional_PET['Year'] <= 2005) & (Regional_PET['Month'] >= 10) & (Regional_PET['Month'] <= 12) ]
SELECTED1990_2005_OND


"""
Finding the LPG (MAM & OND) 2006 - 2021
"""

SELECTED2006_2020_OND = Regional_PET[(Regional_PET['Year'] >= 2006) & (Regional_PET['Year'] <= 2020) & (Regional_PET['Month'] >= 10) & (Regional_PET['Month'] <= 12) ]

SELECTED2006_2020_MAM = Regional_PET[(Regional_PET['Year'] >= 2006) & (Regional_PET['Year'] <= 2020) & (Regional_PET['Month'] >= 3) & (Regional_PET['Month'] <= 5) ]
SELECTED2006_2020_MAM.head()


"""
Rearranging the LPGs to plottabel both spatially and as charts and maps and getting the sum of OND days per season
"""

SELECTED_2006_2020_MAM_T_PET = SELECTED2006_2020_MAM.drop(['Year', 'Month'], axis=1).T.mean(axis = 1).to_frame().rename(columns = {0:'Sum'}).reset_index()

SELECTED_2006_2020_OND_T_PET = SELECTED2006_2020_OND.drop(['Year', 'Month'], axis=1).T.mean(axis = 1).to_frame().rename(columns = {0:'Sum'}).reset_index()

SELECTED_1990_2005_OND_T_PET = SELECTED1990_2005_OND.drop(['Year', 'Month'], axis=1).T.mean(axis = 1).to_frame().rename(columns = {0:'Sum'}).reset_index()

SELECTED_1990_2005_MAM_T_PET = SELECTED1990_2005_MAM.drop(['Year', 'Month'], axis=1).T.mean(axis = 1).to_frame().rename(columns = {0:'Sum'}).reset_index()
```

```
SELECTED_1990_2005_MAM_T_PET
SELECTED_1990_2005_OND_T_PET
```

```
[ ]
SELECTED_2006_2020_MAM_T_PET.to_csv('SELECTED_2006_2020_MAM_T_PET.csv', encoding='utf-8')
SELECTED_1990_2005_MAM_T_PET.to_csv('SELECTED_1990_2005_MAM_T_PET.csv', encoding='utf-8')
SELECTED_2006_2020_OND_T_PET.to_csv('SELECTED_2006_2020_OND_T_PET.csv', encoding='utf-8')
SELECTED_1990_2005_OND_T_PET.to_csv('SELECTED_1990_2005_OND_T_PET.csv', encoding='utf-8')
```

```
[ ]
"""
Computing for regional LGP, using regional PET and regional PPT
then finding the summation and of each location in terms of season, afterwhich are plotted spatially.
"""

Regional_PET = pd.read_csv('/content/drive/MyDrive/CSV_FINAL_2022_08_31/PET_REGIONAL.csv')
Regional_Rainfall = pd.read_csv('/content/drive/MyDrive/CSV_FINAL_2022_08_31/Rainfall_Regional_dateset.csv')

Regional_LGP = (Regional_Rainfall.iloc[:, 3:155]).ge(Regional_PET.iloc[:, 3:155]/2)
Regional_LGP
Regional_LGP_2 = Regional_LGP.replace({True: 1, False: 0})
Regional_LGP_2
Regional_LGP_2['Year'] = regional_date['Year']
Regional_LGP_2['Month'] = regional_date['Month']
Regional_LGP_2.head()
```

```
[ ]
"""
Filtering by years and months to identify the MAM and OND LGP values

"""

"""
Filtering by seasons including OND and MAM for both epochs and findingh their LPG  per season in each location.

"""

"""
Finding the LPG (MAM & OND) 1991 - 2005
"""
SELECTED1990_2005_MAM = Regional_LGP_2[(Regional_LGP_2['Year'] >= 1991) & (Regional_LGP_2['Year'] <= 2005) & (Regional_LGP_2['Month'] >= 3) & (Regional_LGP_2['Month'] <= 5) ]
SELECTED1990_2005_MAM
SELECTED1990_2005_OND = Regional_LGP_2[(Regional_LGP_2['Year'] >= 1991) & (Regional_LGP_2['Year'] <= 2005) & (Regional_LGP_2['Month'] >= 10) & (Regional_LGP_2['Month'] <= 12) ]
SELECTED1990_2005_OND

"""
Finding the LPG (MAM & OND) 2006 - 2021
"""

SELECTED2006_2020_OND = Regional_LGP_2[(Regional_LGP_2['Year'] >= 2006) & (Regional_LGP_2['Year'] <= 2020) & (Regional_LGP_2['Month'] >= 10) & (Regional_LGP_2['Month'] <= 12) ]

SELECTED2006_2020_MAM = Regional_LGP_2[(Regional_LGP_2['Year'] >= 2006) & (Regional_LGP_2['Year'] <= 2020) & (Regional_LGP_2['Month'] >= 3) & (Regional_LGP_2['Month'] <= 5) ]
SELECTED2006_2020_MAM.head()

"""
Rearranging the LPGs to plottabel both spatially and as charts and maps and getting the sum of OND days per season
"""

SELECTED_2006_2020_MAM_T = SELECTED2006_2020_MAM.drop(['Year', 'Month'], axis=1).T.sum(axis = 1).to_frame().rename(columns = {0:'Sum'}).reset_index()

SELECTED_2006_2020_OND_T = SELECTED2006_2020_OND.drop(['Year', 'Month'], axis=1).T.sum(axis = 1).to_frame().rename(columns = {0:'Sum'}).reset_index()

SELECTED_1990_2005_OND_T = SELECTED1990_2005_OND.drop(['Year', 'Month'], axis=1).T.sum(axis = 1).to_frame().rename(columns = {0:'Sum'}).reset_index()

SELECTED_1990_2005_MAM_T = SELECTED1990_2005_MAM.drop(['Year', 'Month'], axis=1).T.sum(axis = 1).to_frame().rename(columns = {0:'Sum'}).reset_index()
```

SELECTED_1990_2005_MAM_T

[ ]
```
"""
Saving the PET as CSV for plotting ready
"""
SELECTED_2006_2020_MAM_T.to_csv('SELECTED_2006_2020_MAM_T_LPG.csv', encoding='utf-8')
SELECTED_1990_2005_MAM_T.to_csv('SELECTED_1990_2005_MAM_T_LPG.csv', encoding='utf-8')
SELECTED_2006_2020_OND_T.to_csv('SELECTED_2006_2020_OND_T_LPG.csv', encoding='utf-8')
SELECTED_1990_2005_OND_T.to_csv('SELECTED_1990_2005_OND_T_LPG.csv', encoding='utf-8')
```

[ ]
```
"""
Saving the LPGs as CSV for plotting ready
"""
SELECTED_2006_2020_MAM_T.to_csv('SELECTED_2006_2020_MAM_T_LPG.csv', encoding='utf-8')
SELECTED_1990_2005_MAM_T.to_csv('SELECTED_1990_2005_MAM_T_LPG.csv', encoding='utf-8')
SELECTED_2006_2020_OND_T.to_csv('SELECTED_2006_2020_OND_T_LPG.csv', encoding='utf-8')
SELECTED_1990_2005_OND_T.to_csv('SELECTED_1990_2005_OND_T_LPG.csv', encoding='utf-8')
```

[ ]
```
df_new2 = df_new.replace({True: 1, False: 0})
df_new2
```

[ ]
```
df_new2['Year'] = columns['Year']
df_new2['Month'] = columns['Month']
PET_LPG_COUNTS = df_new2

PET_LPG_COUNTS
```

[ ]
```
PET_LPG_COUNTS
```

[ ]
```
"""
Creating a copy of the dataframe for summation analysis per year for the LPG
"""

PET_LPG_COUNTS_copy = PET_LPG_COUNTS.copy()
```

[ ]
```
"""
dropping the unecessary columns to compute the sum of number of LPG

"""
dropped_df = PET_LPG_COUNTS_copy.drop(['Year', 'Month'], axis=1)
dropped_df.head()
```

[ ]
```
"""
Doing the row sum for each location to get the number of crop growing days in each location

"""

dropped_df_T = dropped_df.T
dropped_df_T_sum = dropped_df_T.sum(axis = 1).to_frame().reset_index()
dropped_df_T_sum
dropped_df_T_sum.head()
dropped_df_T_sum['Year']=columns['Year']
dropped_df_T_sum['Month']=columns['Month']
# df_new2['Year'] = columns['Year']
# df_new2['Month'] = columns['Month']

import seaborn as sn
fig = px.bar(dropped_df_T_sum, x="index", y=0)
fig.show()
# ax = sns.barplot(x="index", y=0, hue="Year", data=dropped_df_T_sum)
```

```python
# dropped_df_T_sum
# dropped_df_T
"""
The plot shows the areas that had the hisgest number of crop growing days from 1991 to 2020. The data has not been filtered by season yet
"""
```

```python
[ ]
"""
Filtering by seasons including OND and MAM for both epochs and findingh their LPG  per season in each location.

"""

dropped_df
dropped_df
dropped_df['Year']=columns['Year']
dropped_df['Month']=columns['Month']
dropped_df.head()

"""
Finding the LPG (MAM & OND) 1991 - 2005
"""
SELECTED1990_2005_MAM = dropped_df[(dropped_df['Year'] >= 1991) & (dropped_df['Year'] <= 2005) & (dropped_df['Month'] >= 3)
& (dropped_df['Month'] <= 5) ]
SELECTED1990_2005_MAM
SELECTED1990_2005_OND = dropped_df[(dropped_df['Year'] >= 1991) & (dropped_df['Year'] <= 2005) & (dropped_df['Month'] >= 10)
& (dropped_df['Month'] <= 12) ]
SELECTED1990_2005_OND

"""
Finding the LPG (MAM & OND) 2006 - 2021
"""

SELECTED2006_2020_OND = dropped_df[(dropped_df['Year'] >= 2006) & (dropped_df['Year'] <= 2020) & (dropped_df['Month'] >= 10)
& (dropped_df['Month'] <= 12) ]

SELECTED2006_2020_MAM = dropped_df[(dropped_df['Year'] >= 2006) & (dropped_df['Year'] <= 2020) & (dropped_df['Month'] >= 3)
& (dropped_df['Month'] <= 5) ]

"""
Rearranging the LPGs to plottabel both spatially and as charts and maps and getting the sum of OND days per season
"""

SELECTED_2006_2020_MAM_T = SELECTED2006_2020_MAM.drop(['Year', 'Month'], axis=1).T.sum(axis = 1).to_frame().rename(columns = {0:'Sum'}).reset_index()

SELECTED_2006_2020_OND_T = SELECTED2006_2020_OND.drop(['Year', 'Month'], axis=1).T.sum(axis = 1).to_frame().rename(columns = {0:'Sum'}).reset_index()

SELECTED_1990_2005_OND_T = SELECTED1990_2005_OND.drop(['Year', 'Month'], axis=1).T.sum(axis = 1).to_frame().rename(columns = {0:'Sum'}).reset_index()

SELECTED_1990_2005_MAM_T = SELECTED1990_2005_MAM.drop(['Year', 'Month'], axis=1).T.sum(axis = 1).to_frame().rename(columns = {0:'Sum'}).reset_index()




SELECTED_1990_2005_MAM_T
```

```python
[ ]
"""
SAVING THE LPGs AS CSV FOR MAP GENERATION OF LGP MAPS PER SEASON
"""

SELECTED_2006_2020_MAM_T
SELECTED_1990_2005_MAM_T
SELECTED_2006_2020_OND_T
SELECTED_1990_2005_OND_T

SELECTED_2006_2020_MAM_T.to_csv('SELECTED_2006_2020_MAM_T_LPG.csv', encoding='utf-8')
SELECTED_1990_2005_MAM_T.to_csv('SELECTED_1990_2005_MAM_T_LPG.csv', encoding='utf-8')
SELECTED_2006_2020_OND_T.to_csv('SELECTED_2006_2020_OND_T_LPG.csv', encoding='utf-8')
SELECTED_1990_2005_OND_T.to_csv('SELECTED_1990_2005_OND_T_LPG.csv', encoding='utf-8')
```

```
[ ]
"""
 LPG MAM 2006 TO 2020 GRAPH
"""
fig = px.bar(SELECTED_2006_2020_MAM_T, x="index", y='Sum')
fig.show()
```

```
[ ]
"""
 MAM 1990 TO 2005 GRAPH
"""
fig = px.bar(SELECTED_1990_2005_MAM_T, x="index", y='Sum')
fig.show()
```

```
[ ]
"""
 OND 2006 TO 2020 GRAPH
"""
fig = px.bar(SELECTED_2006_2020_OND_T, x="index", y='Sum')
fig.show()
```

```
[ ]

"""
 OND 1990 TO 2005 GRAPH
"""
fig = px.bar(SELECTED_1990_2005_OND_T, x="index", y='Sum')
fig.show()
```

```
[ ]
"""
finding the sum of number of LPG per day as a single count with a column, then later merging it with the whole dataset
"""
PET_LPG_COUNTS_copy_sum_per_day = dropped_df.sum(axis = 1).to_frame()
PET_LPG_COUNTS_copy_sum_per_day.rename(columns = {0:'Sum'}).astype(str)
```

```
[ ]
"""
combining the columns with the year and months with the LPG counts
"""
columns.reset_index(drop=True, inplace=True)
PET_LPG_COUNTS_copy_sum_per_day.reset_index(drop=True, inplace=True)
concatenated_summationLPG_ = pd.concat([PET_LPG_COUNTS_copy_sum_per_day, columns], axis=1)
concatenated_summationLPG_.rename(columns = {0:'Sum'})
```

```
[ ]
concatenated_summationLPG_[(concatenated_summationLPG_['Year'] == 2017) & (concatenated_summationLPG_[0] == 1)]
```

```
[ ]
# concatenated_summationLPG_[(concatenated_summationLPG_['Year'] == 2017) & (concatenated_summationLPG_[0] == 1)]
selected_columns = concatenated_summationLPG_[(concatenated_summationLPG_[0] == 1)]
selected_columns.head()
# df["A"][(df["B"] > 50) & (df["C"] == 900)]
```

```
[ ]
# """"""
# Drawing the number of days that the Pet was twice as much as rainfall from 1990 - 2005
# showing only a few days that had the said condition as can be seen in the graph.

# Number of crop growth days in each year, based on potential PET and received rainfall

# """"""

fig = px.bar(selected_columns, x="Year", y=0)
fig = px.histogram(selected_columns, x="Year", y=0)
# fig = px.bar(selected_columns, x="Year", y=0)
fig.show()
```

```
[ ]
"""
Filtering the daily PET data based on MAM and OND seasons, for basically kriging for computation on LGD and combination with other dat
asets on googlea earth negine
This entails transforming to csv for later processing in excel to save on time
"""
```

```
Compututed_daily_PET.head()

PET_MAM_1991_2005 = Compututed_daily_PET[(Compututed_daily_PET['Year'] <= 2005) & (Compututed_daily_PET['Month'] >= 3) &
(Compututed_daily_PET['Month'] <= 5) ]
PET_MAM_1991_2005_T = PET_MAM_1991_2005.set_index('Year').T
PET_MAM_1991_2005_T_mean = PET_MAM_1991_2005_T.mean(axis=1).to_frame().reset_index()
PET_MAM_1991_2005_T_mean.to_csv('PET_MAM_1991_2005_T_mean.csv', encoding='utf-8')

PET_OND_1991_2005 = Compututed_daily_PET[(Compututed_daily_PET['Year'] <= 2005) & (Compututed_daily_PET['Month'] >= 10) &
 (Compututed_daily_PET['Month'] <= 12) ]
PET_OND_1991_2005_T = PET_OND_1991_2005.set_index('Year').T
PET_OND_1991_2005_T_mean = PET_OND_1991_2005_T.mean(axis=1).to_frame().reset_index()
PET_OND_1991_2005_T_mean.to_csv('PET_OND_1991_2005_T_mean.csv', encoding='utf-8')

PET_OND_2006_2021 = Compututed_daily_PET[(Compututed_daily_PET['Year'] >= 2006) & (Compututed_daily_PET['Month'] >= 3) & (
Compututed_daily_PET['Month'] <= 5) ]
PET_OND_2006_2021_T = PET_OND_2006_2021.set_index('Year').T
PET_OND_2006_2021_T_mean = PET_OND_2006_2021_T.mean(axis=1).to_frame().reset_index()
PET_OND_2006_2021_T_mean.to_csv('PET_OND_2006_2021_T_mean.csv', encoding='utf-8')


PET_MAM_2006_2021 = Compututed_daily_PET[(Compututed_daily_PET['Year'] >= 2006) & (Compututed_daily_PET['Month'] >= 10)
& (Compututed_daily_PET['Month'] <= 12) ]
PET_MAM_2006_2021_T = PET_MAM_1991_2005.set_index('Year').T
PET_MAM_2006_2021_T_mean = PET_MAM_2006_2021_T.mean(axis=1).to_frame().reset_index()
PET_MAM_2006_2021_T_mean.to_csv('PET_MAM_2006_2021_T_mean.csv', encoding='utf-8')


PET_MAM_2006_2021_T.mean(axis=1)

for_latitude = pd.read_csv('/content/Temperature_csv_exports_ALL_1990-2020.csv')
for_latitude
LATLONG = for_latitude[['Place','Latitude','Longitude']]
LATLONG.to_csv('LATLONG.csv', encoding='utf-8')

# LATLONG_2 = LATLONG.rename(columns = {'Place':'index'}, inplace = True)
# PET_MAM_2006_2021_T_mean_merged = pd.merge(PET_MAM_2006_2021_T_mean, LATLONG_2, on="index")

# df.rename(columns = {'old_col1':'new_col1', 'old_col2':'new_col2'}, inplace = True)
```

Processing the predicted or future AEZ CSV data for the sake of interplolation and processing of LGP, PET and Rainfall Rasters.

```
[ ]
Rainfall_rcp85 = pd.read_csv('/content/drive/MyDrive/CSV_FINAL_2022_08_31/Rainfall_RCP85.csv').reset_index().set_index('index').T.a
stype(str).reset_index()
Temperature_rcp85 = pd.read_csv('/content/drive/MyDrive/CSV_FINAL_2022_08_31/TEMPERATURE_RCP85.csv').reset_index().set_ind
ex('index').T.reset_index()
Temperature_rcp45 = pd.read_csv('/content/drive/MyDrive/CSV_FINAL_2022_08_31/TEMPERATURE_RCP45.csv').reset_index().set_ind
ex('index').T.reset_index()
Rainfall_rcp45 = pd.read_csv('/content/drive/MyDrive/CSV_FINAL_2022_08_31/Rainfall_RCP45.csv').reset_index().set_index('index').T.re
set_index()
Temperature_rcp85.head()
Rainfall_rcp45.head()
```

Converting data column to interable feature

```
[ ]
from datetime import datetime
Predicted_date = Temperature_rcp85[['index']].astype(str)


PREDICTED_DATES = pd.DataFrame(columns=['Year','Month'])

for data in range(len(Temperature_rcp85)):
 # print(ppt_llpg_fitered.iloc[data,0])
 date_coverted = datetime.strptime((Temperature_rcp85.iloc[data,0]), '%d/%m/%Y')
 Year = date_coverted.date().year
 Month = date_coverted.date().month


 # print(date_coverted)

 PREDICTED_DATES = PREDICTED_DATES.append({'Year':Year,'Month':Month}, ignore_index=True)
```

PREDICTED_DATES

```
# regional_date3['ID2']=rain_date['ID']
# regional_date
```

Joining the date colum with the entire dataframe, for filtering and selection

```
[ ]
Temperature_rcp85[['Year','Month']] = PREDICTED_DATES[['Year','Month']]
Rainfall_rcp85[['Year','Month']] = PREDICTED_DATES[['Year','Month']]
Rainfall_rcp45[['Year','Month']] = PREDICTED_DATES[['Year','Month']]
Temperature_rcp45[['Year','Month']] = PREDICTED_DATES[['Year','Month']]
Rainfall_rcp85.head()
Temperature_rcp85.head()
Temperature_rcp45.head()
```

Comparing CSV data of rainfal to develop LGP

```
[ ]
Rainfall_rcp85
Rainfall_rcp45.head()
PET_rcp85 = pd.read_csv('/content/drive/MyDrive/CSV_FINAL_2022_08_31/PET_rcp85_Transposed.csv')
PET_rcp45 = pd.read_csv('/content/drive/MyDrive/CSV_FINAL_2022_08_31/PET_rcp45_Transposed.csv')
PET_rcp45.head()
Rainfall_rcp45
Rainfall_rcp85.head()
PET_rcp45.head()
```

Selecting for the various products including MAM and OND

```
[ ]

Temperature_rcp85_select = Temperature_rcp85.iloc[:, 1:462]
Temperature_rcp45.head()
Temperature_rcp85_select
Rainfall_rcp85_select = Rainfall_rcp85.iloc[:, 1:462]
Rainfall_rcp85_select
Rainfall_rcp45_select = Rainfall_rcp45.iloc[:,1:462]

Rainfall_rcp45_select[['Year','Month']] = PREDICTED_DATES[['Year','Month']]
Rainfall_rcp85_select[['Year','Month']] = PREDICTED_DATES[['Year','Month']]
Rainfall_rcp85_select
Rainfall_rcp45_select
```

```
[ ]
Temperature_rcp85_select = Temperature_rcp85.iloc[:, 1:462]
Temperature_rcp45_select = Temperature_rcp45.iloc[:, 1:462]
Temperature_rcp85_select[['Year','Month']] = PREDICTED_DATES[['Year','Month']]
Temperature_rcp45_select[['Year','Month']] = PREDICTED_DATES[['Year','Month']]
Temperature_rcp45_select.head()
```

Calling the PET data that have been calculated in R FOR 2040

```
[ ]
PET_rc45 = (pd.read_csv('/content/drive/MyDrive/CSV_FINAL_2022_08_31/PET_rcp45_Transposed.csv')).iloc[:,0:461]
PET_rc85 = (pd.read_csv('/content/drive/MyDrive/CSV_FINAL_2022_08_31/PET_rcp85_Transposed.csv')).iloc[:,0:461]
PET_rc45[['Year','Month']] = PREDICTED_DATES[['Year','Month']]
PET_rc85[['Year','Month']] = PREDICTED_DATES[['Year','Month']]
```

```
[ ]
# concat_temp_station[(concat_temp_station['Year'] >= 1991) & (concat_temp_station['Year'] <= 2005) & (concat_temp_station['Month'] >=
  3) & (concat_temp_station['Month'] <= 5) ]
RAIN_rc85_MAM = (Rainfall_rcp85_select[(Rainfall_rcp85_select['Year'] >= 2021) & (Rainfall_rcp85_select['Year'] <= 2040) & (Rainfall
_rcp85_select['Month'] >= 3) & (Rainfall_rcp85_select['Month'] <= 5) ]).iloc[:,0:461]
RAIN_rc85_OND = (Rainfall_rcp85_select[(Rainfall_rcp85_select['Year'] >= 2021) & (Rainfall_rcp85_select['Year'] <= 2040) & (Rainfall_
rcp85_select['Month'] >= 10) & (Rainfall_rcp85_select['Month'] <= 12) ]).iloc[:,0:461]
RAIN_rc45_MAM = (Rainfall_rcp45_select[(Rainfall_rcp45_select['Year'] >= 2021) & (Rainfall_rcp45_select['Year'] <= 2040) & (Rainfall
_rcp45_select['Month'] >= 3) & (Rainfall_rcp45_select['Month'] <= 5) ]).iloc[:,0:461]
RAIN_rc45_OND = (Rainfall_rcp45_select[(Rainfall_rcp45_select['Year'] >= 2021) & (Rainfall_rcp45_select['Year'] <= 2040) & (Rainfall_
rcp45_select['Month'] >= 10) & (Rainfall_rcp45_select['Month'] <= 12) ]).iloc[:,0:461]

# PET_rc45_MAM = (PET_rc45[(PET_rc45['Year'] >= 2021) & (PET_rc45['Year'] <= 2040) & (PET_rc45['Month'] >= 3) & (PET_rc45['M
onth'] <= 5) ]).iloc[:,0:461]
# PET_rc45_OND = (PET_rc45[(PET_rc45['Year'] >= 2021) & (PET_rc45['Year'] <= 2040) & (PET_rc45['Month'] >= 10) & (PET_rc45['M
```

```
onth'] <= 12) ]).iloc[:,0:461]
# PET_rc85_MAM = (PET_rc85[(PET_rc85['Year'] >= 2021) & (PET_rc85['Year'] <= 2040) & (PET_rc85['Month'] >= 3) & (PET_rc85['M
onth'] <= 5) ]).iloc[:,0:461]
# PET_rc85_OND = (PET_rc85[(PET_rc85['Year'] >= 2021) & (PET_rc85['Year'] <= 2040) & (PET_rc85['Month'] >= 10) & (PET_rc85['M
onth'] <= 12) ]).iloc[:,0:461]
# PET_rc45_MAM
```

```
[ ]
RAIN_rc85_MAM_2 = RAIN_rc85_MAM.astype('float').T.mean(axis=1).T.to_frame().reset_index()
RAIN_rc85_OND_2 = RAIN_rc85_OND.astype('float').T.mean(axis=1).T.to_frame().reset_index()
RAIN_rc45_MAM_2 = RAIN_rc45_MAM.astype('float').T.mean(axis=1).T.to_frame().reset_index()
RAIN_rc45_OND_2 = RAIN_rc45_OND.astype('float').T.mean(axis=1).T.to_frame().reset_index()

RAIN_rc85_MAM_2.to_csv('RAIN_rc85_MAM_2.csv', index=True, encoding='utf-8')
RAIN_rc85_OND_2.to_csv('RAIN_rc85_OND_2.csv', index=True, encoding='utf-8')
RAIN_rc45_MAM_2.to_csv('RAIN_rc45_MAM_2.csv', index=True, encoding='utf-8')
RAIN_rc45_OND_2.to_csv('RAIN_rc45_OND_2.csv', index=True, encoding='utf-8')
```

```
[ ]
TEMP_rc45_MAM.to_csv('TEMP_rc45_MAM.csv', index=True, encoding='utf-8')
TEMP_rc45_OND.to_csv('TEMP_rc45_OND.csv', index=True, encoding='utf-8')
TEMP_rc85_MAM.to_csv('TEMP_rc85_MAM.csv', index=True, encoding='utf-8')
TEMP_rc85_OND.to_csv('TEMP_rc85_OND.csv', index=True, encoding='utf-8')
```

making sure the columns have the same name, so as to compare them

```
[ ]
# # RAIN_rc85_MAM.head()
# # PET_rc85_MAM = PET_rc85_MAM.astype('int')
# RAIN_rc85_MAM = RAIN_rc85_MAM.astype('float')
# PET_rc85_MAM = PET_rc85_MAM.astype('float')
# RAIN_rc85_MAM
# PET_rc85_MAM
# # lgp_rc85_MAM  = RAIN_rc85_MAM.loc[RAIN_rc85_MAM > (PET_rc85_MAM/2)]

# PET_rc85_MAM.reset_index(drop=True)#
# PET_rc85_MAM
# list(RAIN_rc85_MAM)
# PET_rc85_MAM.columns = list(RAIN_rc85_MAM)
# PET_rc85_MAM

PET_rc85_MAM.columns = list(RAIN_rc85_MAM)
PET_rc85_OND.columns = list(RAIN_rc85_MAM)
PET_rc45_MAM.columns = list(RAIN_rc85_MAM)
PET_rc45_OND.columns = list(RAIN_rc85_MAM)

PET_rc45_OND

lgp_rc85_MAM = ((((RAIN_rc85_MAM.astype('float')).reset_index()).ge((PET_rc85_MAM.astype('float')/2).reset_index())).replace({True:
1, False: 0})).iloc[:,1:462]).T.sum(axis=1).T.to_frame().reset_index()
lgp_rc85_OND = ((((RAIN_rc85_OND.astype('float')).reset_index()).ge(((PET_rc85_OND.astype('float'))/2).reset_index())).replace({True: 1
, False: 0})).iloc[:,1:462]).T.sum(axis=1).T.to_frame().reset_index()
lgp_rc45_MAM = ((((RAIN_rc45_MAM.astype('float')).reset_index()).ge(((PET_rc45_MAM.astype('float'))/2).reset_index())).replace({True
: 1, False: 0})).iloc[:,1:462]).T.sum(axis=1).T.to_frame().reset_index()
lgp_rc45_OND = (((((RAIN_rc45_OND.astype('float')).reset_index()).ge(((PET_rc45_OND.astype('float'))/2).reset_index())).replace({True:
1, False: 0}))).iloc[:,1:462]).T.sum(axis=1).T.to_frame().reset_index()

# # .sum(axis=1).to_frame()
# RAIN_rc85_MAM
# PET_rc85_MAM
PET_rc45_OND
```

```
[ ]
```

```
[ ]
PET_rc85_MAM_2 = PET_rc85_MAM.T.reset_index().mean(axis=1).T.to_frame().reset_index()
PET_rc85_OND_2 = PET_rc85_OND.T.reset_index().mean(axis=1).T.to_frame().reset_index()
PET_rc45_MAM_2 = PET_rc45_MAM.T.reset_index().mean(axis=1).T.to_frame().reset_index()
PET_rc45_OND_2 = PET_rc45_OND.T.reset_index().mean(axis=1).T.to_frame().reset_index()

PET_rc85_MAM_2.to_csv('PET_rc85_MAM_2.csv', index=True, encoding='utf-8')
PET_rc85_OND_2.to_csv('PET_rc85_OND_2.csv', index=True, encoding='utf-8')
```

```
PET_rc45_MAM_2.to_csv('PET_rc45_MAM_2.csv', index=True, encoding='utf-8')
PET_rc45_OND_2.to_csv('PET_rc45_OND_2.csv', index=True, encoding='utf-8')
```

```
[ ]
PET_rc85_MAM.to_csv('lgp_rc85_MAM.csv', index=True, encoding='utf-8')
PET_rc85_OND.to_csv('lgp_rc85_OND.csv', index=True, encoding='utf-8')
PET_rc45_MAM.to_csv('lgp_rc45_MAM.csv', index=True, encoding='utf-8')
PET_rc45_OND.to_csv('lgp_rc45_OND.csv', index=True, encoding='utf-8')
```

```
[ ]
lgp_rc85_MAM

lgp_rc85_MAM.to_csv('lgp_rc85_MAM.csv', index=True, encoding='utf-8')
lgp_rc85_OND.to_csv('lgp_rc85_OND.csv', index=True, encoding='utf-8')
lgp_rc45_MAM.to_csv('lgp_rc45_MAM.csv', index=True, encoding='utf-8')
lgp_rc45_OND.to_csv('lgp_rc45_OND.csv', index=True, encoding='utf-8')
```

```
[ ]
TEMP_rc45_MAM = ((Temperature_rcp45_select[(Temperature_rcp45_select['Year'] >= 2021) & (Temperature_rcp45_select['Year'] <= 20
40) & (Temperature_rcp45_select['Month'] >= 3) & (Temperature_rcp45_select['Month'] <= 5) ]).iloc[:,0:461]).T.mean(axis=1).T.to_frame()
.reset_index()
TEMP_rc45_OND = (Temperature_rcp45_select[(Temperature_rcp45_select['Year'] >= 2021) & (Temperature_rcp45_select['Year'] <= 2040
) & (Temperature_rcp45_select['Month'] >= 10) & (Temperature_rcp45_select['Month'] <= 12) ]).iloc[:,0:461].T.mean(axis=1).T.to_frame().
reset_index()
TEMP_rc85_MAM = (Temperature_rcp85_select[(Temperature_rcp85_select['Year'] >= 2021) & (Temperature_rcp85_select['Year'] <= 204
0) & (Temperature_rcp85_select['Month'] >= 3) & (Temperature_rcp85_select['Month'] <= 5) ]).iloc[:,0:461].T.mean(axis=1).T.to_frame().r
eset_index()
TEMP_rc85_OND = (Temperature_rcp85_select[(Temperature_rcp85_select['Year'] >= 2021) & (Temperature_rcp85_select['Year'] <= 2040
) & (Temperature_rcp85_select['Month'] >= 10) & (Temperature_rcp85_select['Month'] <= 12) ]).iloc[:,0:461].T.mean(axis=1).T.to_frame().
reset_index()
TEMP_rc45_OND
```

```
[ ]
TEMP_rc45_MAM.to_csv('TEMP_rc45_MAM.csv', index=True, encoding='utf-8')
TEMP_rc45_OND.to_csv('TEMP_rc45_OND.csv', index=True, encoding='utf-8')
TEMP_rc85_MAM.to_csv('TEMP_rc85_MAM.csv', index=True, encoding='utf-8')
TEMP_rc85_OND.to_csv('TEMP_rc85_OND.csv', index=True, encoding='utf-8')
```

8.2.2 GEE Code (Baseline Mapping)

```
LGP PRODUCTS 2
Map.setOptions('SATELLITE');
Map.centerObject(table, 9);

var startDate = '1991-01-01';
var endDate = '2005-12-31';

var start = '2006-01-01';
var end = '2020-12-31';

////////////////////////////////////////////////////////////////////////////
///////////////////////////////////Aridity Index

var dataset_AI_ond = ee.ImageCollection('IDAHO_EPSCOR/TERRACLIMATE')
        .filter(ee.Filter.date('1991-01-01',          '2005-12-30')).select(['pet','pr']).sort('system:time_start',
true).filter(ee.Filter.calendarRange(3, 5, 'month'));


var dataset_AI_mam = ee.ImageCollection('IDAHO_EPSCOR/TERRACLIMATE')
```

```
                    .filter(ee.Filter.date('1991-01-01',                    '2005-12-30')).select(['pet','pr']).sort('system:time_start',
true).filter(ee.Filter.calendarRange(10, 12, 'month'));

var dataset_AI_mam_2 = ee.ImageCollection('IDAHO_EPSCOR/TERRACLIMATE')
        .filter(ee.Filter.date('2006-01-01',                    '2020-12-30')).select(['pet','pr']).sort('system:time_start',
true).filter(ee.Filter.calendarRange(3, 5, 'month'));



var dataset_AI_2_ond_2 = ee.ImageCollection('IDAHO_EPSCOR/TERRACLIMATE')
        .filter(ee.Filter.date('2006-01-01',                    '2020-12-30')).select(['pet','pr']).sort('system:time_start',
true).filter(ee.Filter.calendarRange(10, 12, 'month'));



// print(dataset_AI);

function AI(collection){
 var ratio = (collection.select(['pet']).divide(collection.select(['pr']))).multiply(100);
 var clipped_ratio = ratio.clip(table);
 return ratio;
}



var AI_OND_1990 = (dataset_AI_ond.map(AI)).mean().clip(table);

var AI_MAM_1990 = (dataset_AI_mam.map(AI)).mean().clip(table);

var AI_OND_2020 =  (dataset_AI_2_ond_2.map(AI)).mean().clip(table);

var AI_MAM_2020 = (dataset_AI_mam_2.map(AI)).mean().clip(table);

print(AI_MAM_2020);
Map.addLayer(AI_MAM_2020,{},'AI_MAM_2020');



//////////////////////////////////////////////////////////////
/////////////////////////////////////////////Potential Evapotranspiration (PET)

var dataset_PET_ond = ee.ImageCollection('IDAHO_EPSCOR/TERRACLIMATE')
        .filter(ee.Filter.date('1991-01-01',                    '2005-12-30')).select(['pet']).sort('system:time_start',
true).filter(ee.Filter.calendarRange(3, 5, 'month'));



var dataset_PET_mam = ee.ImageCollection('IDAHO_EPSCOR/TERRACLIMATE')
        .filter(ee.Filter.date('1991-01-01',                    '2005-12-30')).select(['pet']).sort('system:time_start',
true).filter(ee.Filter.calendarRange(10, 12, 'month'));

var dataset_PET_mam_2 = ee.ImageCollection('IDAHO_EPSCOR/TERRACLIMATE')
        .filter(ee.Filter.date('2006-01-01',                    '2020-12-30')).select(['pet']).sort('system:time_start',
true).filter(ee.Filter.calendarRange(3, 5, 'month'));
```

```
var dataset_PET_2_ond_2 = ee.ImageCollection('IDAHO_EPSCOR/TERRACLIMATE')
            .filter(ee.Filter.date('2006-01-01',                    '2020-12-30')).select(['pet']).sort('system:time_start',
true).filter(ee.Filter.calendarRange(10, 12, 'month'));


function PET(collection){
  var ratio = (collection.select(['pet']));
  var clipped_ratio = ratio.clip(table);
  return ratio;
}



var PET_OND_1990 = (dataset_PET_ond.map(PET)).mean().clip(table);

var PET_MAM_1990 = (dataset_PET_mam.map(PET)).mean().clip(table);

var PET_OND_2020 =  (dataset_PET_2_ond_2 .map(PET)).mean().clip(table);

var PET_MAM_2020 = (dataset_PET_mam_2.map(PET)).mean().clip(table);

print(PET_MAM_2020);
// Map.addLayer(PET_MAM_2020,{},'PET_MAM_2020');




//////////////////////////////////////////////////////////////////////////////
///////////////////////////////////interpolating LPG values to generate LPG output raster for modelling
var KRIGING_LPG_1990_2005_MAM = table13.kriging({
  propertyName: 'Sum',
  shape: 'exponential',
  range: 100 * 1000,
  sill: 1.0,
  nugget: 0.1,
  maxDistance: 100 * 1000,
  reducer: 'mean',
});

var LPG_1990_2005_MAM_MAP = KRIGING_LPG_1990_2005_MAM.clip(table);
Map.addLayer(LPG_1990_2005_MAM_MAP,{},'LPG_1990_2005_MAM_MAP');
Export.image.toDrive({image:LPG_1990_2005_MAM_MAP,            scale:            1000,            description:
'LPG_1990_2005_MAM_MAP', fileNamePrefix: 'LPG_1990_2005_MAM_MAP',
   region: table, maxPixels: 1e13});

var KRIGING_LPG_1990_2005_OND = table14.kriging({
  propertyName: 'Sum',
  shape: 'exponential',
  range: 100 * 1000,
  sill: 1.0,
```

```
 nugget: 0.1,
 maxDistance: 100 * 1000,
 reducer: 'mean',
});


var LPG_1990_2005_OND_MAP = KRIGING_LPG_1990_2005_OND.clip(table);
Map.addLayer(LPG_1990_2005_OND_MAP,{},'LPG_1990_2005_OND_MAP');
Export.image.toDrive({image:LPG_1990_2005_OND_MAP, scale: 1000, description: 'LPG_1990_2005_OND_MAP',
fileNamePrefix: 'LPG_1990_2005_OND_MAP',
  region: table, maxPixels: 1e13});


var KRIGING_LPG_2006_2020_MAM = table12.kriging({
 propertyName: 'Sum',
 shape: 'exponential',
 range: 100 * 1000,
 sill: 1.0,
 nugget: 0.1,
 maxDistance: 100 * 1000,
 reducer: 'mean',
});


var LPG_2006_2020_MAM_MAP = KRIGING_LPG_2006_2020_MAM.clip(table);
Map.addLayer(LPG_2006_2020_MAM_MAP,{},'LPG_2006_2020_MAM_MAP');
Export.image.toDrive({image:LPG_2006_2020_MAM_MAP,         scale:         1000,         description:
'LPG_2006_2020_MAM_MAP', fileNamePrefix: 'LPG_2006_2020_MAM_MAP',
  region: table, maxPixels: 1e13});


var KRIGING_LPG_2006_2020_OND = table11.kriging({
 propertyName: 'Sum',
 shape: 'exponential',
 range: 100 * 1000,
 sill: 1.0,
 nugget: 0.1,
 maxDistance: 100 * 1000,
 reducer: 'mean',
});

var LPG_2006_2020_OND_MAP = KRIGING_LPG_2006_2020_OND.clip(table);
Map.addLayer(LPG_2006_2020_OND_MAP,{},'LPG_2006_2020_OND_MAP');
Export.image.toDrive({image:LPG_2006_2020_OND_MAP, scale: 1000, description: 'LPG_2006_2020_OND_MAP',
fileNamePrefix: 'LPG_2006_2020_OND_MAP',
  region: table, maxPixels: 1e13});




/////////////////////////////////////////////////

var KRIGING_PET_MAM_1991_2005 = table6.kriging({
 propertyName: 'Sum',
 shape: 'exponential',
 range: 100 * 1000,
```

```
  sill: 1.0,
  nugget: 0.1,
  maxDistance: 100 * 1000,
  reducer: 'mean',
});

var krig_PET_MAM_91_05 = KRIGING_PET_MAM_1991_2005.clip(table);
Map.addLayer(krig_PET_MAM_91_05,{},'krig_PET_MAM_91_05');
Export.image.toDrive({image:krig_PET_MAM_91_05,  scale:  1000,  description:  'krig_PET_MAM_91_05',
fileNamePrefix: 'krig_PET_MAM_91_05',
   region: table, maxPixels: 1e13});

var KRIGING_PET_MAM_2006_2021 = table9.kriging({
  propertyName: 'Sum',
  shape: 'exponential',
  range: 100 * 1000,
  sill: 1.0,
  nugget: 0.1,
  maxDistance: 100 * 1000,
  reducer: 'mean',
});

var krig_PET_MAM_06_21 = KRIGING_PET_MAM_2006_2021.clip(table);
Map.addLayer(krig_PET_MAM_06_21,{},'krig_PET_MAM_06_21');
Export.image.toDrive({image:krig_PET_MAM_06_21,  scale:  1000,  description:  'krig_PET_MAM_06_21',
fileNamePrefix: 'krig_PET_MAM_06_21',
   region: table, maxPixels: 1e13});

var KRIGING_PET_OND_1991_2005 = table8.kriging({
  propertyName: 'Sum',
  shape: 'exponential',
  range: 100 * 1000,
  sill: 1.0,
  nugget: 0.1,
  maxDistance: 100 * 1000,
  reducer: 'mean',
});

var krig_PET_OND_91_05 = KRIGING_PET_OND_1991_2005.clip(table);
Map.addLayer(krig_PET_OND_91_05,{},'krig_PET_OND_91_05');
Export.image.toDrive({image:krig_PET_OND_91_05,  scale:  1000,  description:  'krig_PET_OND_91_05',
fileNamePrefix: 'krig_PET_OND_91_05',
   region: table, maxPixels: 1e13});


var KRIGING_PET_MAM_2006_2021 = table9.kriging({
  propertyName: 'Sum',
  shape: 'exponential',
  range: 100 * 1000,
  sill: 1.0,
  nugget: 0.1,
  maxDistance: 100 * 1000,
```

```
  reducer: 'mean',
});

var krig_PET_OND_06_21 = KRIGING_PET_MAM_2006_2021.clip(table);
Map.addLayer(krig_PET_OND_06_21,{},'krig_PET_OND_06_21');
Export.image.toDrive({image:krig_PET_OND_06_21,    scale:    1000,    description:    'krig_PET_OND_06_21',
fileNamePrefix: 'krig_PET_OND_06_21',
  region: table, maxPixels: 1e13});


// print('kriging',kriging_test )
// Map.addLayer(KRIGING.clip(table),{},'Kriging');


/////////////////////////////////////////////////////////////////////////////
/////////////////////////////////////////////////////////////////
////MAN-KENDALL ANALYSIS OF TREND USING TIME SERIES (RAINFALL, TEMPERATURE,
EVAPOTRANSPIRATION DURING MAM & OND PERIODS)


var NASA_2 = ee.ImageCollection("NASA/FLDAS/NOAH01/C/GL/M/V001").select("Evap_tavg")
  .filterDate(startDate, endDate).sort('system:time_start', false);

// var mean_PET_3_5_2 = NASA.mean();
var                                 temperature_dataset_2                                 =
ee.ImageCollection('ECMWF/ERA5/DAILY').select('mean_2m_air_temperature').filterDate(startDate,
endDate).sort('system:time_start', false);
// print('TEMP DATA',temperature_dataset_2)
var    rainfall_2    =    ee.ImageCollection("UCSB-CHG/CHIRPS/DAILY").select('precipitation').filterDate(startDate,
endDate)
  .sort('system:time_start', false);


var    rainfall_3    =    ee.ImageCollection("UCSB-CHG/CHIRPS/DAILY").select('precipitation').filterDate(start,
end).sort('system:time_start', false);

var                                 temperature_dataset_3                                 =
ee.ImageCollection('ECMWF/ERA5/DAILY').select('mean_2m_air_temperature').filterDate(start,
end).sort('system:time_start', false);
// print('TEMP DATA',temperature_dataset_2)




function clip_temp(collection){
  var clipped = collection.clip(table);
  return clipped;
}

function multiply(image_collection){
  var image_mm = image_collection.multiply(86400);
  var clipped_tavg = image_mm.clip(table);
  return clipped_tavg;
```

```
}

function temp(image_collection){
  var image_mm = image_collection;
  var clipped_temp_degree = image_mm.clip(table);
  return clipped_temp_degree;
}



//////////////////Filtering the images for the MAM & OND Periods
// var Evapotranspiration_MAM = NASA_2.filter(ee.Filter.calendarRange(3, 5, 'month')).map(multiply);

// var Evapotranspiration_OND = NASA_2.filter(ee.Filter.calendarRange(10, 12, 'month')).map(multiply);

var        Temperature_MAM_90_05        =        (temperature_dataset_2.filter(ee.Filter.calendarRange(3,        5,
'month')).map(temp).mean()).subtract(273.15).clip(table);
Map.addLayer(Temperature_MAM_90_05,{},'Temperature_MAM_90_05');
Export.image.toDrive({image:Temperature_MAM_90_05, scale: 1000, description: 'Temperature_MAM_90_05',
fileNamePrefix: 'Temperature_MAM_90_05',
   region: table, maxPixels: 1e13});




var        Temperature_OND_90_05        =        (temperature_dataset_2.filter(ee.Filter.calendarRange(10,        12,
'month')).map(temp).mean()).subtract(273.15).clip(table);
Map.addLayer(Temperature_OND_90_05,{},'Temperature_OND_90_05');
Export.image.toDrive({image:Temperature_OND_90_05, scale: 1000, description: 'Temperature_OND_90_05',
fileNamePrefix: 'Temperature_OND_90_05',
   region: table, maxPixels: 1e13});




var Precipitation_MAM_90_05 = (rainfall_2.filter(ee.Filter.calendarRange(3, 5, 'month')).map(clip_temp).mean());
Export.image.toDrive({image:Precipitation_MAM_90_05, scale: 1000, description: 'Precipitation_MAM_90_05',
fileNamePrefix: 'Precipitation_MAM_90_05',
   region: table, maxPixels: 1e13});

var Precipitation_OND_90_05 = (rainfall_2.filter(ee.Filter.calendarRange(10, 12, 'month')).map(clip_temp).mean());
Export.image.toDrive({image:Precipitation_OND_90_05, scale: 1000, description: 'Precipitation_OND_90_05',
fileNamePrefix: 'Precipitation_OND_90_05',
   region: table, maxPixels: 1e13});




var        Temperature_MAM_06_21        =        (temperature_dataset_3.filter(ee.Filter.calendarRange(3,        5,
'month')).map(temp).mean()).subtract(273.15);
Map.addLayer(Temperature_MAM_06_21,{},'Temperature_MAM_06_21');
Export.image.toDrive({image:Temperature_MAM_06_21, scale: 1000, description: 'Temperature_MAM_06_21',
fileNamePrefix: 'Temperature_MAM_06_21',
   region: table, maxPixels: 1e13});
```

```
var        Temperature_OND_06_21        =        (temperature_dataset_3.filter(ee.Filter.calendarRange(10,        12,
'month')).map(temp).mean()).subtract(273.15);
Map.addLayer(Temperature_OND_06_21,{},'Temperature_OND_06_21');
Export.image.toDrive({image:Temperature_OND_06_21, scale: 1000, description: 'Temperature_OND_06_21',
fileNamePrefix: 'Temperature_OND_06_21',
    region: table, maxPixels: 1e13});


var Precipitation_MAM_06_21 = rainfall_3.filter(ee.Filter.calendarRange(3, 5, 'month')).map(clip_temp).mean();
Export.image.toDrive({image:Precipitation_MAM_06_21, scale: 1000, description: 'Precipitation_MAM_06_21',
fileNamePrefix: 'Precipitation_MAM_06_21',
    region: table, maxPixels: 1e13});


var Precipitation_OND_06_21 = rainfall_3.filter(ee.Filter.calendarRange(10, 12, 'month')).map(clip_temp).mean();
Export.image.toDrive({image:Precipitation_OND_06_21, scale: 1000, description: 'Precipitation_OND_06_21',
fileNamePrefix: 'Precipitation_OND_06_21',
    region: table, maxPixels: 1e13});


print(Precipitation_OND_06_21);



/////computing MI for preparation to compute the climate regimes

var                              MI_90_05_MAM                                            =
(((Precipitation_MAM_90_05.subtract(krig_PET_MAM_91_05)).divide(krig_PET_MAM_91_05))).rename('MI_MA
M_90');
print('mi', MI_90_05_MAM );
Export.image.toDrive({image:MI_90_05_MAM, scale: 1000, description: 'MI_90_05_MAM', fileNamePrefix:
'MI_90_05_MAM',
    region: table, maxPixels: 1e13});


var                              MI_90_05_OND                                            =
(((Precipitation_OND_90_05.subtract(krig_PET_OND_91_05)).divide(krig_PET_OND_91_05))).rename('MI_OND_
90');

Export.image.toDrive({image:MI_90_05_OND, scale: 1000, description: 'MI_90_05_OND', fileNamePrefix:
'MI_90_05_OND',
    region: table, maxPixels: 1e13});



var                              MI_06_20_MAM                                            =
(((Precipitation_MAM_06_21.multiply(krig_PET_MAM_06_21)).divide(krig_PET_MAM_06_21))).rename('MI_M
AM_06');
Export.image.toDrive({image:MI_06_20_MAM, scale: 1000, description: 'MI_06_20_MAM', fileNamePrefix:
'MI_06_20_MAM',
    region: table, maxPixels: 1e13});



var                              MI_06_20_OND                                            =
(((Precipitation_OND_06_21.multiply(krig_PET_OND_06_21)).divide(krig_PET_OND_06_21))).rename('MI_OND
_06');
Export.image.toDrive({image:MI_06_20_OND, scale: 1000, description: 'MI_06_20_OND', fileNamePrefix:
'MI_06_20_OND',
```

```
      region: table, maxPixels: 1e13});



// print('test',TR_MAM_05_20 );

Map.addLayer(TR_MAM_05_20,{},'TR_MAM_05_20');
Export.image.toDrive({image:TR_MAM_05_20, scale: 1000, description: 'TR_MAM_05_20', fileNamePrefix:
'TR_MAM_05_20',
   region: table, maxPixels: 1e13});

///////////////////////
/////////////////////computing Climate Regimes (CR)
var                                  CI_OND_90_05                                      =
(TR_OND_90_05.multiply(LPG_1990_2005_OND_MAP).multiply(MI_90_05_OND)).rename('CI_OND_90');

Map.addLayer(CI_OND_90_05,{},'CI_OND_90_05');
Export.image.toDrive({image:CI_OND_90_05, scale: 1000, description: 'CI_OND_90_05', fileNamePrefix:
'CI_OND_90_05',
   region: table, maxPixels: 1e13});

var                                  CI_OND_06_20                                      =
(TR_OND_05_20.multiply(LPG_2006_2020_OND_MAP).multiply(MI_06_20_OND)).rename('CI_OND_06');

Map.addLayer(CI_OND_06_20,{},'CI_OND_06_20');
Export.image.toDrive({image:CI_OND_06_20, scale: 1000, description: 'CI_OND_06_20', fileNamePrefix:
'CI_OND_06_20',
   region: table, maxPixels: 1e13});

var                                  CI_MAM_90_05                                      =
(TR_MAM_90_05.multiply(LPG_1990_2005_MAM_MAP).multiply(MI_90_05_MAM)).rename('CI_MAM_90');


Map.addLayer(CI_MAM_90_05,{},'CI_MAM_90_05');
Export.image.toDrive({image:CI_MAM_90_05, scale: 1000, description: 'CI_MAM_90_05', fileNamePrefix:
'CI_MAM_90_05',
   region: table, maxPixels: 1e13});

print('CI_MAM_90_05', CI_MAM_90_05);

var                                  CI_MAM_06_20                                      =
(TR_MAM_05_20.multiply(LPG_2006_2020_MAM_MAP).multiply(MI_06_20_MAM)).rename('CI_MAM_06');

Map.addLayer(CI_MAM_06_20,{},'CI_MAM_06_20');
Export.image.toDrive({image:CI_MAM_06_20, scale: 1000, description: 'CI_MAM_06_20', fileNamePrefix:
'CI_MAM_06_20',
   region: table, maxPixels: 1e13});



///////////////////////////slope in percentage
```

```
// A digital elevation model.
var dem = ee.Image('NASA/NASADEM_HGT/001').select('elevation').clip(table);

// Calculate slope. Units are percentage
var slope = (ee.Terrain.slope(dem)).multiply(0.27777777);

// Calculate aspect. Units are degrees where 0=N, 90=E, 180=S, 270=W.
var aspect = ee.Terrain.aspect(dem);

Map.addLayer(slope, {}, 'Slope');

var terrain = ee.Terrain.products(dem);
// print('ee.Terrain.products bands', terrain.bandNames());
// Map.addLayer(terrain.select('hillshade'), {min: 0, max: 255}, 'Hillshade');




// var slopereclass = ee.Image(1)
//       .where(slope.gte(0).and(slope.lte(2)), 1)
//       .where(slope.gt(2).and(slope.lte(5)), 2)
//       .where(slope.gt(5).and(slope.lte(8)), 3)
//       .where(slope.gt(8).and(slope.lte(16)),4)
//       .where(slope.gt(16).and(slope.lte(30)),5)
//       .where(slope.gt(30).and(slope.lte(45)),6)
//       .where(slope.gt(45).and(slope.lte(100)),7);

Map.addLayer(slopereclass.clip(table),{},'slopereclass%');
var slopereclass_2 = slopereclass.clip(table);

Export.image.toDrive({image:slope, scale: 1000, description: 'slope', fileNamePrefix: 'slope',
   region: table, maxPixels: 1e13});




/////////////////////////////////////////////////////////////////
//////////////////Computing the Aridity index of each season (MAM & OND)
/////////////////////////////////////////////////////////////////

var                          AI_90_05_MAM                              =
((Precipitation_MAM_90_05.divide(krig_PET_MAM_91_05)).multiply(100)).rename('AI_MAM_90');
print('mi',  AI_90_05_MAM );
Map.addLayer(AI_90_05_MAM,{},'AI_90_05_MAM');

Export.image.toDrive({image:AI_90_05_MAM,  scale:  1000,  description: 'AI_90_05_MAM', fileNamePrefix:
'AI_90_05_MAM',
   region: table, maxPixels: 1e13});

var                          AI_90_05_OND                              =
((Precipitation_OND_90_05.divide(krig_PET_OND_91_05)).multiply(100)).rename('AI_OND_90');
Map.addLayer(AI_90_05_OND,{},'AI_90_05_OND');
```

```
Export.image.toDrive({image:AI_90_05_OND, scale: 1000, description: 'AI_90_05_OND', fileNamePrefix:
'AI_90_05_OND',
   region: table, maxPixels: 1e13});


var                              AI_06_20_MAM                                    =
((Precipitation_MAM_06_21.divide(krig_PET_MAM_06_21)).multiply(100)).rename('AI_MAM_06');
Map.addLayer(AI_06_20_MAM,{},'AI_06_20_MAM');
Export.image.toDrive({image:AI_06_20_MAM, scale: 1000, description: 'AI_06_20_MAM', fileNamePrefix:
'AI_06_20_MAM',
   region: table, maxPixels: 1e13});

var                              AI_06_20_OND                                    =
((Precipitation_OND_06_21.divide(krig_PET_OND_06_21)).multiply(100)).rename('AI_OND_06');
Map.addLayer(AI_06_20_OND,{},'AI_06_20_OND');
Export.image.toDrive({image:AI_06_20_OND, scale: 1000, description: 'AI_06_20_OND', fileNamePrefix:
'AI_06_20_OND',
   region: table, maxPixels: 1e13});

////////////////////////////////////////////////////////////////////////////////////////////////////////////////
//////////soil dataset comprising of agricultural zones suitable areas and soil drainage extracted from soil classification
data


Map.addLayer(soil_ag_suit,{},'soil_agri_suit');
Export.image.toDrive({image:soil_ag_suit, scale: 1000, description: 'soil_ag_suit', fileNamePrefix: 'soil_ag_suit',
   region: table, maxPixels: 1e13});

Map.addLayer(soil_drainage,{},'soil_drainage');
Export.image.toDrive({image:soil_drainage, scale: 1000, description: 'soil_drainage', fileNamePrefix: 'soil_drainage',
   region: table, maxPixels: 1e13});



////////////////////////////////////////////////////////////////////////////////////////////////////////////////
/////////////////////contrained elevation data

var constrained_slope = ee.Image(1)
      .where(slope.gte(0).and(slope.lte(8)), 1)
      .where(slope.gt(8).and(slope.lte(15)), 2)
      .where(slope.gt(16).and(slope.lte(30)), 3)
      .where(slope.gt(30).and(slope.lte(100)),4);

var constrained_slope_clip = constrained_slope.clip(table);

Map.addLayer(constrained_slope_clip,{},'constrained_slope_clip');
Export.image.toDrive({image:constrained_slope_clip, scale: 1000, description: 'constrained_slope_clip',
fileNamePrefix: 'constrained_slope_clip',
   region: table, maxPixels: 1e13});


////////////////////////////////////////////////////////////////////////////////////////////////////////////////
```

```
///////////////////////////ASSESSING DRY MATTER & productivity USING DAILY NDVI
var dataset_mod = ee.ImageCollection('MODIS/061/MOD13A2')
        .filter(ee.Filter.date('2006-01-01', '2020-12-31'));
var ndvi = dataset_mod.select('NDVI');

var dataset = ee.ImageCollection('MODIS/061/MOD13A2')
        .filter(ee.Filter.date('1991-01-01', '2005-12-31'));

var ndvi_2 = dataset.select('NDVI');




var    MAM_NDVI_1990    =    (((ndvi_2.select('NDVI').filter(ee.Filter.calendarRange(3,    5,
'month')).max()).clip(table)).multiply(1.615).pow(1.318)).unitScale(58000, 315000);

var    OND_NDVI_1990    =    ((ndvi_2.select('NDVI').filter(ee.Filter.calendarRange(10,    12,
'month')).max().clip(table)).multiply(1.615).pow(1.318)).unitScale(58000, 315000);

var    OND_NDVI_2020    =    ((ndvi.select('NDVI').filter(ee.Filter.calendarRange(10,    12,
'month')).max().clip(table)).multiply(1.615).pow(1.318)).unitScale(58000, 315000);

var    MAM_NDVI_2020    =    ((ndvi.select('NDVI').filter(ee.Filter.calendarRange(3,    5,
'month')).max().clip(table)).multiply(1.615).pow(1.318)).unitScale(58000, 315000);

Map.addLayer(MAM_NDVI_2020,{},'MAM_NDVI_2020_DM');
Export.image.toDrive({image:MAM_NDVI_2020, scale: 1000, description: 'MAM_NDVI_2020', fileNamePrefix:
'MAM_NDVI_2020',
   region: table, maxPixels: 1e13});

Map.addLayer(OND_NDVI_2020,{},'OND_NDVI_2020_DM');
Export.image.toDrive({image:OND_NDVI_2020, scale: 1000, description: 'OND_NDVI_2020', fileNamePrefix:
'OND_NDVI_2020',
   region: table, maxPixels: 1e13});

Map.addLayer(OND_NDVI_1990,{},'OND_NDVI_1990_DM');
Export.image.toDrive({image:OND_NDVI_1990, scale: 1000, description: 'OND_NDVI_1990', fileNamePrefix:
'OND_NDVI_1990',
   region: table, maxPixels: 1e13});

Map.addLayer(MAM_NDVI_1990,{},'MAM_NDVI_1990_DM');
Export.image.toDrive({image:MAM_NDVI_1990, scale: 1000, description: 'MAM_NDVI_1990', fileNamePrefix:
'MAM_NDVI_1990',
   region: table, maxPixels: 1e13});




///////////////////////////////////
/////////////////////////////////////////
/////////////////////////Computing AEZ of MAM and OND
```

```
var      AEZ_1990_MAM      =      (CI_MAM_90_05.multiply((AI_90_05_MAM).pow(-1)).multiply((slope).pow(-
1)).multiply(soil_drainage).multiply(MAM_NDVI_1990))
Map.addLayer(AEZ_1990_MAM,{},'AEZ_1990_MAM');
Export.image.toDrive({image:AEZ_1990_MAM, scale: 1000, description: 'AEZ_1990_MAM', fileNamePrefix:
'AEZ_1990_MAM',
   region: table, maxPixels: 1e13});

var      AEZ_1990_OND      =      (CI_OND_90_05.multiply((AI_90_05_OND).pow(-1)).multiply((slope).pow(-
1)).multiply(soil_drainage).multiply(OND_NDVI_1990))
Map.addLayer(AEZ_1990_OND,{},'AEZ_1990_OND');
Export.image.toDrive({image:AEZ_1990_OND, scale: 1000, description: 'AEZ_1990_OND', fileNamePrefix:
'AEZ_1990_OND',
   region: table, maxPixels: 1e13});

var      AEZ_2020_OND      =      (CI_OND_06_20.multiply((AI_06_20_OND).pow(-1)).multiply((slope).pow(-
1)).multiply(soil_drainage).multiply(OND_NDVI_2020))
Map.addLayer(AEZ_2020_OND,{},'AEZ_2020_OND');
Export.image.toDrive({image:AEZ_2020_OND, scale: 1000, description: 'AEZ_2020_OND', fileNamePrefix:
'AEZ_2020_OND',
   region: table, maxPixels: 1e13});

var      AEZ_2020_MAM      =      (CI_MAM_06_20.multiply((AI_06_20_MAM).pow(-1)).multiply((slope).pow(-
1)).multiply(soil_drainage).multiply(MAM_NDVI_2020))
Map.addLayer(AEZ_2020_OND,{},'AEZ_2020_OND');
Export.image.toDrive({image:AEZ_2020_OND, scale: 1000, description: 'AEZ_2020_MAM', fileNamePrefix:
'AEZ_2020_MAM',
   region: table, maxPixels: 1e13});


function fuzzyfication(image){
 var min = image.reduceRegion(ee.Reducer.min(),table.geometry(),1000);
 var max = image.reduceRegion(ee.Reducer.max(),table.geometry(),1000);
}
```

8.2.3   GEE Code (Future Mapping)

```
/////////////////////////////////////////////////////
```

```
////////////////////////////CLIMAT EREGIMES = WEIGHTED OVERLAY OF MI,LGP,TR
////////////////////////MI = ((P - PET)/PET)*100

var MULTI_BAND_PET = (PET_rc45_MAM_2.addBands(PET_rc85_OND_2_2)
.addBands(PET_rc85_MAM_2_2).addBands(PET_rc45_OND_2_2)).rename(['PET_rc45_MAM_2','PET_rc85_OND
_2_2','PET_rc85_MAM_2_2','PET_rc45_OND_2_2']);
print(MULTI_BAND_PET);


var MULTI_BAND_TEMP = (TEMP_rc45_MAM_2.addBands(TEMP_rc45_OND_2)
.addBands(TEMP_rc85_MAM_2).addBands(TEMP_rc85_OND_2)).rename(['TEMP_rc45_MAM_2','TEMP_rc45_O
ND_2','TEMP_rc85_MAM_2','TEMP_rc85_OND_2']);

var MULTI_BAND_LGP = (lgp_rc45_MAM_2.addBands(lgp_rc45_OND_2)
.addBands(lgp_rc85_MAM_2).addBands(lgp_rc85_OND_2)).rename(['lgp_rc45_MAM_2','lgp_rc45_OND_2','lgp_rc
85_MAM_2','lgp_rc85_OND_2']);

var MULTI_BAND_RAIN = (RAIN_rc45_MAM_2_2.addBands(RAIN_rc45_OND_2_2)
.addBands(RAIN_rc85_MAM_2_2).addBands(RAIN_rc85_OND_2_2)).rename(['RAIN_rc45_MAM_2_2','RAIN_rc
45_OND_2_2','RAIN_rc85_MAM_2_2','RAIN_rc85_OND_2_2']);


/////////////////////////////////////////////computing the moisture index

function products(MULTIBAND1,MULTIBAND2,MULTIBAND3,MULTIBAND4){
  var MI = ((MULTIBAND4.subtract(MULTIBAND1)).divide(MULTIBAND1));
  return MI.rename(['MI_rc45_MAM','MI_rc45_OND_2','MI_rc85_MAM_2','MI_rc85_OND_2']);
}
var                          MI_OUTPUT                          =
products(MULTI_BAND_PET,MULTI_BAND_TEMP,MULTI_BAND_LGP,MULTI_BAND_RAIN);
print(MI_OUTPUT);
Map.addLayer(MI_OUTPUT,{},'MI_OUTPUT');
Export.image.toDrive({image:MI_OUTPUT, scale: 1000, description: 'MI_OUTPUT', fileNamePrefix: 'MI_OUTPUT',
   region: table, maxPixels: 1e13});

/////////////////////////////computing climate regimes

function CR_computing(MI,MULTIBAND1,MULTIBAND2,MULTIBAND3,MULTIBAND4){
  var                          CR                          =
((MI).multiply(MULTIBAND3).multiply(MULTIBAND2)).rename(['CR_rc45_MAM','CR_rc45_OND_2','CR_rc85_
MAM_2','CR_rc85_OND_2']);
  return CR;
}
var                          CR_OUTPUT                          =
CR_computing(MI_OUTPUT,MULTI_BAND_PET,MULTI_BAND_TEMP,MULTI_BAND_LGP,MULTI_BAND_
RAIN);
print(CR_OUTPUT);
Map.addLayer(CR_OUTPUT,{},'CR_OUTPUT');
Export.image.toDrive({image:CR_OUTPUT,    scale:    1000,    description:    'CR_OUTPUT',    fileNamePrefix:
'CR_OUTPUT',
   region: table, maxPixels: 1e13});

/////////////////////////////computing Aridity Index
function AI_computing(MI,MULTIBAND1,MULTIBAND2,MULTIBAND3,MULTIBAND4){
  var                          AI                          =
((MULTIBAND4).divide(MULTIBAND1)).rename(['AI_rc45_MAM','AI_rc45_OND_2','AI_rc85_MAM_2','AI_rc8
5_OND_2']);
  return AI;
}
```

```
var                                            AI_OUTPUT                                          =
AI_computing(MI_OUTPUT,MULTI_BAND_PET,MULTI_BAND_TEMP,MULTI_BAND_LGP,MULTI_BAND_
RAIN);
print(AI_OUTPUT);
Export.image.toDrive({image:AI_OUTPUT, scale: 1000, description: 'AI_OUTPUT', fileNamePrefix: 'AI_OUTPUT',
   region: table, maxPixels: 1e13});

Map.addLayer(AI_OUTPUT,{},'AI_OUTPUT');

/////////////////////////////////////////
///////////////////computing sub AEZ from the foavailable outputs
function AEZ(MULTIBAND1,MULTIBAND2,MULTIBAND3){
 var AEZ_COMPUTED = MULTIBAND1.multiply(MULTIBAND2).multiply(MULTIBAND3);
 return
AEZ_COMPUTED.rename(['AEZ_rc45_MAM','AEZ_rc45_OND_2','AEZ_rc85_MAM_2','AEZ_rc85_OND_2']);
}

var AEZ_output = AEZ(AI_OUTPUT,CR_OUTPUT,MI_OUTPUT);

Map.addLayer(AEZ_output,{},'AEZ_output');

/////////////////////////////////////////
///////////////////After attaining the computation, we now download the data and process it in a GIS environment, in
////////order to utilize the various methods such as fuzzification found there
```

9   APPENDIX 3 – SIGNED TURNITIN REPORT

1Assessment of impacts of climate change on AEZ and agriculture in Lower Eastern Kenya turnitin 2 09.05.2024.docx

12/05/2024   11/05/2024   12/05/2024

ORIGINALITY REPORT

7% SIMILARITY INDEX   **6**% INTERNET SOURCES   **4**% PUBLICATIONS   **2**% STUDENT PAPERS

PRIMARY SOURCES

1	gis.stackexchange.com Internet Source	1%
2	www.tutorialspoint.com Internet Source	<1%
3	efdinitiative.org Internet Source	<1%
4	geoinnova.org Internet Source	<1%
5	"Handbook of Climate Change Resilience", Springer Science and Business Media LLC, 2020 Publication	<1%
6	lup.lub.lu.se Internet Source	<1%
7	"Global soil organic carbon sequestration potential map (GSOCseq v1.1) - Technical manual", Food and Agriculture Organization of the United Nations (FAO), 2022	<1%

Publication

8	ouci.dntb.gov.ua Internet Source	<1%
9	www.coursehero.com Internet Source	<1%
10	"Climate Change Adaptation in Africa", Springer Nature, 2017 Publication	<1%
11	link.springer.com Internet Source	<1%
12	pdffox.com Internet Source	<1%
13	www.frontiersin.org Internet Source	<1%
14	Submitted to University of KwaZulu-Natal Student Paper	<1%
15	Innovations as Key to the Green Revolution in Africa, 2011. Publication	<1%
16	journals.ametsoc.org Internet Source	<1%
17	ir.haramaya.edu.et Internet Source	<1%
18	library.wur.nl Internet Source	<1%

UNIVERSITY OF NAIROBI

Declaration of Originality Form

This form must be completed and signed for all works submitted to the University for Examination.

Name of student: _____ Lilian Wangui Ndungu _____

Registration Number: _____ F80/54871/2019 _____

Faculty/School/Institute: _____ Engineering _____

Department: _____ Geospatial and Space Technology _____

Course Name: _____ Doctor of Philosophy Degree in Geographic Information System (GIS)

Title of the work

Assessing the Impact of Climate Change on Agro-Ecological Zones and Agriculture in Kenya's Lower Eastern Region

DECLARATION

1. I understand what Plagiarism is and I am aware of the University's policy in this regard.
2. I declare that this _____ Thesis _____ (Thesis, project, essay, assignment, paper, report etc) is my original work and has not been submitted elsewhere for examination, award of a degree or publication. Where other people's work, or my own work has been used, this has properly been acknowledged and referenced in accordance with the University of Nairobi's requirements.
3. I have not sought or used the services of any professional agencies to produce this work
4. I have not allowed, and shall not allow anyone to copy my work with the intention of passing it off as his/her own work
5. I understand that any false claim in respect of this work shall result in disciplinary action in accordance with University Plagiarism Policy.

Signature: _____

Date: _____ 11/05/2024 _____

158